The role of free- and liposomal-N-acetylcysteine in paraquat-induced cytotoxicity

by

Panagiotis Mitsopoulos

Department of Biology

Submitted in partial fulfillment of the requirements
for the Master‟s degree

Faculty of Graduate Studies
Lakehead University
Thunder Bay, Ontario

September 23, 2009

Table of Contents

Acknowledgements

I would first and foremost like to thank Dr. Zacharias Suntres, who has been an exceptional supervisor throughout the course of my studies, allowing me significant input in regards to the direction of our project and being pivotal to the development of my independent research skills. I also thank my committee members, Drs. Neelam Khaper, David Law, and Lada Malek, who have provided valuable guidance over the course of my studies; Dr. Bruce Cook, whom I had the pleasure of working with to begin this project, and Misagh Alipour for providing me with lyophilized L-NAC for my experiments. I thank Dr. Marina Ulanova who, together with Dr. Khaper, fostered a sense of community among the faculty, staff, and students and furthered our knowledge by promoting weekly journal clubs and seminars to discuss science as well as our own projects. Next I would like to thank the students and staff who have worked with me over the course of my studies and have made my days, and long nights, enjoyable in the lab: Sean Bryan, a good friend who has genuinely influenced my outlook on life as we tackled the joys and frustrations of laboratory research together; Rebecca Barnes and Sean Gravelle for providing strong examples and helping to bring out my best; and Pouya Sadeghi Aval, Jeff Werner, Lindsay Sutherland, Jessica Rosengren, Marlon Hagerty, Nicole Hawdon, Pam Tallon, Melanie Heney, Sarah Khan, Lee Shewchuk, Adiel Mallik, Jesse Gordon, Bryan Gray, and Patricia Lyle for their assistance and good memories. I would also like to thank my mother, father, brother and sister for their support and love. Lastly, I acknowledge the Northern Ontario School of Medicine, and NSERC for funding.

Abbreviations

A549 - human alveolar type II-like epithelial cell line

ANX - annexin V

ARDS - acute respiratory distress syndrome

ATCC - American Type Culture Collection

CDK - cyclin-dependent kinase

cDNA - complimentary deoxyribonucleic acid

CEES - chloroethyl ethyl sulfide

CM-H_2DCFDA - 5-(and-6)-chloromethyl-2′,7′-dichlorodihydrofluorescein diacetate, acetyl ester

DNA - deoxyribonucleic acid

DPPC - dipalmitoyl-phosphatidylcholine

EL - empty liposomes

GPx - glutathione peroxidise

G_{red} - glutathione reductase

GSH - glutathione (reduced form)

GSSG - glutathione (oxidized form)

GST - glutathione S-transerase

H_2O_2 - hydrogen peroxide

JC-1 - 5,5′,6,6′-tetrachloro-1,1′,3,3′-tetraethylbenzimidazolylcarbocyanine iodide

i.p. - intraperitoneal

IL - interleukin

K_d - sorption coefficient

LDH - lactate dehydrogenase

L-NAC - liposomal-N-acetylcysteine

LPS - lipopolysaccharide

MAPK - mitogen activated protein kinase

MTT - 3-(4,5-dimethylthiazol-2-yl)-2,5-diphenyltetrazolium bromide

NAC - N-acetylcysteine

NADH - nicotinamide adenine dinucleotide

NADPH - nicotinamide adenine dinucleotide phosphate

NaSAL - sodium salicylate

NF-κB - nuclear factor-kappa B

PBS - phosphate buffered saline

PCR - polymerase chain reaction

PEG - polyethylene glycol

PI - propidium iodide

PQ - paraquat

PS - phosphatidylserine

qPCR - quantitative polymerase chain reaction

RNA - ribonucleic acid

ROS - reactive oxygen species

rRNA - ribosomal ribonucleic acid

SEM - standard error of mean

SOD - superoxide dismutase

TNF-α - tumor necrosis factor α

TRAIL - TNF-related apoptosis-inducing ligand

TUNEL - terminal deoxynucleotidyl transferase mediated dUTP nick-end labelling

UPLC - ultra-performance liquid chromatography

Abstract

Paraquat (PQ), one of the most commonly used herbicides worldwide, is highly toxic to humans and exposure can result in severe clinical situations with no effective treatments available. The toxicity of PQ has been attributed to its ability to continuously produce reactive oxygen species (ROS) via redox cycling. Oxidants have been shown to induce the expression of several early response genes and to activate transcription factors, which may contribute to the inflammatory response associated with PQ injury. In order to further elucidate the mechanism(s) of PQ injury, we investigated its effects on the cellular status and gene expression profile of immortalized human alveolar epithelial A549 cells *in vitro*. Incubation of cells with PQ resulted in time- and concentration-dependent increases in intracellular PQ levels, which correlated with increases in intracellular ROS levels, and decreases in intracellular glutathione (GSH) content, mitochondrial membrane potential, and cell viability. Messenger RNA analysis revealed differential gene expression in response to PQ exposure, particularly increases in the expression of pro-inflammatory genes (i.e. IL1A, IL6, IL18), which correlated with increases in the secretion of pro-inflammatory cytokines (i.e. IL-8, IL-6). Recognizing that ROS play a major role in PQ-induced cytotoxicity, modulating the levels of antioxidants may serve as a potential treatment strategy. Since the delivery of many natural antioxidants exhibit poor bioavailability and cannot easily cross biological barriers, we investigated the *in vitro* effects of the thiol-containing antioxidant N-acetylcysteine (NAC) delivered to A549 cells either in its free or liposome-encapsulated form (L-NAC). Pre-treatment of cells with NAC or L-NAC protected against PQ-induced cytotoxicity (i.e. decreased ROS levels and LDH leakage; increased GSH content, cellular antioxidant potential, and cell viability), and messenger RNA analysis revealed

modulation of gene expression, particularly inflammatory mediators (i.e. IL8, IL10, IL18), which correlated with modulation of inflammatory cytokine secretion (i.e. IL-8). These cytoprotective effects were more evident in cells pre-treated with L-NAC, which is attributable to the increased levels of intracellular NAC achieved via liposomal delivery. These data provide evidence for further studies investigating the protective effects of L-NAC in PQ- and other oxidant-mediated lung injuries *in vivo*.

Preface

Paraquat (PQ) is an agent that, when introduced into humans and animals, enters the blood and is accumulated in the alveolar type I and II epithelial cells and Clara cells of the lung (Suntres 2002). Due to the chemical nature of PQ (it does not directly interact with cellular processes, it primarily acts to produce ROS through a process of redox cycling, and it is specifically accumulated in the lung), this agent is used as a model to simulate oxidant-induced lung injuries (Bus and Gibson 2008). The inflammatory response induced by PQ also contributes to oxidant-induced lung injuries and is similar to that seen following challenge of lungs to a variety of other toxins and certain oxidative stress-mediated pulmonary diseases, including acute lung injury and acute respiratory distress syndrome (ARDS) (Bus and Gibson 1984). Recognizing that PQ mediates its toxic effects primarily via the generation of ROS, it may follow that an increase in cellular thiol content via pre-treatment with N-acetylcysteine (NAC) or liposomal-NAC (L-NAC; liposomes have been used to enhance the delivery of drugs (Stone and Smith 2004)) will protect against its associated cytotoxicity. Accordingly, the objectives of this study are to: (i) characterize the uptake and cytotoxic effects of PQ in alveolar type II-like A549 cells; (ii) characterize the uptake of NAC and L-NAC in A549 cells; (iii) examine the effectiveness of NAC and L-NAC against PQ-induced cytotoxicity and delineate the mechanism(s) by which these antioxidant formulations confer their cytoprotection; and (iv) assess whether L-NAC confers a greater cytoprotective effect against PQ-induced cytotoxicity than NAC. The results of this *in vitro* study will help to delineate the mechanism(s) of PQ-induced cytotoxicity, provide insights into the mechanism(s) of possible NAC cytoprotection, and may also provide evidence

for future studies regarding the therapeutic use of NAC or L-NAC in animal models of oxidative stress-related pulmonary injury.

CHAPTER I

Introduction

1.1 - Paraquat

1.1.1 - History

Paraquat (1,1′-dimethyl-4,4′-bipyridinium chloride; PQ) is a fast-acting, non-selective broadleaf weed herbicide that acts on contact and is now frequently used in over 120 countries worldwide (Roberts *et al.* 2002). First synthesized in 1882 by Weidel and Rosso by the reaction of 4,4‟-bipyridine with methyl iodide (Bromilow 2004), PQ was later used as an oxidation-reduction indicator (methyl viologen) in 1932 when it was found to undergo a single electron reduction to a blue-coloured free radical mono-cation, with a redox potential of -0.446 V (Bromilow 2004); a second reduction to the fully reduced and colourless 1,1′-dimethyl-4,4′-dihydrobipyridyl has a redox potential of -0.88 V. Its herbicidal properties were later discovered in 1955 at Jealott‟s Hill International Research Centre, Bracknell, UK (Bromilow 2004), and PQ was introduced into the market as a herbicide in 1962 by the Plant Protection Division Ltd of Imperial Chemical Industries (ICI; now Syngenta) (Dinis-Oliveira *et al.* 2008). Paraquat is now sold under many trade names in concentrated formulations (10 - 30 % active PQ ion) that contain PQ alone (i.e. Gramoxone®), PQ and diquat, or PQ and urea herbicides as the active ingredients.

1.1.2 - Use as herbicide

PQ is a desiccant and defoliant able to strongly adsorb to organic matter, and quickly induces its toxicity on contact via its rapid penetration through the leaf surface. Leaves turn visibly brown within a few hours due to scorching under strong light conditions in the presence of oxygen, with complete desiccation occurring within a few days (Bromilow 2004). Though readily translocated in the xylem, PQ is poorly translocated in the phloem and is thus not effective at controlling perennial plants (Preston *et al.* 2005). However, unlike many other herbicides that rely on translocation within the plant for their activity, the mechanisms employed by PQ do not require the plant to be in an active stage of growth. Thus, PQ can be applied in the dry season or winter months provided there is leaf present.

1.1.3 - Interaction with soil

The use of PQ is not considered to have a significant environmental impact for various reasons: in addition to reducing soil erosion, it does not present the risk of leaching to groundwater (Roberts *et al.* 2002); it becomes inactive and biologically unavailable when bound to soil particles (Roberts *et al.* 2002); and there is a reduced loss of soil organic carbon into the atmosphere. The PQ di-cation sorbs strongly to the negatively-charged soil clay particles, having a sorption coefficient (K_d) of over 1000 L/kg, which is notably high since leaching is considered insignificant for compounds having $K_d > 10$ L/kg (Bromilow 2004). Due to its

inactivity in soils, the herbicide may be applied in a variety of situations, including pre-emergence or pre-plant, without risk of phytotoxicity (Bromilow 2004).

1.1.4 - Environmental degradation

PQ can be degraded into less toxic derivatives in the environment, predominantly by ultraviolet radiation originating from the sun (particularly between 290 – 310 nm wavelengths) (Slade 1966), but also by naturally occurring soil microorganisms (Roberts *et al.* 2002, Bromilow 2004, Amondham *et al.* 2006). The main intermediates of photochemical and microbial degradation of PQ are of relatively low toxicity and will decompose easily as they do not strongly sorb to soil particles, freeing them for further microbial degradation (Bromilow 2004). PQ has not been shown to be metabolized by plants themselves, as any degradation of PQ in the plant has been attributed to photochemical means (Slade 1966). The degradation of PQ in the environment does not occur at appreciable rates, indicating that in agricultural practices its degradation in soil is negligible. However, the natural deactivation capacity of soil is several times the recommended application rate, suggesting this is not an issue.

1.1.5 - Mechanisms of plant toxicity

Upon its rapid absorption into the plant, PQ exerts its toxic effects almost immediately by interfering with photosynthesis. The PQ cation diverts electrons from the iron-sulfur centers of

photosystem I in chloroplasts (Bromilow 2004), thereby replacing ferredoxin as an artificial final electron acceptor and consequently inhibiting the formation of NADPH. The newly formed PQ radical is then rapidly reoxidized by molecular oxygen produced in chloroplasts, forming the superoxide radical and regenerating the PQ cation, which is free to divert more electrons from photosystem I (Bromilow 2004). This PQ redox cycling in plants forms copious amounts of superoxide anion, which can generate hydroxyl radicals either directly or via a hydrogen peroxide intermediate and damage cellular lipids, proteins, and nucleic acids (Bromilow 2004). Consequently PQ is most effective during the day while photosynthesis is occurring, as opposed to overnight when there is a relative lack of reducing equivalents for the redox cycling of PQ.

PQ can be applied safely if used according to the manufacturer‟s instructions, and essentially has no environmental impact as it is strongly adsorbed to soil particles and is degraded by soil microorganisms and ultraviolet light. Nevertheless, due to the extensive herbicidal use of PQ, many cases of human PQ intoxication have followed and there remain no effective treatments.

1.2 - Cellular Redox Balance

1.2.1 - Reactive oxygen species

Reactive oxygen species (ROS) are small molecules capable of oxidation, and include oxygen ions, free radicals (highly reactive molecules possessing unpaired valence shell electrons), peroxides, and derivatives of oxygen that do not contain unpaired electrons (i.e. hydrogen

peroxide) (Ciencewicki *et al.* 2008, Rahman *et al.* 2006). Although they play a role in important cellular processes, such as initiating certain signal transduction pathways (Bilska and Wlodek 2005), ROS are capable of causing deleterious effects such as damage to cellular organelles, proteins, lipids, and nucleic acids, and play a role in many diseases (Aitio 2006).

Cells are constantly exposed to ROS, which can be formed endogenously via the reduction of molecular oxygen to water following mitochondrial electron transport during cellular respiration, by cellular enzymes such as cyclooxygenases, lipoxygenases, peroxidases, cytochrome P450 oxidase and xanthine oxidase, and can be released by inflammatory cells (i.e. phagocytes such as neutrophils and macrophages) (Ciencewicki *et al.* 2008, Rahman *et al.* 2006, Mak 2008, Gram 1997). The primary ROS formed *in vivo* are superoxide anion and hydrogen peroxide (H_2O_2). Superoxide is formed via the reduction of molecular oxygen, while H_2O_2 is formed through non-enzymatic or enzymatic dismutation of superoxide (Rahman *et al.* 2006, Mak 2008). The most reactive and harmful ROS is the hydroxyl radical which can be formed via both the Fenton and Haber-Weiss reactions (Mak 2008), but also from the reaction of superoxide with nitric oxide to produce reactive molecule peroxynitrite, which decomposes to form nitrogen dioxide and the hydroxyl radical (Ciencewicki *et al.* 2008, Rahman *et al.* 2006, Gram 1997). Other examples of ROS include the peroxyl radical and singlet oxygen (Rahman *et al.* 2006), and exogenous sources derive from, among other things, ozone, cigarette smoke, and other air pollutants.

1.2.2 - Antioxidants

The cell is normally equipped with a variety of antioxidant defences which limit the extent of oxidation taking place and maintain a redox balance *in vivo*. There are two recognized classes of antioxidants: enzymatic and non-enzymatic. Enzymatic antioxidants include catalase, superoxide dismutase (SOD), glutathione reductase (G_{red}), glutathione peroxidise (GPx), and thioredoxins, which degrade ROS to less toxic molecules (Rahman *et al.* 2006, Mak 2008). Non-enzymatic antioxidants include ascorbic acid, α-tocopherol, β-carotene, melatonin, and low-molecular weight thiol-containing compounds (i.e. the reduced form of glutathione, metallothionein, and others) (Rahman *et al.* 2006, Mak 2008). These antioxidants can directly interact with ROS to control their levels, and are regulated by feedback mechanisms such that balanced levels of both antioxidants and ROS are maintained in the cell (Rahman *et al.* 2006, Mak 2008).

Glutathione is one of the most important cellular antioxidants. In its reduced (GSH) form, glutathione is able to scavenge free radicals non-enzymatically via its free thiol group and enzymatically via GPx and GSH S-transferase (GST), which protect against H_2O_2 and toxic compounds, respectively (Arakawa and Ito 2007, Kelly 1998). The oxidized dimer (GSSG) of glutathione, can be reduced to GSH by G_{red}, a NADPH/$NADP^+$ - dependent enzyme, to restore the redox potential (Arakawa and Ito 2007). However, this activity will be inhibited by a reduced NADPH/$NADP^+$ redox level, whereupon GSSG is exported from the cell to restore GSH redox state (van de Poll *et al.* 2006). This will reduce the GSH pool, so that the cellular reductive potential becomes dependent on glutathione *de novo* synthesis (van de Poll *et al.*

2006). Glutathione is synthesized from the amino acids glutamate, glycine, and cysteine, and is an almost exclusively intracellular process that occurs in the cytoplasm (van de Poll *et al.* 2006). Depletion of any of these amino acids may lead to changes in GSH metabolism, though cysteine is most frequently the rate-limiting constituent due to its small pool size (van de Poll *et al.* 2006).

1.2.3 - Oxidative stress

When cellular redox balance is compromised and an oxidizing environment prevails, the cell is considered to be in a state of oxidative stress. In this type of environment, ROS can cause extensive cellular damage. For instance, ROS can react with base pairs and the deoxyribose phosphate backbone of DNA, the main target of radical damage, resulting in damage and scission of strands (Gram 1997). Reactive oxygen species can also initiate the lipid peroxidation of polyunsaturated fatty acids, affecting phospholipids that constitute biological membranes (Rahman *et al.* 2006). The hydroxyl radical can abstract a hydrogen atom from polyunsaturated fatty acids to form a conjugated diene radical, resulting in the formation of epoxides, peroxides, and lipid peroxyradicals (Gram 1997, Shek *et al.* 1994). Subsequently, this newly formed radical may abstract a hydrogen atom from another polyunsaturated fatty acid, resulting in a potentially cytotoxic chain reaction (Gram 1997). In addition, lipid peroxidation products such as lipid radicals or aldehydes may cause DNA strand breaks, DNA adducts, and DNA-protein cross-links (Gram 1997). ROS may also damage amino acids and proteins resulting in denaturation and inhibition of enzymatic activity (Rahman *et al.* 2006, Gram 1997). If unmanaged, oxidative stress can lead to the death of the cell (Gram 1997).

1.3 - Oxidant-related Pulmonary Injuries

1.3.1 - Lung architecture and function

The lung is a heterogeneous organ composed of more than 40 different cell types (Shek *et al.* 1994). Two of these cell types, alveolar epithelial type I and II cells, are the main constituents of the alveolar epithelium. Type I cells, which comprise 33 % of total alveolar epithelial cells and cover 93 % of the alveolar surface area, are responsible for gas exchange in the lung between the air space and capillaries (Dinis-Oliveira *et al.* 2008). In contrast, alveolar type II cells comprise 67 % of total epithelial cells in the lung, yet merely cover 7 % of the alveolar surface area (Dinis-Oliveira *et al.* 2008). These precursors of type I cells function in active transport of water and ions, and are responsible for the secretion of surfactant in the lung (Dinis-Oliveira *et al.* 2008). Surfactant, which is mainly composed of phospholipids, is responsible for preventing lung collapse upon exhalation and is able to protect the lung from exposure to the wide array of environmental toxins (Shek *et al.* 1994).

1.3.2 - Oxidative stress in the lung

The lung is particularly vulnerable to oxidant-mediated damage as it is constantly and directly exposed to ambient air containing ozone, nitrogen dioxide, diesel exhaust, cigarette smoke, and other airborne oxidant gases and particulates, all of which can cause damage via ROS (Ciencewicki *et al.* 2008, Rahman *et al.* 2006). It is also vulnerable to injury induced by

bacterial infections and foreign toxic compounds, among other things. The most prominent cell types affected by various toxicants are the capillary endothelial cells, Clara cells, and both type I and type II alveolar epithelial cells (Shek *et al.* 1994). Reactive oxygen species have been implicated in the pathogenesis of many diseases (i.e. acute lung injury, acute respiratory distress syndrome, etc.) through a variety of mechanisms. Physiologically, ROS can cause the remodelling of extracellular matrix and blood vessels, and stimulate mucous secretion and alveolar repair processes. At the biochemical level, ROS can inactivate antiproteases, induce apoptosis, regulate cell proliferation, and modulate the immune system in the lungs. Finally at the molecular level, ROS have been implicated in initiating inflammatory processes in the lung through the activation of nuclear factor-κB (NF-κB) and activator protein-1, various signal transduction pathways, chromatin remodelling, and gene expression of pro-inflammatory mediators (Rahman *et al.* 2006).

Acute lung injury and its more severe form, ARDS, are syndromes of acute pulmonary inflammation characterized by sudden reduction in gas exchange, static compliance, and non-hydrostatic pulmonary edema (Ciencewicki *et al.* 2008). These inflammatory disorders of the lung are commonly caused by pneumonia, sepsis, trauma and/or aspiration (Chopra *et al.* 2009). Oxidative stress has been suggested to be involved in the pathogenesis of ARDS, and ROS are believed to play an important role in pulmonary vascular endothelial damage, which is hypothesized to be responsible for the clinical manifestations of ARDS (Ciencewicki *et al.* 2008). The inflammatory response results in large numbers of neutrophils and macrophages migrating to the lungs, which contribute to a state of oxidative stress (Ciencewicki *et al.* 2008, Chopra *et al.* 2009). One potential approach to alleviating such injuries is to target the increased

oxidative stress in the lung, which may regulate major cellular events such as gene expression and cellular signalling pathways leading to inflammation (Sadowska *et al.* 2007). This may be achieved via the restoration of cellular antioxidant defences, or through anti-inflammatory agents by attenuating the activity of inflammatory cells and their production of ROS.

1.4 - PQ Toxicity in Humans

Human exposure to PQ can cause severe clinical situations. The most common cause of PQ-induced mortality is through ingestion of the concentrated formula, which is commonly between 10 - 30 % PQ ion (Bateman 2008). Improper storage of the concentrated PQ formulation in various containers, often cola bottles and coffee mugs, resulted in death due to mistaken ingestion attributable to its dark colour. To circumvent this and to reduce the amount of PQ absorbed in the gut, current PQ formulations contain a stenching agent as well as an emetic (Bateman 2008). PQ exposure has also been implicated as an etiological factor of Parkinson‟s disease (i.e. as a result of chronic, non-pneumotoxic levels since PQ is able to cross the blood-brain barrier) (Dinis-Oliveira *et al.* 2006a, Bove *et al.* 2005) and is associated with an increased risk of certain cancers, particularly of the skin (Spiewak 2001).

1.4.1 - Human exposure to PQ

Most poisonings due to PQ result from ingestion of the compound, but can also occur through inhalation, skin absorption, injection, and ocular exposure. Ingestion of PQ can cause

gastrointestinal irritation and death through general organ failure (high dose) or respiratory dysfunction (lower dose) (Bus and Gibson 1984, Clark *et al.* 1966, Eddleston *et al.* 2003). Inhalation of PQ does not usually result in severe clinical cases, particularly in open spaces, due to its low vapour pressure and its tendency to form large droplets (median diameter is 100μm) which has difficulty reaching the alveoli of humans, but cases have been reported of inhalation in enclosed spaces causing toxicity (Chester and Ward 1984). Intact human skin has a low permeability to PQ (permeability coefficient of 0.73) since PQ is very hydrophilic (Walker *et al.* 1983). One study had six volunteers percutaneously exposed to PQ and found that only minute quantities (0.23 - 0.29 % of dose) had been absorbed over a 24-hour period, depending on the site tested (Wester *et al.* 1984). However, extensive skin contaminations have been reported (Soloukides *et al.* 2007). Cases of lethal injection have also been reported, with the minimum lethal dose via intraperitoneal (i.p.), subcutaneous, intravenous, or intramuscular injection being considerably less than that from ingestion (Choi *et al.* 2008). Finally, contact with the eyes can cause retinal damage, but does not usually lead to systemic toxicity (Cant and Lewis 1968).

1.4.2 - PQ toxicokinetics

Following ingestion, PQ is rapidly distributed in most tissues with the highest concentrations found in the kidney and lung (Bus and Gibson 1984, Clark *et al.* 1966, Smith 1985, Smith and Heath 1975) . PQ is eliminated from the body largely unchanged through the kidneys into the urine, and over 90% of the initial dose is excreted unchanged within 12 to 24 hours of ingestion, assuming renal function is not compromised (Bus and Gibson 1984, Clark *et al.* 1966, Smith

1985, Smith and Heath 1975). However, PQ is preferentially taken up in the lung, and results in pulmonary toxicity (Suntres 2002).

1.4.3 - PQ lung injury

Systemic PQ accumulates to lethal concentrations in the lung over time, and as a result is the primary site of chronic PQ injury. PQ is actively uptaken by alveolar type I and II epithelial cells and Clara cells against a concentration gradient, a process attributed to the chemical structure of PQ as it is mistakenly recognized as a substrate for the polyamine uptake system in these cells (Smith *et al.* 1990, Hoet and Nemery 2000). Once inside the cell, the PQ cation is reduced by cellular diaphorases, including NADPH-cytochrome P450 reductase, NADH:ubiquinone oxidoreductase (complex I), xanthine oxidase, and nitric oxide synthase, to form $PQ^{\cdot+}$ (Ciencewicki *et al.* 2008, Gram 1997, Day and Crapo 1996, Bus *et al.* 1976). This radical is quickly oxidized by molecular oxygen to form the superoxide anion and re-generate the PQ cation, with a very fast reaction rate of 7.7×10^{8} $M^{-1}s^{-1}$ (Dinis-Oliveira *et al.* 2008). The redox potential of PQ ($PQ^{2+}/PQ^{\cdot+}$) is very high (E'_0 = -0.45 V), while that of O_2 ($O_2/O_2^{\cdot-}$) is lower (E'_0 = -0.16 V), thus facilitating electron flow from the reduced PQ to O_2 (Farrington *et al.* 1973). Therefore, as long as reducing equivalents for PQ are present, the cation will continuously be reduced and then re-oxidized in a process termed "redox cycling," which will result in the continuous generation of superoxide anion, leading to other toxic ROS. Other toxic outcomes of PQ redox cycling include: the depletion of NADPH, the primary source of reducing equivalents for the intracellular reduction of PQ, which will affect NADPH-requiring

biochemical processes, and lipid peroxidation of polyunsaturated fatty acids (Gram 1997, Bus and Gibson 1984, Freeman *et al.* 1985).

The continuous formation of superoxide generates an imbalance in the oxidant/antioxidant ratio, leading to the generation of other ROS, mainly hydrogen peroxide and hydroxyl radical, and a state of oxidative stress. Hydrogen peroxide is formed by the dismutation of superoxide anion, as well as by the reduction of superoxide anion to O_2^{-2} by the PQ radical, which exists as H_2O_2 in aqueous solution at physiologic pH (Gram 1997, Quinlan *et al.* 1994). The hydroxyl radical can be formed by the Haber-Weiss reaction, which can be catalyzed by traces of transition metal ions or metal chelates (i.e. the Fenton reaction) (Gram 1997).

NADPH is an essential co-factor for the maintenance of normal biochemical and physiological functions. It is a cofactor of glutathione reductase in the generation of GSH from GSSG, and the lack of NADPH may also interfere with the synthesis of proteins and lipids (Bus *et al.* 1976, Quinlan *et al.* 1994). The pentose phosphate pathway, the main source of cellular NADPH generation, is upregulated during PQ injury (the rate-limiting enzyme is glucose-6-phosphate dehydrogenase), which directly correlates with the degree of inhibition of fatty-acid synthesis (Dinis-Oliveira *et al.* 2008). Ironically, this attempt by the cell to restore NADPH levels may simply exacerbate PQ-induced cytotoxicity as more reducing equivalents will be available for PQ redox cycling. Lipid peroxidation, the final consequence of PQ redox cycling, is an irreversible reaction that occurs when polyunsaturated fatty acids react with ROS in the presence of transition metals, and is one of the most important causes of cell membrane damage (Gram 1997, Bus *et al.* 1976).

1.4.4 - Lung pathophysiology

Two stages are associated with the lung injury induced by PQ in humans: initially there is a destructive phase in which the alveolar epithelium is destroyed and inflammatory cells infiltrate the lung, followed by a proliferative phase where fibroblasts lay down collagen leading to pulmonary fibrosis, with injury occurring due to limited gas exchange (Ciencewicki *et al.* 2008, Rahman *et al.* 2006, Bus and Gibson 1984, Smith 1985, Smith and Heath 1975). The destructive phase is characterized by early damage to the alveolar epithelium, particularly type I and II cells (Bus and Gibson 1984, Smith and Heath 1975). In type I cells, swelling is observed followed by vacuolation and disruption of organelles, increased numbers and swelling of mitochondria, and the appearance of dark granules in the cytoplasm (Bus and Gibson 1984, Smith and Heath 1975). Over time they show hydropic degeneration in the form of numerous large vacuolated swellings projecting into the alveolus (Smith and Heath 1975). Type II cells have also been observed to form ultrastructural lesions, but these are generally not apparent until after the first lesions are seen in type I cells (Smith 1985, Smith and Heath 1975, Smith and Heath 1976). Type II cells undergo swelling of their mitochondria, vacuolation of lamellar bodies, and disruption of endoplasmic reticulum (Bus and Gibson 1984, Smith and Heath 1975). Within days, as PQ continues to accumulate in these cells, ROS accumulate to toxic levels and play a major role in the destruction of the alveolar epithelium (Bus and Gibson 1984).

The proliferation of type II cells is thought to be a non-specific reaction to alveolar epithelial damage, but may only occur when epithelial cell damage is moderate (Fukuda *et al.* 1985). When the damage is severe, it is thought that type II cells die and are replaced with epithelial

cells of bronchiolar origin (Fukuda *et al.* 1985). However, due to the targeted destruction of type II cells in addition to type I cells by PQ, no precursors are available to replace the destroyed type I cells and, thus, the basement membrane may become completely denuded (Bus and Gibson 1984).

Alveolar pulmonary oedema, capillary congestion, hyaline membranes, and an acute inflammatory exudate may induce dyspnoea in man, but are rarely directly fatal (Smith and Heath 1975). The reason for the liberation of the oedema fluid into the alveolar spaces is somewhat unclear, since PQ does not damage the pulmonary capillaries (Smith and Heath 1975). It may be due to increased vascular permeability, or perhaps the loss of pulmonary surfactant that is normally generated by type II cells (Smith and Heath 1975). This may then withdraw fluid from the alveolar capillaries to produce oedema. It has also been suggested that the loss of surfactant leads to the formation of hyaline membranes (Smith and Heath 1975). This phase of destruction produces many inflammatory mediators, which attract inflammatory cells (i.e. mainly polymorphonuclear leukocytes, including neutrophils and eosinophils) to the site of injury (Bus and Gibson 1984, Smith 1985, Smith and Heath 1975).

The inflammatory response which is initiated in the destructive phase is maintained through the proliferative phase. This phase is morphologically characterized by the infiltration and proliferation of profibroblasts into the alveolar spaces, their differentiation into fibroblasts, and the development of fibrosis (Bus and Gibson 1984). This intra-alveolar migration of connective tissue cells through gaps in the epithelial basement membrane is one of the most important events responsible for the development of intra-alveolar fibrosis (Fukuda *et al.* 1985). The

release of factors including fibronectin, a chemoattractant and growth factor for fibroblasts, from macrophages in the alveolitis may be responsible for the recruitment and migration of these cells (Fukuda *et al.* 1985). These fibroblasts produce extensive amounts of collagen that contribute to pulmonary fibrosis. Histologically, following the proliferative phase there is a dense mass of fibroblastic tissue with nearly complete obliteration of normal lung architecture (Smith and Heath 1975).

If the injury is mild and only small gaps are present in the epithelial lining covering the basement membrane, regenerating epithelial cells will re-establish the epithelial lining (Smith and Heath 1975). If this is the case, intra-alveolar fibrosis will not develop. Denuded basement membranes are thought to act as scaffolding for epithelial cell regeneration (Fukuda *et al.* 1985). If the alveolar injury is severe and the gaps in the epithelial lining are large, the regenerating epithelial cells may grow over a layer of fibrinous exudate deposited on the surface of the epithelial basement membrane and thus will not establish contact with the existing basement membrane (Fukuda *et al.* 1985). This may lead to a duplication of the basement membrane, with the original basement membrane appearing convoluted, perhaps contributing to the loss of normal alveolar architecture seen in such injuries (Fukuda *et al.* 1985).

These processes are presumed to be a reparative mechanism for alveolitis, but ultimately will result in the obliteration of normal alveolar architecture, limited gas exchange, and may lead to death via anoxia (Gram 1997, Bus and Gibson 1984). The destruction of the alveolar epithelium during the destructive phase allows proteolytic enzymes secreted from inflammatory cells to degrade the exposed basement membrane (Eddleston *et al.* 2003, Smith and Heath 1975).

It seems that the formation of a fluid exudate during the destructive phase is not necessary for the initiation of the proliferative phase. It was found that PQ caused extensive necrosis of alveolar cells but not of mesenchymal structures, and that alveolar and peritoneal macrophages were more readily killed by PQ than fibroblasts (Dinis-Oliveira *et al.* 2008). In addition, it appears that the presence of macrophages results in a more rapid proliferation of fibroblasts, suggesting PQ may actively stimulate the proliferation of fibroblasts using macrophages as an intermediate.

1.4.5 - Clinical treatments

The clinical treatment strategies for PQ poisoning generally focus on removing PQ from the gastrointestinal tract to limit its absorption (i.e. using activated charcoal and Fuller‟s earth, due to its strong adsorption to these compounds), increasing its elimination from the body (i.e. forced diuresis, gastric lavage) and its excretion from the blood (i.e. hemoperfusion), and limiting pulmonary damage with anti-inflammatory agents (Eddleston *et al.* 2003, Choi *et al.* 2008, Ruiz-Bailen *et al.* 2001, Drault *et al.* 1999, Lopez Lago *et al.* 2002, Lheureux *et al.* 1995). These strategies have had limited success.

Objective

Characterize the uptake and cytotoxic effects of PQ in A549 cells. The uptake of PQ in A549 cells will be assessed via ultra-performance liquid chromatographic analysis of a concentration- and time-course of PQ exposure. The cytotoxicity of PQ in A549 cells will be assessed via the MTT viability assay and by assessing intracellular GSH content, ROS levels, mitochondrial membrane potential, apoptosis, cellular gene expression, and inflammatory cytokine release.

Methods

1.1 - Cell culture

Human alveolar type II-like epithelial A549 cells (American Type Culture Collection # CCL-185; ampule passage no. 80; ATCC, Manassas, VA, USA) were maintained in Costar 0.2 µm vent cap cell culture flasks (Corning, Corning, NY, USA) with standard Dulbecco‟s modified Eagle‟s medium nutrient mixture F-12 Ham (Sigma-Aldrich, Oakville, ON, Canada) supplemented with 10 % iron-fortified bovine calf serum (SAFC Biosciences, Lenexa, KS, USA), 2 mM L-glutamine (Gibco, Carlsbad, CA), and antibiotic/antimycotic (100 U/mL penicillin, 100 µg/mL streptomycin, and 0.25 µg/mL amphotericin B; Gibco). Cultures were incubated at 37 ºC in a humidified atmosphere of 5 % CO_2 in air until 80 % confluence. Cell counts and viabilities were assessed using a Vi-Cell XR Cell Viability Analyzer (Beckman Coulter, Mississauga, ON, Canada).

1.2 - Paraquat (PQ) preparation

PQ (Paraquat dichloride x-hydrate, Sigma-Aldrich) was dissolved in ddH_2O to produce a 100 mM stock solution, and was added to serum-free culture media to form specific treatment concentrations. PQ stock solutions were stored at 4 °C in the absence of light.

1.3 - Viability (MTT)

The MTT (3-(4,5-dimethylthiazol-2-yl)-2,5-diphenyltetrazolium bromide) assay is used as a quantitative index of cell viability in which the mitochondrial and cytosolic dehydrogenases of living cells reduce the yellow tetrazolium salt to produce a purple formazan dye that can be measured spectrophotometrically (Volobоueva *et al.* 2005). A549 cells were seeded into sterile flat-bottom 96-well plates (Corning) at a concentration of 10,000 cells/well and incubated overnight. Cells were challenged with 150 μL of control or PQ-containing media (various concentrations and times; serum-free). Following challenge, culture media was replaced with control media containing 10 % yellow MTT (Thiazolyl Blue Tetrazolium Bromide; Sigma-Aldrich, St. Louis, MO, USA) reagent and cells were incubated at 37 °C for an additional 4 hours, during which the MTT was converted to purple formazan crystals in living cells. Following this, the incubation media was aspirated and 50 μL dimethylsulfoxide per well was added to solubilise the formazan crystals. Following agitation, absorbance was measured spectrophotometrically at a wavelength of 570 nm (650 nm correction wavelength) using a PowerWave XS Microplate Spectrophotometer (BioTek, Winooski, VT, USA). Viability of treated wells were assessed relative to control wells, which were taken to have 100 % viability.

1.4 - Ultra-performance liquid chromatography

Liquid chromatography was performed on an Acquity Ultra-Performance Liquid Chromatograph (UPLC) composed of an Acquity Binary Solvent Manager, Sample Manager, and Photodiode

Array (PDA) Detector (Waters, Milford, MA, USA). Conditions for the optimization of PQ and GSH detection using UPLC were based on high-performance liquid chromatography methodology outlined by Raggi et al. (Raggi *et al.* 1998). Briefly, cells were grown in sterile 150 cm^2 culture flasks (Corning) to 80 % confluence, then challenged with control or PQ-containing media (serum-free) for a pre-determined amount of time. Following challenge, cells were harvested via trypsinization, washed twice with PBS, and stored at -80 ºC overnight via liquid nitrogen snap-freezing. Frozen samples were thawed and lysed via sonication (20 s, 100 % amplitude; Sonic Dismembrator Model 500, Fisher Scientific, Pittsburgh, PA, USA). Lysates were centrifuged at 16,000 × g and 4 ºC for 5 min (Eppendorf Centrifuge 5415 R), and injected onto an Acquity UPLC HSS T3 analytical column (2.1 mm I.D. x 150 mm length, 1.8 µm particle size; Waters) with a Vanguard pre-column (2.1 mm I.D. x 5 mm length; Waters), at 30 ºC. The mobile phase consisted of 23 mM ammonium formate (pH 3.0) at a flow rate of 0.250 mL/min. PQ and GSH concentrations were measured at 257.7 and 202.1 nm, respectively, using Empower 2 software.

1.5 - Total protein assay

Total protein of treated samples was assessed using the Micro Lowry Total Protein Kit – Peterson‟s Modification (Sigma-Aldrich), in accordance with the manufacturer‟s instructions. Cell lysates were thawed and 10 µL aliquots were diluted to 1.0 mL with 0.1 M NaCl (used to eliminate ampholyte interference). 100 µL of deoxycholate solution was added and left to stand at room temperature for 10 minutes after mixing, followed by the addition of 100 µL of

trichloroacetic acid (72% w/v) to precipitate the protein. After centrifugation for 5 minutes at 500 × g, supernatants were decanted and pellets were dissolved in 1.0 mL Lowry‟s reagent solution. This was transferred to a 24-well plate and allowed to stand at room temperature for 20 minutes. Following this, 500 µL of Folin & Ciocalteu‟s phenol reagent working solution was added while mixing the sample, and colour was allowed to develop for 30 minutes at room temperature. Absorbance was measured spectrophotometrically at 570 nm using a PowerWave XS Microplate Spectrophotometer (BioTek), and converted to protein concentration using a standard curve of known values.

1.6 - Reactive oxygen species levels

CM-H_2DCFDA (5-(and-6)-chloromethyl-2′,7′-dichlorodihydrofluorescein diacetate, acetyl ester) is used as a cell-permeant indicator of ROS. This molecule remains nonfluorescent until the acetate groups are removed by intracellular esterases and oxidation occurs within the cell. In addition, esterase cleavage of the lipophilic blocking groups yields a charged form of the dye that is much better retained by cells than the parent compound. This chloromethyl derivative of H_2DCFDA allows for covalent binding to intracellular components, permitting even longer retention within the cell. Cells seeded into sterile flat-bottom 6-well plates (Corning) at 0.5×10^6 cells/well and grown overnight to 80 % confluence were challenged with control or PQ-containing (0.25 mM or 1.0 mM) serum-free media for 1, 4, or 8 h. Following challenge, cells were washed with PBS and stained for 30 minutes with CM-H_2DCFDA (Molecular Probes, Eugene, OR, USA) under standard incubation conditions. Stained cells were washed with PBS

and detached from the plate surface using Fisherbrand disposable sterile cell scrapers (Fisher Scientific) and suspended in PBS for flow cytometric analysis using the FL1-H channel of a BD FACSCalibur Flow Cytometer (BD Biosciences, San Jose, CA) with BD CellQuest Pro Software. A minimum of 10,000 gated events were acquired per trial. Fluorescence was directly proportional to levels of intracellular ROS.

1.7 - Hydrogen peroxide levels

Levels of hydrogen peroxide (H_2O_2) in treated cells were measured via electrochemical detection. Cells seeded into sterile flat-bottom 6-well plates (Corning) at 0.5×10^6 cells/well and grown to 80 % confluence overnight were challenged for 6 h with 2.0 mL of control or PQ-containing (0.1, 0.25, 0.5, 1.0 mM) media (serum-free). Immediately following challenge, incubation media was analyzed using the Apollo 4000 Free Radical Analyzer (World Precision Instruments, Sarasota, FL, USA) in the 10 nA range. Raw data was interpolated to H_2O_2 concentrations using a standard curve of known values.

1.8 - Mitochondrial membrane potential

Mitochondrial membrane potential was assessed using the MitoProbe JC-1 Assay Kit for Flow Cytometry (Molecular Probes). Cells seeded into sterile flat-bottom 6-well plates (Corning) at 0.5×10^6 cells/well and grown overnight to 80 % confluence were challenged with control or

PQ-containing (0.25 mM or 1.0 mM) serum-free media for 1, 4, or 8 h. Following challenge, cells were washed with PBS and stained for 30 minutes with JC-1 (5,5′,6,6′-tetrachloro-1,1′,3,3′-tetraethylbenzimidazolylcarbocyanine iodide), a cationic dye that exhibits potential-dependent accumulation in mitochondria, under standard incubation conditions. Stained cells were then detached from the plate surface using Fisherbrand disposable sterile cell scrapers (Fisher Scientific) and suspended in PBS for flow cytometric analysis using the FL1-H and FL2-H channels of a BD FACSCalibur Flow Cytometer (BD Biosciences) with BD CellQuest Pro Software. A minimum of 10,000 gated events were acquired per trial. Mitochondrial depolarization was indicated by decreased red fluorescence intensity due to concentration-dependent formation of red fluorescent J-aggregates.

1.9 - Annexin V

Phosphatidylserine (PS) translocation, an indicator of apoptosis, was assessed via flow cytometric analysis of control and treated cells dually stained with annexin V and propidium iodide (PI) using the Vybrant Apoptosis Assay Kit #2 – Alexa Fluor 488 annexin V / propidium iodide (Molecular Probes). In normal viable cells, PS is located on the cytoplasmic surface of the cell membrane, but becomes translocated from the inner to the outer leaflet in apoptotic cells. The human vascular anticoagulant annexin V is a 35 – 36 kD Ca^{2+}-dependent phospholipid-binding protein that possesses a high affinity for PS. Thus, annexin V labelled with a fluorophore can identify apoptotic cells by binding to PS on the outer leaflet. However, because annexin V conjugates are able to pass through the compromised membranes of dead cells and

bind to PS in the interior of the cell, propidium iodide, a cell-impermeant dead cell stain that binds to DNA, was used in combination with annexin V staining to distinguish necrotic from apoptotic cells.

Cells seeded into sterile 25 cm^2 culture flasks (Corning) at 1.25×10^6 cells and grown to 80 % confluence overnight were challenged with control or PQ-containing (0.25 mM or 1.0 mM) serum-free media for 1, 4, or 8 h. Following challenge, cells were washed with PBS and suspended via trypsinization in 100 µL annexin-binding buffer at 1×10^6 cells/mL. Cells were then incubated at room temperature with Alexa Fluor 488 annexin V (ANX) and PI stains in the absence of light. Following 15 minute incubation, dually-stained samples were diluted by adding 400 µL annexin-binding buffer and immediately analyzed flow cytometrically on a BD FACSCalibur Flow Cytometer (BD Biosciences) using the BD CellQuest Pro Software on the FL1-H (ANX) and FL3-H (PI) channels, acquiring a minimum of 10,000 gated events per trial. ANX^-/ PI^- cells were considered live, ANX^+/ PI^- cells apoptotic, and $ANX^{+/-}/ PI^+$ cells necrotic.

1.10 - Quantitative polymerase chain reaction (qPCR)

1.10.1 - RNA isolation

RNA isolation was performed using the RT^2 qPCR-Grade RNA Isolation Kit (SA Biosciences, Frederick, MD, USA) in accordance with the manufacturer"s instructions using certified RNase-free barrier tips (Ambion Applied Biosystems, Foster City, CA, USA). Cells seeded into sterile

25 cm^2 culture flasks (Corning) at 1.5×10^6 cells and incubated to 80 % confluence overnight were washed with PBS and treated with control or 0.25 mM PQ-containing media (serum-free) for 1, 4, or 8 h. Adherent cells were washed once with PBS and detached via trypsinization. Following centrifugation (500 × g for 5 min at 4 ˚C), cells were washed with PBS and lysed using the provided lysis and binding buffer, which contained chaotropic components that stabilized RNA and inhibited RNase activity. Lysates were placed in RNAse-free microfuge tubes (Ambion Applied Biosystems) and RNA was extracted using a silica membrane spin column. Upon loading of the RNA onto the column, genomic DNA was digested with an RNase-free DNase enzyme and, following washes to remove degraded genomic DNA, salts, and other cellular components, low ionic strength conditions eluted the pure RNA from the column. Aliquots were stored at -80 ˚C.

1.10.2 - Experion

The concentration and integrity of extracted RNA was assessed using the Experion RNA StdSens analysis kit (Bio-Rad) on an Experion Automated Electrophoresis Station (Bio-Rad), in accordance with the manufacturer‟s instructions. Briefly, 1 µL aliquots of denatured RNA samples and ladder were loaded onto a microfluidic chip containing channels that, once primed with a gel matrix, allowed for separation, staining, detection, and data analysis of the samples by measuring the 18 and 28 S rRNA peaks. Only high-quality RNA samples were used for subsequent gene expression analysis.

1.10.3 - First strand cDNA synthesis

First strand complementary DNA (cDNA) synthesis reactions were performed using an RT^2 First Strand Kit (SA Biosciences) in accordance with the manufacturer"s instructions. Briefly, to eliminate contaminating genomic DNA from samples prior to reverse transcription, 2.0 µg RNA was added to a DNA elimination buffer and incubated for 5 min at 42 ˚C using an MJ Mini Personal Thermal Cycler (Bio-Rad), and placed on ice for one minute. Following this, the solution was incubated at 42 ˚C for 15 min with random hexamers and oligo-dT to prime reverse transcription, and a reverse transcriptase to synthesize cDNA product. The reaction was terminated by heating to 95 ˚C for 5 min. This was placed on ice and diluted with 91 µL ddH_2O in preparation for real-time PCR.

1.10.4 - Real-time PCR

Quantitative real-time PCR analysis was performed using the Human Stress & Toxicity PathwayFinder RT^2 Profiler PCR Array (Table 1.1; SA Biosciences) on an iQ5 Multicolor Real-Time PCR Detection System (Bio-Rad) in accordance with the manufacturer"s instructions. Briefly, cDNA synthesized via reverse-transcription of extracted RNA was added to 2X RT^2 Real-Time SYBR Green/Fluorescein PCR Master Mix (SA Biosciences) and protected from light. Following gentle mixing, 25 µL was pipetted into each well of the array (containing pre-dispensed gene-specific primer sets), with wells sealed using optical thin-wall 8-cap strips, and bubbles removed following brief centrifugation. Real-time PCR was performed using a two-step

cycling program involving an initial single cycle of 95 ˚C for 10 min (required to activate the HotStart DNA polymerase), followed by 40 cycles of 95 ˚C for 15 s, then 60 ˚C for 1 min (SYBR Green fluorescence was recorded during the annealing step of each cycle). Following the qPCR reaction, a first derivative dissociation curve was performed as a quality control measure. Briefly, the reaction was heated to 95 ˚C for 1 min, cooled to 65 ˚C for 2 min, then ramped from 65 to 95 ˚C at a rate of 2 ˚C/min with optics on. The formation of a single peak at temperatures greater than 80 ˚C indicated the presence of a single PCR product in the reaction mixture.

1.11 - Bio-Plex

Bio-Plex cytokine assays are multiplex bead-based assays designed to quantitate multiple cytokines in diverse matrices, including cell culture supernatants. Cells were seeded into sterile 25 cm^2 culture flasks (Corning) at 1.35×10^6 cells and incubated overnight, then washed with PBS and treated with 2 mL of control, 0.25 or 1.0 mM PQ-containing media (serum-free) for 1, 4, or 8 h. Following incubation, media of treated cells were analyzed for levels of various cytokines using a Human Grp I Cytokine 7-Plex Panel kit (Bio-Rad) specific for interleukins 1β, 6, 8, 10, and 15, TNF-α, and eotaxin, using a Bio-Plex 200 System (Bio-Rad) in accordance with the manufacturer‟s instructions. Antibodies specifically directed against the cytokines of interest were covalently coupled to colour-coded polystyrene beads, which were allowed to react with sample containing the cytokines of interest. Biotinylated detection antibodies specific for a different epitope on the cytokines were added, resulting in the formation of a sandwich of

antibodies around each cytokine. Streptavidin-phycoerythrin was then added to bind the biotinylated detection antibodies, allowing the reaction mixture to be detected. Each well was analyzed via the flow-based Bio-Plex suspension array system, which identified and quantitated each specific reaction based on bead colour and fluorescence, and cytokine concentrations were assessed using Bio-Plex Manager software via a standard curve derived from a recombinant cytokine standard.

1.12 - Statistics

Data were presented as mean ± S.E.M ($n \geq 3$) and analyzed for statistical significance using the paired Student‟s t-test, with $p < 0.05$ considered significant. For normalized data, a paired one sample t-test was performed comparing means to a hypothetical mean of 1 ($p < 0.05$).

Table 1.1: Human Stress & Toxicity PathwayFinder RT^2 Profiler PCR Array gene table.

Unigene	GeneBank	Symbol	Description	Gene Name
Hs.480653	NM_001154	ANXA5	Annexin A5	ANX5/ENX2
Hs.367437	NM_000051	ATM	Ataxia telangiectasia mutated	AT1/ATA
Hs.631546	NM_004324	BAX	BCL2-associated X protein	Bax zeta
Hs.516966	NM_138578	BCL2L1	BCL2-like 1	BCL-XL/S
Hs.2490	NM_033292	CASP1	Caspase 1, apoptosis-related cysteine peptidase (interleukin 1, beta, convertase)	ICE/IL1BC
Hs.5353	NM_001230	CASP10	Caspase 10, apoptosis-related cysteine peptidase	ALPS2/FLICE2
Hs.655983	NM_001228	CASP8	Caspase 8, apoptosis-related cysteine peptidase	ALPS2B/CAP4
Hs.502302	NM_001752	CAT	Catalase	MGC138422
Hs.57907	NM_002989	CCL21	Chemokine (C-C motif) ligand 21	6Ckine/CKb9
Hs.514107	NM_002983	CCL3	Chemokine (C-C motif) ligand 3	G0S19-1/LD78ALPHA
Hs.75703	NM_002984	CCL4	Chemokine (C-C motif) ligand 4	ACT2/G-26
Hs.430646	NM_005190	CCNC	Cyclin C	CycC
Hs.523852	NM_053056	CCND1	Cyclin D1	BCL1/D11S287E
Hs.79101	NM_004060	CCNG1	Cyclin G1	CCNG
Hs.370771	NM_000389	CDKN1A	Cyclin-dependent kinase inhibitor 1A (p21, Cip1)	CAP20/CDKN1
Hs.291363	NM_007194	CHEK2	CHK2 checkpoint homolog (S. pombe)	CDS1/CHK2
Hs.408767	NM_001885	CRYAB	Crystallin, alpha B	CRYA2/CTPP2
Hs.1349	NM_000758	CSF2	Colony stimulating factor 2 (granulocyte-macrophage)	GMCSF
Hs.632586	NM_001565	CXCL10	Chemokine (C-X-C motif) ligand 10	C7/IFI10
Hs.72912	NM_000499	CYP1A1	Cytochrome P450, family 1, subfamily A, polypeptide 1	AHH/AHRR
Hs.12907	NM_000773	CYP2E1	Cytochrome P450, family 2, subfamily E, polypeptide 1	CPE1/CYP2E
Hs.1644	NM_000780	CYP7A1	Cytochrome P450, family 7, subfamily A, polypeptide 1	CP7A/CYP7
Hs.290758	NM_001923	DDB1	Damage-specific DNA binding protein 1, 127kDa	DDBA/UV-DDB1
Hs.505777	NM_004083	DDIT3	DNA-damage-inducible transcript 3	CEBPZ/CHOP
Hs.445203	NM_001539	DNAJA1	DnaJ (Hsp40) homolog, subfamily A, member 1	DJ-2/DjA1
Hs.380282	NM_007034	DNAJB4	DnaJ (Hsp40) homolog, subfamily B, member 4	DNAJW/DjB4
Hs.654393	NM_005225	E2F1	E2F transcription factor 1	E2F-1/RBBP3
Hs.326035	NM_001964	EGR1	Early growth response 1	AT225/G0S30
Hs.212088	NM_001979	EPHX2	Epoxide hydrolase 2, cytoplasmic	CEH/SEH
Hs.435981	NM_001983	ERCC1	Excision repair cross-complementing rodent repair deficiency, complementation group 1 (includes overlapping antisense sequence)	COFS4/UV20
Hs.469872	NM_000122	ERCC3	Excision repair cross-complementing rodent repair	BTF2/GTF2H

			deficiency, complementation group 3 (xeroderma pigmentosum group B complementing)	
Hs.2007	NM_000639	FASLG	Fas ligand (TNF superfamily, member 6)	APT1LG1/CD178
Hs.1424	NM_002021	FMO1	Flavin containing monooxygenase 1	FMO1
Hs.642706	NM_001461	FMO5	Flavin containing monooxygenase 5	FMO5
Hs.80409	NM_001924	GADD45A	Growth arrest and DNA-damage-inducible, alpha	DDIT1/GADD45
Hs.616962	NM_004864	GDF15	Growth differentiation factor 15	GDF-15/MIC-1
Hs.76686	NM_000581	GPX1	Glutathione peroxidase 1	GSHPX1
Hs.271510	NM_000637	GSR	Glutathione reductase	MGC78522
Hs.2006	NM_000849	GSTM3	Glutathione S-transferase M3 (brain)	GST5/GSTB
Hs.517581	NM_002133	HMOX1	Heme oxygenase (decycling) 1	HO-1/bK286B10
Hs.530227	NM_005526	HSF1	Heat shock transcription factor 1	HSTF1
Hs.520028	NM_005345	HSPA1A	Heat shock 70kDa protein 1A	HSP70-1/HSP72
Hs.690634	NM_005527	HSPA1L	Heat shock 70kDa protein 1-like	HSP70-HOM/hum70t
Hs.432648	NM_021979	HSPA2	Heat shock 70kDa protein 2	HSPA2
Hs.90093	NM_002154	HSPA4	Heat shock 70kDa protein 4	APG-2/HS24
Hs.605502	NM_005347	HSPA5	Heat shock 70kDa protein 5 (glucose-regulated protein, 78kDa)	BIP/GRP78
Hs.654614	NM_002155	HSPA6	Heat shock 70kDa protein 6 (HSP70B')	HSP70B
Hs.702021	NM_006597	HSPA8	Heat shock 70kDa protein 8	HSC54/HSC70
Hs.520973	NM_001540	HSPB1	Heat shock 27kDa protein 1	CMT2F/DKFZp586P1322
Hs.523560	NM_001040141	HSP90AA2	Heat shock protein 90kDa alpha (cytosolic), class A member 2	HSP90ALPHA/HSPCA
Hs.509736	NM_007355	HSP90AB1	Heat shock protein 90kDa alpha (cytosolic), class B member 1	D6S182/HSP90-BETA
Hs.595053	NM_002156	HSPD1	Heat shock 60kDa protein 1 (chaperonin)	CPN60/GROEL
Hs.1197	NM_002157	HSPE1	Heat shock 10kDa protein 1 (chaperonin 10)	CPN10/GROES
Hs.36927	NM_006644	HSPH1	Heat shock 105kDa/110kDa protein 1	DKFZp686M05240/HSP105
Hs.274313	NM_002178	IGFBP6	Insulin-like growth factor binding protein 6	IBP6
Hs.83077	NM_001562	IL18	Interleukin 18 (interferon-gamma-inducing factor)	IGIF/IL-18
Hs.1722	NM_000575	IL1A	Interleukin 1, alpha	IL-1A/IL1
Hs.126256	NM_000576	IL1B	Interleukin 1, beta	IL-1/IL1-BETA
Hs.654458	NM_000600	IL6	Interleukin 6 (interferon, beta 2)	BSF2/HGF
Hs.36	NM_000595	LTA	Lymphotoxin alpha (TNF superfamily, member 1)	LT/TNFB
Hs.567303	NM_002392	MDM2	Mdm2, transformed 3T3 cell double minute 2, p53 binding protein (mouse)	HDMX/hdm2
Hs.407995	NM_002415	MIF	Macrophage migration inhibitory	GIF/GLIF

			factor (glycosylation-inhibiting factor)	
Hs.647371	NM_005953	MT2A	Metallothionein 2A	MT2
Hs.654408	NM_003998	NFKB1	Nuclear factor of kappa light polypeptide gene enhancer in B-cells 1 (p105)	DKFZp686C01211/EBP-1
Hs.81328	NM_020529	NFKBIA	Nuclear factor of kappa light polypeptide gene enhancer in B-cells inhibitor, alpha	IKBA/MAD-3
Hs.706746	NM_000625	NOS2A	Nitric oxide synthase 2A (inducible, hepatocytes)	HEP-NOS/INOS
Hs.147433	NM_182649	PCNA	Proliferating cell nuclear antigen	MGC8367
Hs.354056	NM_000941	POR	P450 (cytochrome) oxidoreductase	CPR/CYPOR
Hs.180909	NM_002574	PRDX1	Peroxiredoxin 1	MSP23/NKEFA
Hs.706768	NM_005809	PRDX2	Peroxiredoxin 2	NKEFB/PRP
Hs.201978	NM_000962	PTGS1	Prostaglandin-endoperoxide synthase 1 (prostaglandin G/H synthase and cyclooxygenase)	COX1/COX3
Hs.643267	NM_005053	RAD23A	RAD23 homolog A (S. cerevisiae)	HHR23A
Hs.655835	NM_005732	RAD50	RAD50 homolog (S. cerevisiae)	RAD50-2/hRad50
Hs.414795	NM_000602	SERPINE1	Serpin peptidase inhibitor, clade E (nexin, plasminogen activator inhibitor type 1), member 1	PAI/PAI-1
Hs.443914	NM_000454	SOD1	Superoxide dismutase 1, soluble (amyotrophic lateral sclerosis 1 (adult))	ALS/ALS1
Hs.487046	NM_000636	SOD2	Superoxide dismutase 2, mitochondrial	IPO-B/MNSOD
Hs.241570	NM_000594	TNF	Tumor necrosis factor (TNF superfamily, member 2)	DIF/TNF-alpha
Hs.279594	NM_001065	TNFRSF1A	Tumor necrosis factor receptor superfamily, member 1A	CD120a/FPF
Hs.478275	NM_003810	TNFSF10	Tumor necrosis factor (ligand) superfamily, member 10	APO2L/Apo-2L
Hs.654481	NM_000546	TP53	Tumor protein p53	LFS1/TRP53
Hs.654499	NM_007120	UGT1A4	UDP glucuronosyltransferase 1 family, polypeptide A4	HUG-BR2/UDPGT
Hs.191334	NM_003362	UNG	Uracil-DNA glycosylase	DGU/DKFZp781L1143
Hs.98493	NM_006297	XRCC1	X-ray repair complementing defective repair in Chinese hamster cells 1	RCC
Hs.647093	NM_005431	XRCC2	X-ray repair complementing defective repair in Chinese hamster cells 2	DKFZp781P0919
Hs.534255	NM_004048	B2M	Beta-2-microglobulin	B2M
Hs.412707	NM_000194	HPRT1	Hypoxanthine phosphoribosyltransferase 1 (Lesch-Nyhan syndrome)	HGPRT/HPRT
Hs.523185	NM_012423	RPL13A	Ribosomal protein L13a	RPL13A
Hs.544577	NM_002046	GAPDH	Glyceraldehyde-3-phosphate dehydrogenase	G3PD/GAPD
Hs.520640	NM_001101	ACTB	Actin, beta	PS1TP5BP1

Results

Effect of PQ on viability of A549 cells. Initially, a concentration and time response of A549 cells to PQ was carried out to determine an appropriate range of PQ concentrations for subsequent experiments. Viability of PQ-challenged A549 cells decreased in both a concentration- and time-dependent manner relative to control cells as determined by the MTT colorimetric assay (Figure 1.1). Significant cell death was observed following challenge with as low as 0.1 mM PQ for 24 h, approximately 50 % of cells were dead using 0.25 mM PQ with the greatest number of cells dying following 1.0 mM PQ exposure (Figure 1.1 A). This final concentration was further investigated to determine the progression of cell death over time (Figure 1.1 B). It was found that significant cell death was achieved following 1 h of incubation, approximately 50 % after 8 h, with the greatest number of cells dying at 24 h post-PQ exposure. Based on these results, all subsequent experiments were carried out using 0.25 and / or 1.0 mM PQ for 1, 4, 8, and / or 24 h.

Uptake of PQ and intracellular GSH content in PQ-challenged cells. To further investigate the mechanism(s) leading to cell death in A549 cells following PQ challenge, challenged cells were analyzed for PQ uptake and intracellular GSH content. The uptake of PQ in A549 cells increased in both a concentration- and time-dependent manner following PQ exposure, with concomitant decreases in intracellular GSH content as determined by UPLC analysis (Figure 1.2). Following 24 h exposure, uptake was detected with as low as 0.10 mM PQ, and increased linearly ($R^2 = 0.971$) with increasing PQ concentrations (Figure 1.2 A). This correlated with

decreased intracellular GSH levels following 24 h PQ exposure, which was evident with 0.25 mM and greater PQ concentrations. Similarly, PQ uptake was detected as early as 1 h exposure with 1.0 mM PQ, and increased linearly ($R^2 = 0.987$) over a 24 h period (Figure 1.2 B). This again correlated with decreases in intracellular GSH content, as levels were significantly reduced relative to control cells following 4 and 8 h challenge with 1.0 mM PQ, and decreased further after 24 h. Figures 1.2 C-D depict chromatograms with increasing PQ uptake and decreasing GSH content, respectively, in a concentration-dependent manner.

Effect of PQ exposure on intracellular ROS levels. Since it is known that one of the primary actions of PQ is to generate ROS via redox cycling resulting in concomitant decreases in the antioxidant status of cells (i.e. GSH), the role of ROS in PQ-induced toxicity of A549 cells was assessed. Flow cytometric analysis of PQ-challenged cells stained with CM-H_2DCFDA revealed concentration- and time-dependent increases in ROS levels (Figure 1.3). Relative fluorescence increased in a concentration-dependent manner following 4 and 8 h PQ exposure, and in a time-dependent manner at both 0.25 and 1.0 mM PQ, reaching as high as a 3.26-fold increase relative to control cells following 1.0 mM PQ challenge for 8 h (Figure 1.3 A). Representative histograms show increased FL1-H fluorescence intensity with increasing PQ concentrations following 1, 4, and 8 h exposure (Figures 1.3 B-D). In addition, data of H_2O_2 levels from preliminary experiments of PQ-challenged cells suggest that levels in culture media increased following challenge with increasing PQ concentrations for 6 h (Figure 1.4).

Effect of PQ exposure on cellular mitochondrial membrane potential. Flow cytometric analysis of PQ-challenged cells stained with the cell permeable JC-1 dye revealed that PQ depolarizes the mitochondrial membrane as indicated by decreases in FL2-H fluorescence (Figure 1.5). This effect of PQ on A549 cells is concentration- and time-dependent, reaching approximately 50 % less fluorescence in cells challenged with 1.0 mM PQ relative to control cells after 8 h. Representative histograms (Figures 1.5 B-D) show decreased FL2-H fluorescence intensity with increasing PQ concentrations relative to control cells, particularly following 4 and 8 h exposure.

Effect of PQ exposure on apoptosis of A549 cells. PQ-challenged cells did not exhibit significant changes in apoptosis relative to control cells, as indicated by PS translocation via annexin V staining (Figure 1.6) and caspase-3 activation (data not shown), when challenged with 0.25 or 1.0 mM PQ for 1, 4, or 8 h (Figures 1.6 A-C). Representative flow cytometric dot-plots show no apparent changes in apoptotic and necrotic cells following 0, 0.25, and 1.0 mM PQ challenge for 1 h (Figures 1.6 D-F).

Time-course of gene expression in PQ-challenged cells. Gene expression was assessed using a PCR array designed to study genes involved with cellular stress and toxicity. The magnitude of gene expression in cells challenged with 0.25 mM PQ for 1, 4, and 8 h was generally increased relative to control cells (Figure 1.7). The relative fold change of each gene is listed in Table 1.2. As indicated in Table 1.2.1, the expression of many genes relating to oxidative or metabolic

stress, including CAT, GPX1, SOD1, and SOD2, were unchanged relative to control following 1, 4, and 8 h PQ exposure, though GSR expression increased 1.6-fold after 8 h. Similarly, the expression of many heat shock genes were generally not changed relative to control, though the expression of HSPA2 was decreased 1.6-fold and HSPA5 was increased 1.5-fold following 8 h PQ exposure (Table 1.2.2). With respect to proliferation and carcinogenesis related genes (Table 1.2.3), of note was the increased expression of CCNC over time (1.7-fold after 8 h PQ exposure), as well as EGR1 (2- and 2.5-fold after 4 and 8 h, respectively). Significant increases in expression were observed 4 and 8 h post-PQ exposure in certain genes involved with growth arrest and senescence, including CDKN1A (1.5- and 1.8-fold, respectively), DDIT3 (2.1- and 1.8-fold, respectively), and GDF15 (1.8- and 1.7-fold, respectively), while MDM2 was increased 2.5-fold after 8 h (Table 1.2.4). In addition, the expression of certain pro-inflammatory cytokines was increased following 4 and 8 h PQ exposure, including IL18 (1.4- and 1.7-fold, respectively), IL1A (2.39- and 1.7-fold, respectively), IL6 (2.9- and 2.1-fold, respectively), NOS2A (1.6- and 2-fold, respectively), and SERPINE1 (1.5- and 1.8-fold, respectively), while other inflammatory cytokines (i.e. CCL21, CCL3, CCL4, CSF2, CXCL10, IL1B, and LTA) were not expressed in A549 cells challenged with these conditions (Table 1.2.5). The expression of DNA damage and repair genes were largely unchanged following PQ exposure (Table 1.2.6), as were apoptosis signalling genes with the exceptions of ANXA5, CASP10, and CASP8 (Table 1.2.7), each of which progressively increased with increasing PQ exposure time (1.6-, 1.7- and 1.6-fold, respectively, after 8 h).

Measures were taken throughout the quantitative gene expression procedure to ensure that reliable results were obtained. Figure 1.8 depicts representative gels and electropherograms of

extracted RNA samples, achieved using the Experion automated electrophoresis station, indicating high RNA integrity with little or no apparent degradation of 18 and 28 S rRNA. Additionally, a single peak (or zero if no product was amplified) was present in first-derivative dissociation curves for every PCR reaction on all arrays, indicating that only a single PCR product (i.e. the gene of interest) was amplified in each case (Figure 1.9 depicts representative dissociation curves of selected genes).

Effect of PQ challenge on inflammatory cytokine release by A549 cells. Analysis of incubation media of PQ-challenged cells using Bio-Plex technology revealed that levels of secreted IL-8 and IL-6 increase in both a time- and concentration-dependent manner (Figure 1.10). Following a slight increase in IL-8 levels secreted by cells challenged with 1.0 mM PQ for 1 h relative to control cells, IL-8 levels progressively increased after 4 and 8 h (1.93- and 3.17-fold, respectively; Figure 1.10 A). This same effect was seen with increasing PQ concentrations at both 4 and 8 h post-PQ exposure. Similar patterns were seen with regards to IL-6 secretion at 4 and 8 h, where the levels were increased 1.55- and 2.25-fold, respectively, following 1.0 mM PQ challenge relative to control cells (Figure 1.10 B). Levels of secreted IL-1β, IL-10, IL-15, and TNF-α were below detection limits, while eotaxin was only consistently detectable following 1.0 mM PQ challenge for 8 h (1.393 ± 1.023 pg/mL; n = 3).

Discussion

PQ, one of the most commonly used herbicides worldwide, is highly toxic to humans. PQ primarily accumulates in the lung due to its active uptake by type I and II alveolar cells, resulting in destructive and proliferative phases. The initial destruction of the lung by PQ leads to further damage via an inflammatory response, and fibroblasts colonize the lung resulting in pulmonary fibrosis and eventually death via anoxia (Smith *et al.* 1990, Suntres 2002). Since the consequences of PQ-induced toxicity are not unique to the chemical, it can also effectively be used as a model for oxidative stress-related pulmonary injuries. In this study, the effects of PQ in A549 type II-like alveolar cells, and its potential mechanism(s) of action, were investigated *in vitro*.

Challenge of A549 cells with PQ resulted in both concentration- and time-dependent decreases in cell viability as measured via the MTT assay (Figure 1.1), a widely used method of assessing toxicity *in vitro*. These results correspond to those of Weidauer *et al*. 2004 using primary alveolar type II cells isolated from rat lung, where 1.0 mM PQ challenge for 24 h resulted in approximately 20 % viability as assessed via the MTT assay (Weidauer *et al.* 2004). In the present study, the decreases in viability were associated with concomitant time- and concentration-dependent increases in cellular uptake of PQ (Figure 1.2).

PQ is known to undergo redox cycling, a process resulting in the generation of ROS and depletion of intracellular GSH levels, an indicator of cellular redox status. In the present study, the time- and concentration-dependent increases in PQ uptake were associated with both

concentration- and time-dependent decreases in intracellular GSH levels and increases in the presence of ROS. Flow cytometric analysis revealed increased ROS production in a concentration- and time-dependent manner, reaching nearly 3.5-fold greater levels relative to control following 1.0 mM PQ challenge for 8 h (Figure 1.3). It is important to note that the increases in fluorescence (i.e. formation of DCF) following PQ challenge were not a result of direct interactions between PQ and the H_2DCFDA molecule, as these compounds were found to not interact with each other (unlike other molecules including the bacterial toxin pyocyanin) (O'Malley *et al.* 2004). Thus, it is evident that PQ is responsible for increased ROS production in the cell. Additionally, levels of H_2O_2 were investigated in culture media following PQ exposure and preliminary data suggested that levels of this damaging species increased in a concentration-dependent manner in PQ-challenged cells, supporting the aforementioned ROS data. Collectively, these results suggest that the uptake of PQ in A549 cells leads to increased ROS production, including H_2O_2, which is, at least in part, responsible for the significant decreases in intracellular GSH levels observed following PQ exposure, and these events contribute to cell death.

Although PQ is known to produce cell death via necrosis, less is known of its ability to cause cell death via apoptotic mechanism(s). Thus, the effect of PQ on apoptosis was also investigated. Mitochondrial membrane potential, a very early indicator of apoptosis, decreased in a concentration- and time-dependent manner following PQ exposure of A549 cells (Figure 1.5), correlating with the increased levels of ROS under the same conditions. This is in accordance with results obtained by Cheng et al. 2009, in human corneal endothelial cells challenged with PQ, in which there was an approximate 60 % decrease in mitochondrial membrane potential

following 0.5 mM PQ challenge for 24 h. In addition, it should be noted that PQ itself does not have a direct effect on the membrane energy level (Costantini *et al.* 1995). However, no changes in annexin V staining (i.e. PS translocation), were observed in cells post-PQ exposure under the same conditions (Figure 1.6), and cells were negative for caspase-3 activation (data not shown). Although Cappelletti et al. found that incubation of A549 cells with lower doses of PQ (80 and 160 μM) for 24 h with an additional 72 h incubation in PQ-free cell culture media resulted in apoptotic features (i.e. morphological changes and TUNEL staining) (Cappelletti *et al.* 1998), the results presented here provide evidence to suggest that apoptosis does not play a major role in PQ-induced toxicity of A549 cells under the presently studied conditions (i.e. measured immediately following shorter PQ exposure times).

In order to further investigate the intracellular processes taking place during PQ challenge, gene expression was investigated over time (i.e. 1, 4, and 8 h following 0.25 mM PQ exposure) using PCR arrays specific for genes relating to cellular stress and toxicity. The magnitude of gene expression in PQ-challenged cells was generally increased relative to control cells (Figure 1.7), indicating that the cell actively responded to the novel stress.

Expression of many oxidative or metabolic stress-related genes did not change significantly following PQ challenge (i.e. CAT, SOD1, SOD2, and GPX1; Table 1.2.1), corresponding to other studies (Weidauer *et al.* 2004, Lehmann *et al.* 2001, Tomita *et al.* 2005, Tomita *et al.* 2007). For instance, the expression of CAT, SOD1, and SOD2 genes remained unchanged following PQ challenge of primary type II alveolar cells isolated from rats (Lehmann *et al.* 2001) and in the H358 alveolar type II-like cell line (Weidauer *et al.* 2004), while GPX1 gene

expression was similarly unchanged in the lungs of both PQ-challenged rats (Tomita *et al.* 2005) and mice (Tomita *et al.* 2007). Additionally, GSR was up-regulated after 8 h PQ exposure in our study (Table 1.2.1), which is in agreement with its up-regulation in the lungs of PQ-challenged rats (Tomita *et al.* 2005) and mice (Tomita *et al.* 2007). Although the gene expression levels for these antioxidant enzymes (i.e. SOD, CAT) were not up-regulated following PQ exposure, other studies have shown that their respective enzymatic activities were increased following PQ exposure (Saito 1986).

Expression levels of many inflammatory genes were up-regulated following PQ exposure, particularly following 4 and 8 h. These include IL18, IL1A, IL6, NOS2A, and SERPINE1 (Table 1.2.5). IL18, IL1A, and IL6 all code for pro-inflammatory cytokines, while NOS2A codes for inducible nitric oxide synthase, an enzyme involved in the production of nitric oxide, and SERPINE1 codes for plasminogen activator inhibitor-1, which inhibits urokinase plasminogen activator by forming a 1:1 stoichiometric complex (Sato *et al.* 2004). These increases in gene expression correlated with increased secretion of pro-inflammatory cytokines into the cell culture supernatant, including IL-8 and IL-6. Levels of both cytokines were observed to increase in a concentration- and time-dependent manner following PQ challenge (Figure 1.10), though IL-8 protein was substantially more abundant in the cell culture supernatant. It has been well established that one of the initial consequences of PQ injury is the infiltration of neutrophils into the lung (Shek *et al.* 1994, Eddleston *et al.* 2003), a treatment effect mediated by the early production of IL-8, which acts primarily to chemically attract and activate infiltrating neutrophils. Other studies have shown increased IL-8 gene expression in A549 cells, peripheral blood mononuclear cells, and retinal pigment epithelial cells under similar

PQ exposure conditions (Bianchi *et al.* 1993, Fernandes *et al.* 2008). IL-6 functions in inflammation and in the maturation of B cells, and is produced at sites of acute or chronic inflammation. The expression of this cytokine was stimulated at both the gene (Table 1.2.5) and protein level (Figure 1.10 B) following PQ challenge under the studied conditions, which corresponds with gene expression findings in PQ-challenged mice from another study (Tomita *et al.* 2007). Together with IL-8, this cytokine may have a role in the inflammatory response associated with PQ toxicity in the lung.

In addition, levels of IL-1β, IL-10, IL-15, and TNF-α secretion in cell culture supernatants were not detectable, while eotaxin was only consistently detectable following challenge with the 1.0 mM PQ for 8 h (the most damaging condition studied). This suggests that the secretion of eotaxin, a chemoattractant for eosinophils, is also up-regulated during PQ-induced toxicity in A549 cells. Eosinophil infiltration is believed to be another early consequence of PQ toxicity in the lung (Fukuda *et al.* 1985, Candan and Alagozlu 2001) and these results provide evidence to suggest that type II alveolar cells may contribute to their chemoattraction during such injuries. The up-regulation of these inflammatory genes in concert with the increased secretion of certain pro-inflammatory cytokines suggest that type II alveolar cells are, at least in part, responsible for initiating the inflammatory response due to PQ in the lung.

PQ challenge also had an impact on the cell cycle of A549 cells since a variety of such genes were up-regulated in this study. CCNC, which encodes a cyclin that interacts with cyclin-dependent kinase 8 (together inducing the phosphorylation of the carboxy-terminal domain of the large subunit of RNA polymerase II (Rao *et al.* 2009)) and has recently been implicated in cell

cycle transitions between G_0 to G_1 and G_1 to S phase (Rao *et al.* 2009), exhibited increased gene expression (nearly 1.7-fold) after 8 h (Table 1.2.3). This increase in CCNC expression corresponds with findings in BJ Foreskin cells challenged with single-walled carbon nanotubes, which are known to increase intracellular ROS levels (Sarkar *et al.* 2007). CDKN1A is another gene that was up-regulated following PQ exposure, reaching a 1.8-fold increase after 8 h (Table 1.2.4). This gene encodes a cyclin-dependent kinase (CDK) inhibitor that inhibits the activity of cyclin-CDK2 or -CDK4 complexes, thus regulating cell cycle progression at G1 (King and Cidlowski 1998). Furthermore, DDIT3 and GADD45A, both DNA damage-inducible genes whose expressions are known to be up-regulated in a wide variety of cells under genotoxic stress conditions (Oyadomari and Mori 2004), were maximally expressed after 4 h PQ exposure (2.1- and 1.6-fold increases, respectively; Table 1.2.4), corresponding with the more than 3-fold increase in GADD45A following PQ challenge of neuroblastoma (SH-SY5Y) cells (Moran *et al.* 2008). In addition, gene expression of GADD45A and MDM2 (which codes for a protein with p53-regulatory activity (Stoyanova *et al.* 2009)) were found to increase in GPX1-knockout mice challenged with PQ (Cheng *et al.* 2003), correlating with the up-regulation of both genes in this study (MDM2 was up-regulated nearly 2.5-fold following 8 h PQ challenge; Table 1.2.4). Finally, GDF15, which is also involved in growth and differentiation of cells, was increased at 4 and 8 h post-PQ challenge (1.8- and 1.7-fold, respectively; Table 1.2.4). These results suggest that PQ challenge, perhaps through the generation of ROS, has a considerable impact on the cell-cycle of A549 cells, which may lead to growth arrest as a result of the increased expression of the aforementioned genes.

EGR1, which encodes a transcriptional regulator that activates genes (including p53) required for differentiation and mitogenesis (Sperandio *et al.* 2009), was substantially up-regulated with increasing PQ exposure, reaching 2.0- and 2.5-fold increases after 4 and 8 h, respectively (TP53 expression remained unchanged under these conditions; Table 1.2.4). This cancer suppressor gene has not been studied in PQ-induced toxicity, but results from a study using ionizing radiation injury on A549 cells showed that EGR1 has a radiation-inducible promoter that promotes the elevation of growth factors or their receptors (i.e. TGF-β1, TNF-α, or EGFR) (Shareef *et al.* 2007). They found that ionizing radiation induced EGR1 gene expression in A549 cells, which led to increased TNF-α protein. However, they speculated that activation of NF-κB by TNF-α in A549 cells may have led to abrogation of the pro-apoptotic effects of both TNF-α and TRAIL (Shareef *et al.* 2007). Based on these findings, it is possible that the increased levels of intracellular ROS due to PQ in this study are the cause of EGR1 up-regulation, and perhaps a similar mechanism may be in play in this model to help explain the lack of apoptosis observed following PQ challenge, despite the up-regulation of certain apoptotic signalling genes after 8 h (i.e. ANXA5, CASP10, and CASP8; Table 1.2.7).

Finally, it was interesting to note that, though the expression of ACTB was unchanged following 1 and 4 h PQ exposure, it was up-regulated 1.8-fold following 8 h PQ exposure relative to other housekeeping genes (Table 1.2.3), suggesting ACTB was not a reliable housekeeping gene in this model of PQ-induced toxicity. This is supported by a study by Cappelletti et al where 24 h PQ challenge (80 μM) of A549 cells resulted in irreversible actin filament disorganization (Cappelletti *et al.* 1994). The use of ACTB as a housekeeping gene in PQ toxicity studies requires further investigation, particularly as many gene studies involving PQ have utilized it in

this capacity (Lehmann *et al.* 2001, Ishida *et al.* 2006). Expression of B2M, HPRT1, RPL13A, and GAPDH, the housekeeping genes used in these experiments, effectively remained constant under all studied conditions.

The results from this study indicate that exposure of A549 cells to PQ resulted in concentration- and time-dependent cellular PQ uptake, increases in the production of ROS (including H_2O_2), and decreases in intracellular GSH levels, with each of these factors contributing to cell death. Despite the decreases in mitochondrial membrane potential, apoptosis was found to not play a significant role in PQ-induced toxicity under the studied conditions, as evidenced by insignificant PS translocation and caspase-3 activation. However, PQ challenge may have affected the cell-cycle as evidenced by the up-regulation of many genes involved in growth arrest. In addition, gene expression analysis revealed significant increases in certain pro-inflammatory genes, which correlated with increases in the secretion of pro-inflammatory cytokines (i.e. IL-8 and IL-6). Finally, alveolar type II epithelial cells, because of their abundance in the lung and their ability to take up the chemical, contribute to the initiation of the inflammatory response in cases of PQ lung toxicity.

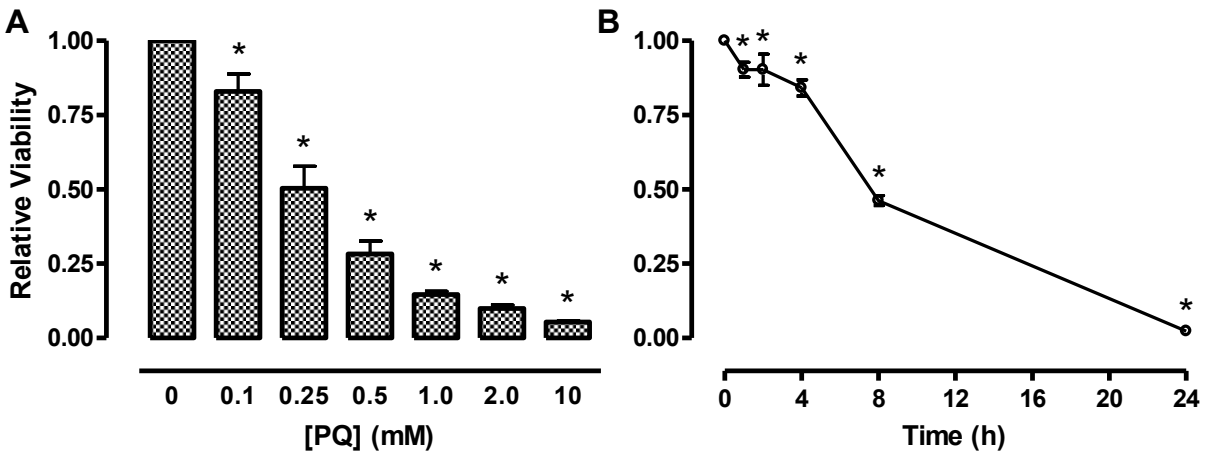

Figure 1.1: Effect of PQ concentration and time of exposure on the viability of A549 cells. Viability of cells challenged with PQ was assessed by measuring the activity of mitochondrial dehydrogenases using the MTT colorimetric assay. Cells seeded into 96-well plates at 10,000 cells/well and grown to 80 % confluence were challenged with (A) increasing concentrations of PQ for 24 h or (B) with 1.0 mM PQ for various time points up to 24 h. Cells were incubated for 4 h with MTT reagent post-PQ challenge and absorbance was measured spectrophotometrically at 570 nm (650 nm correction wavelength). Viability of PQ-challenged cells was assessed relative to control cells. Data points represent mean ± S.E.M. of 5 (A) and 3 (B) independent experiments performed in octuplet. * denotes significant difference relative to control ($p < 0.05$).

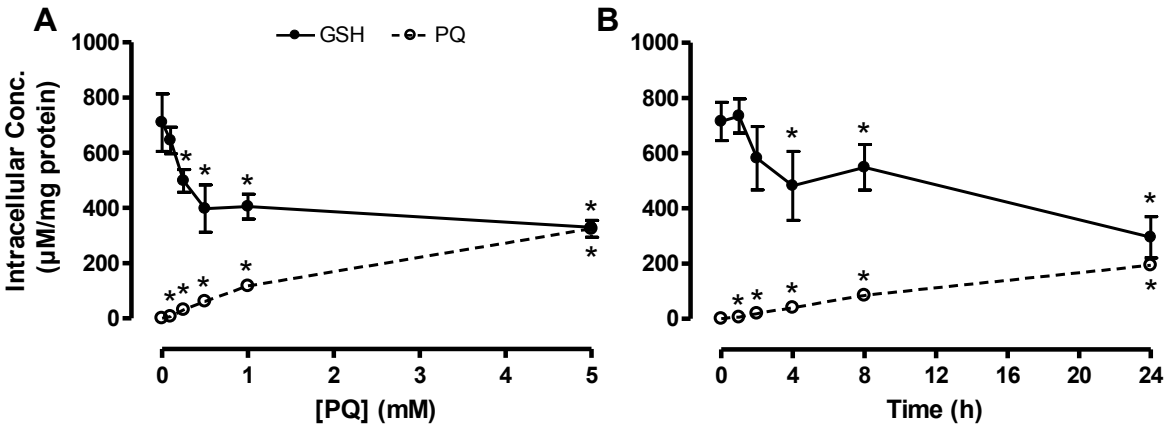
A
B
GSH
PQ
Intracellular Conc. (µM/mg protein)
[PQ] (mM)
Time (h)

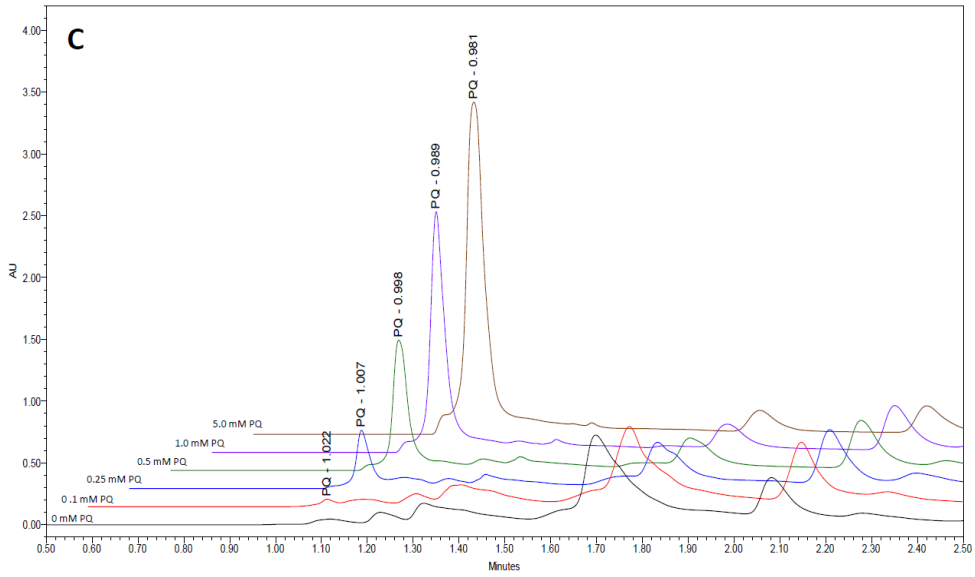
C
PQ - 0.981
PQ - 0.989
PQ - 0.998
PQ - 1.007
PQ - 1.022
5.0 mM PQ
1.0 mM PQ
0.5 mM PQ
0.25 mM PQ
0.1 mM PQ
0 mM PQ
AU
Minutes

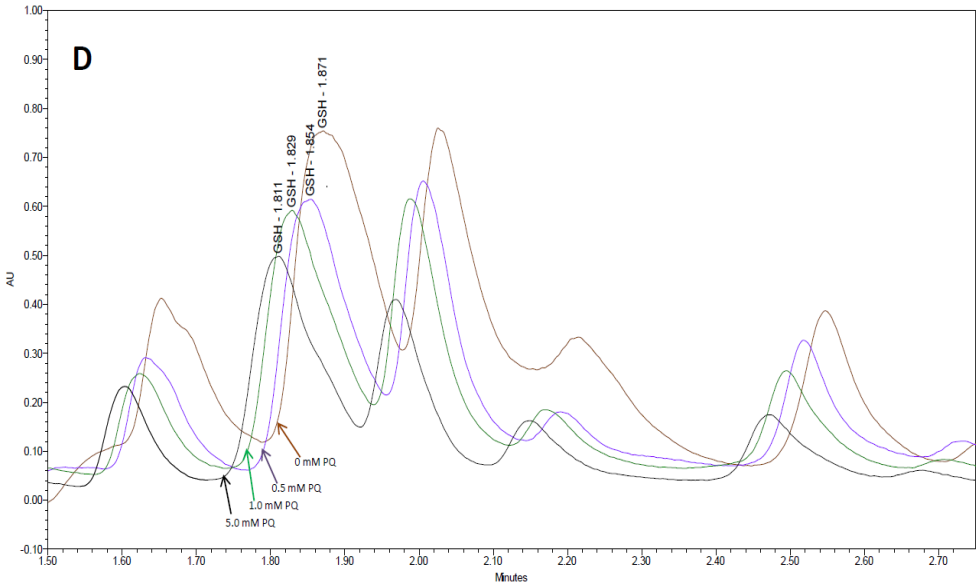
D
GSH - 1.871
GSH - 1.854
GSH - 1.829
GSH - 1.811
0 mM PQ
0.5 mM PQ
1.0 mM PQ
5.0 mM PQ
AU
Minutes

Figure 1.2: PQ uptake and intracellular GSH content in PQ-challenged cells: a concentration and time effect. Cells challenged with increasing concentrations of PQ for 24 h (A) or with 1.0 mM PQ for various times up to 24 h (B) were sonicated, and lysate was assessed concurrently for cellular PQ uptake and intracellular GSH content via UPLC (dotted line: PQ levels; solid line: GSH levels). Lysates were normalized to total protein. Representative UPLC chromatograms show increases in PQ uptake (C) and decreases in GSH content (D) as the PQ treatment concentration increases (PQ treatments are as labelled in figures; retention times are indicated at peak maxima). Data points represent mean ± S.E.M. of 3 independent experiments performed in duplicate. * denotes significant difference relative to control ($p < 0.05$).

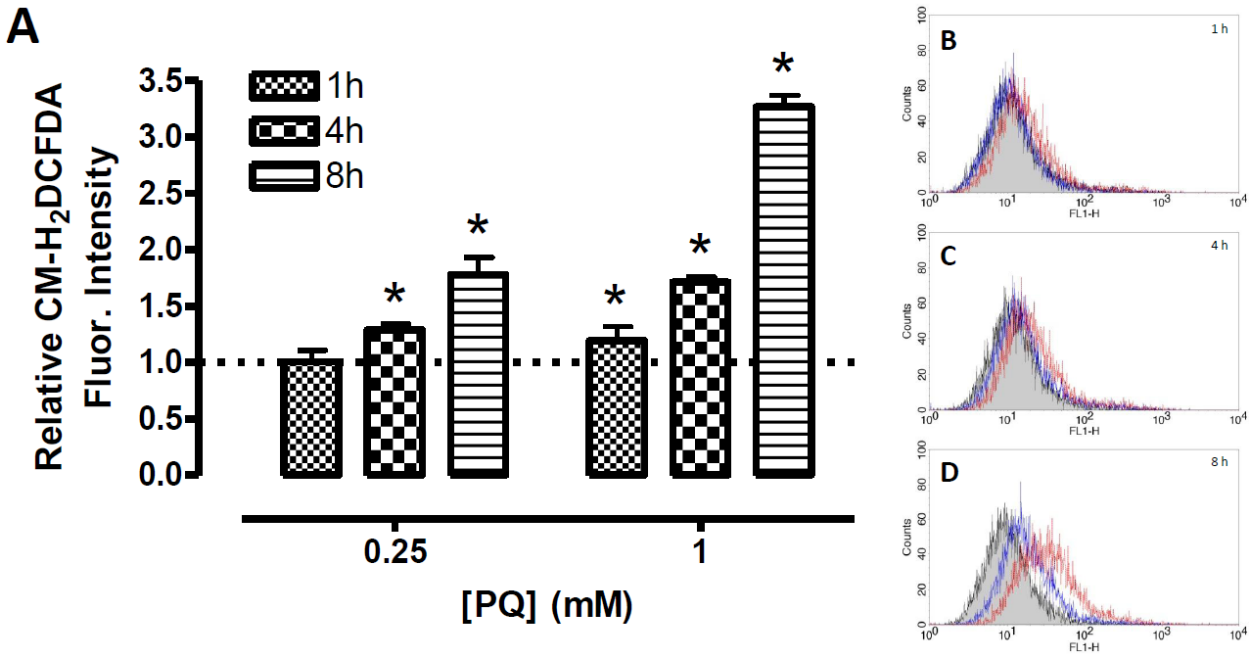

Figure 1.3: Levels of intracellular ROS post-PQ challenge. Following challenge with 0, 0.25 or 1.0 mM PQ for 1, 4, or 8 h, cells were stained with the cell-permeable CM-H_2DCFDA fluorescent probe and analyzed using flow cytometry (minimum 10,000 events; FL1-H). Increases in relative fluorescence indicate a greater abundance of intracellular ROS compared to control cells (A). Representative histograms show FL1-H fluorescence intensity of stained cells following 1 (B), 4 (C), and 8 h (D) PQ exposure (shaded area: 0 mM PQ control; solid blue line: 0.25 mM PQ; dotted red line: 1.0 mM PQ). Bars represent mean ± S.E.M. of 3 independent trials. * denotes significant difference relative to control ($p < 0.05$).

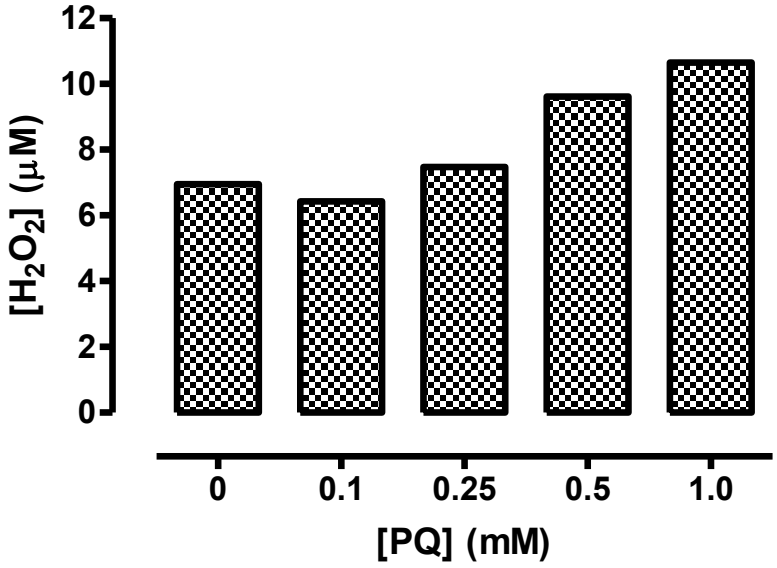

Figure 1.4: Effect of PQ exposure on levels of hydrogen peroxide. Hydrogen peroxide levels were measured in culture media of cells challenged with increasing concentrations of PQ for 6 h. Cells were seeded into 6-well plates at 0.5×10^6 cells/well, incubated overnight, and challenged with 3.0 mL of control or PQ-containing media. Immediately following challenge, data was obtained via electrochemical detection of incubation media using the Apollo 4000 Free Radical Analyzer, and was interpolated to H_2O_2 concentrations (μM) from pA using a standard curve of known values. Bars represent data obtained from 1 independent experiment due to failure of equipment.

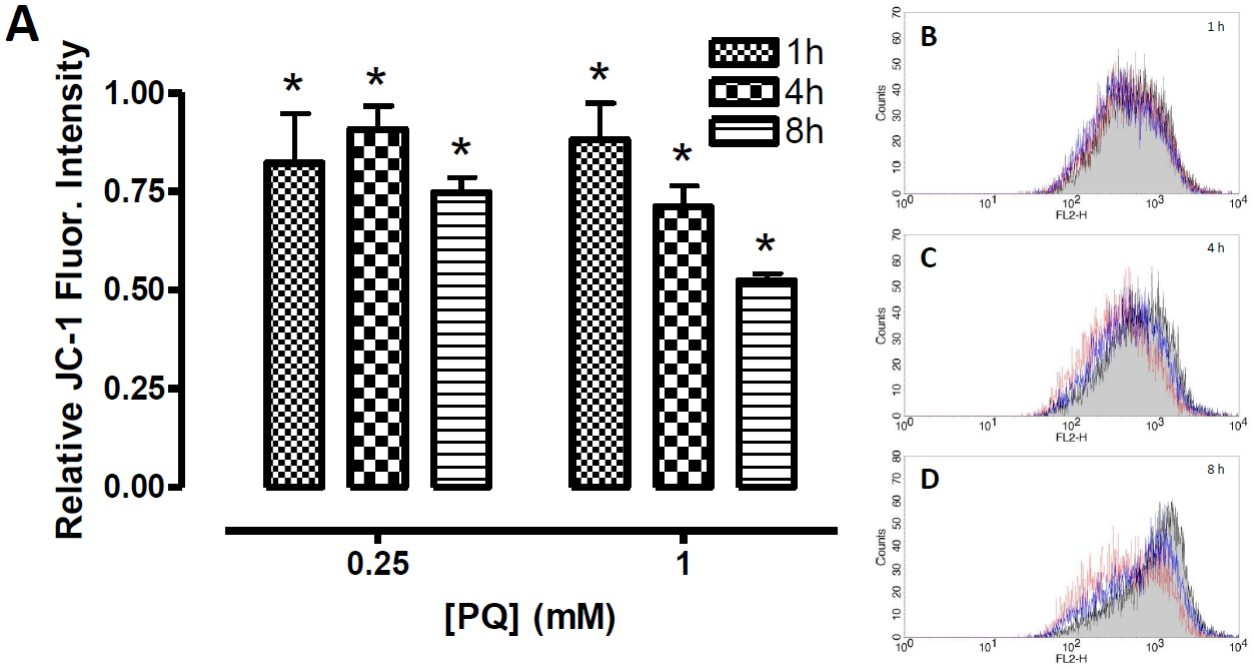

Figure 1.5: Effect of PQ challenge on cellular mitochondrial membrane potential. Cells seeded into 6-well plates at 0.5×10^6 cells/well and challenged with 0, 0.25 or 1.0 mM PQ for 1, 4, and 8 h were stained with the membrane-permeable JC-1 fluorescent dye for 30 min. Normal mitochondrial membrane potential caused aggregation of the dye molecules resulting in red fluorescence emission (measured flow cytometrically using FL2-H channel), while depolarization of mitochondrial membrane potential was indicated by decreased red fluorescence. Representative histograms show FL2-H fluorescence intensity of stained cells following 1 (B), 4 (C), and 8 h (D) PQ exposure (shaded area: 0 mM PQ control; blue solid line: 0.25 mM PQ; dotted red line: 1.0 mM PQ). Bars represent mean ± S.E.M. of 3 independent trials. * denotes significant difference relative to control ($p < 0.05$).

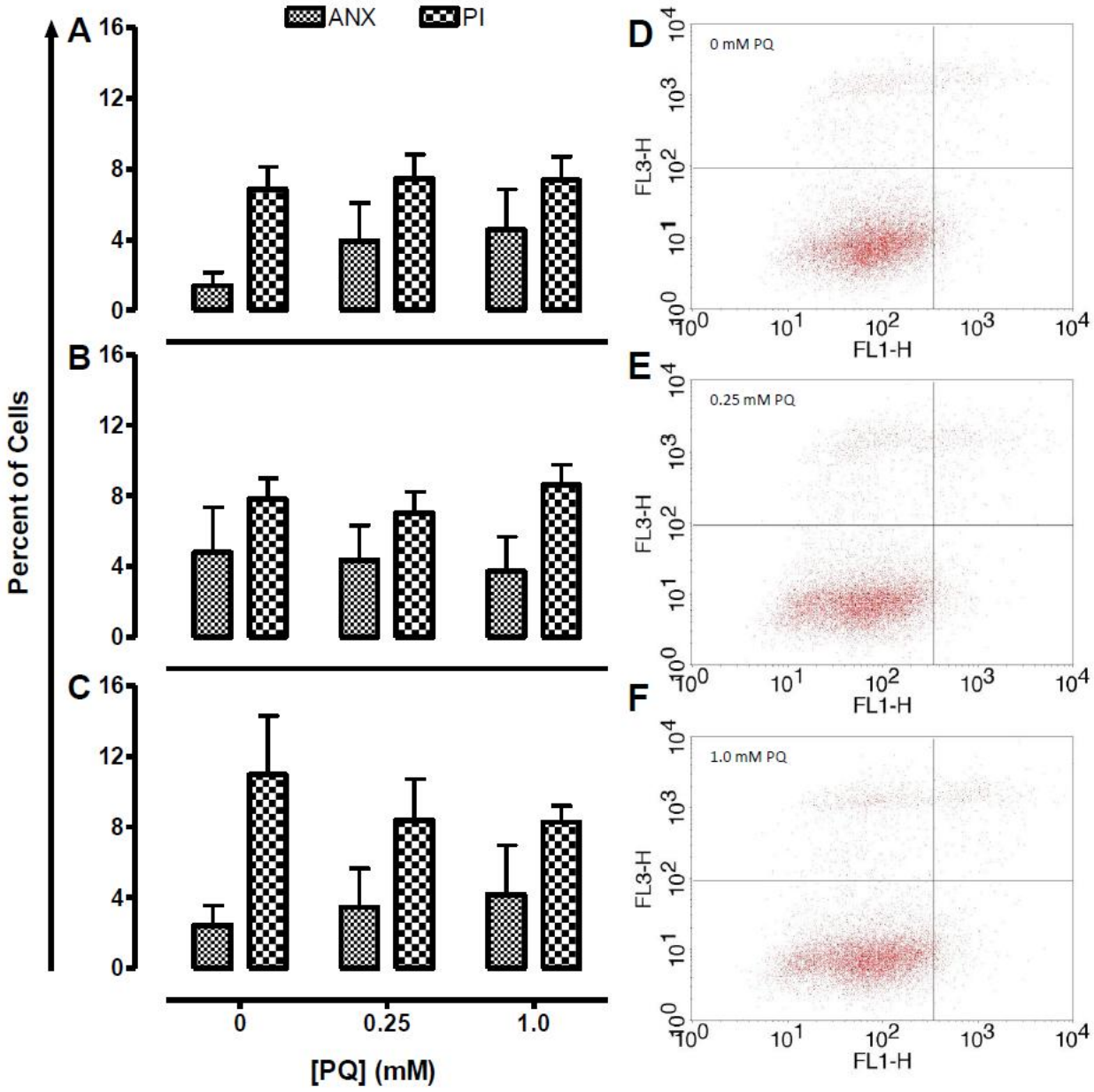
ANX
PI
A
B
C
D
E
F
Percent of Cells
[PQ] (mM)
0
0.25
1.0
0 mM PQ
0.25 mM PQ
1.0 mM PQ
FL3-H
FL1-H

Figure 1.6: Effect of PQ challenge on apoptosis of A549 cells. Following 0, 0.25, or 1.0 mM PQ challenge for 1, 4, or 8 h, cells were suspended via trypsinization and dually stained for 15 minutes with annexin V (ANX) and propidium iodide (PI) for flow cytometric analysis of phosphatidylserine translocation (A-C), an indicator of apoptosis. Representative flow cytometric dot-plots show similar ANX and PI staining among 0, 0.25, and 1.0 mM PQ-challenged cells (1 h exposure; D-F, respectively). Annexin V and PI fluorescences were measured on FL1-H and FL3-H channels, respectively. ANX^-/ PI^- cells were considered live (LL), ANX^+/ PI^- cells apoptotic (LR), and $ANX^{+/-}/ PI^+$ cells necrotic (UL + UR). Bars represent mean ± S.E.M. of 3 independent trials (A-C). LL: lower left; LR: lower right; UL: upper left; UR: upper right.

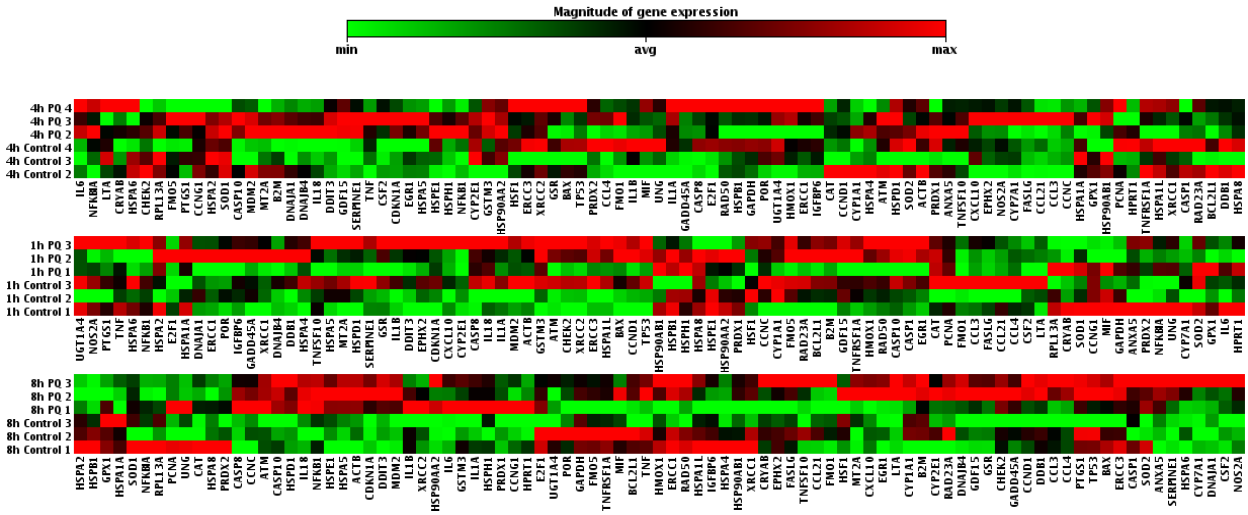

Figure 1.7: Effect of PQ exposure on the magnitude of gene expression in A549 cells. RNA was extracted from cells challenged with 0 or 0.25 mM PQ for 1 (upper panel), 4 (middle panel), or 8 h (lower panel) and analyzed via quantitative reverse-transcription PCR using a gene array. The magnitude of expression of each gene is expressed on a scale ranging from minimal (intense green) to maximal (intense red) expression (n = 3 independent trials).

Table 1.2: Relative expression, via gene array analysis, of genes involved with cellular stress and toxicity in cells challenged with 0.25 mM PQ for 1, 4, or 8 h. Fold change is expressed relative to untreated control using the housekeeping genes B2M, HPRT1, RPL13A, and GAPDH.

Table 1.2.1: Oxidative or metabolic stress-related genes.

Symbol	1 h	4 h	8 h
CAT	1.16 ± 0.15	-1.01 ± 0.10	1.00 ± 0.04
CRYAB	-1.10 ± 0.06	1.24 ± 0.21	1.00 ± 0.15
CYP1A1	-1.08 ± 0.20	-1.01 ± 0.07	1.29 ± 0.06
CYP2E1	0.00 ± 0.00	0.00 ± 0.00	0.00 ± 0.00
CYP7A1	0.00 ± 0.00	0.00 ± 0.00	0.00 ± 0.00
EPHX2	2.03 ± 0.56	0.00 ± 0.00	1.04 ± 0.34
FMO1	0.00 ± 0.00	0.00 ± 0.00	0.00 ± 0.00
FMO5	1.12 ± 0.09	1.16 ± 0.20	-1.18 ± 0.14
GPX1	1.00 ± 0.04	1.01 ± 0.07	-1.10 ± 0.05
GSR	1.15 ± 0.22	1.12 ± 0.19	1.60 ± 0.18
GSTM3	1.32 ± 0.15	1.29 ± 0.11	1.36 ± 0.14
HMOX1	1.06 ± 0.08	1.18 ± 0.10	1.00 ± 0.14
MT2A	1.04 ± 0.07	1.08 ± 0.08	1.35 ± 0.22
POR	1.52 ± 0.46	-1.15 ± 0.26	-1.36 ± 0.88
PRDX1	1.02 ± 0.04	1.00 ± 0.04	1.18 ± 0.09
PRDX2	1.33 ± 0.44	0.00 ± 0.00	0.00 ± 0.00
PTGS1	1.06 ± 0.15	0.00 ± 0.00	0.00 ± 0.00
SOD1	-1.03 ± 0.02	-1.08 ± 0.08	-1.01 ± 0.07
SOD2	1.01 ± 0.04	1.02 ± 0.11	1.26 ± 0.16

Table 1.2.2: Heat shock genes.

Symbol	1 h	4 h	8 h
DNAJA1	1.03 ± 0.09	1.30 ± 0.11	1.05 ± 0.03
DNAJB4	1.04 ± 0.11	1.29 ± 0.06	1.31 ± 0.09
HSF1	-1.04 ± 0.06	1.07 ± 0.04	-1.02 ± 0.06
HSPA1A	1.14 ± 0.13	-1.16 ± 0.03	-1.29 ± 0.03
HSPA1L	1.28 ± 0.21	-1.57 ± 0.47	-1.11 ± 0.18
HSPA2	1.05 ± 0.05	-1.03 ± 0.04	-1.59 ± 0.07
HSPA4	1.14 ± 0.12	-1.00 ± 0.09	-1.08 ± 0.08
HSPA5	-1.01 ± 0.06	1.31 ± 0.09	1.47 ± 0.07
HSPA6	0.00 ± 0.00	0.00 ± 0.00	0.00 ± 0.00
HSPA8	1.46 ± 0.30	-1.04 ± 0.19	-1.14 ± 0.08
HSPB1	1.07 ± 0.06	-1.02 ± 0.09	-1.37 ± 0.09
HSP90AA2	-1.01 ± 0.08	1.24 ± 0.22	1.39 ± 0.13
HSP90AB1	1.08 ± 0.03	1.04 ± 0.09	-1.08 ± 0.22
HSPD1	1.03 ± 0.01	1.05 ± 0.09	1.27 ± 0.07
HSPE1	-1.08 ± 0.04	1.03 ± 0.05	1.16 ± 0.04
HSPH1	1.06 ± 0.03	1.18 ± 0.10	1.19 ± 0.07

Table 1.2.3: Proliferation / carcinogenesis related genes.

Symbol	1 h	4 h	8 h
ACTB	1.13 ± 0.12	1.15 ± 0.14	1.79 ± 0.12
CCNC	1.15 ± 0.22	1.34 ± 0.19	1.67 ± 0.34
CCND1	1.48 ± 0.37	1.08 ± 0.19	1.45 ± 0.34
CCNG1	-1.13 ± 0.04	-1.02 ± 0.05	1.07 ± 0.04
E2F1	0.00 ± 0.00	0.00 ± 0.00	0.00 ± 0.00
EGR1	1.40 ± 0.38	2.04 ± 0.16	2.47 ± 0.82
PCNA	1.02 ± 0.06	-1.01 ± 0.04	1.07 ± 0.03

Table 1.2.4: Growth arrest and senescence related genes.

Symbol	1 h	4 h	8 h
CDKN1A	1.03 ± 0.01	1.48 ± 0.09	1.81 ± 0.18
DDIT3	1.20 ± 0.08	2.14 ± 0.07	1.79 ± 0.00
GADD45A	1.16 ± 0.06	1.59 ± 0.06	1.52 ± 0.14
GDF15	1.05 ± 0.10	1.83 ± 0.09	1.73 ± 0.15
IGFBP6	1.09 ± 0.14	1.09 ± 0.12	-1.26 ± 0.22
MDM2	1.13 ± 0.12	1.24 ± 0.16	2.45 ± 0.16
TP53	1.34 ± 0.21	1.06 ± 0.13	1.15 ± 0.22

Table 1.2.5: Inflammatory genes.

Symbol	1 h	4 h	8 h
CCL21	0.00 ± 0.00	0.00 ± 0.00	0.00 ± 0.00
CCL3	0.00 ± 0.00	0.00 ± 0.00	0.00 ± 0.00
CCL4	0.00 ± 0.00	0.00 ± 0.00	0.00 ± 0.00
CSF2	0.00 ± 0.00	0.00 ± 0.00	0.00 ± 0.00
CXCL10	0.00 ± 0.00	0.00 ± 0.00	0.00 ± 0.00
IL18	1.10 ± 0.05	1.41 ± 0.10	1.70 ± 0.12
IL1A	1.36 ± 0.31	2.39 ± 0.44	1.74 ± 0.14
IL1B	1.38 ± 0.33	0.00 ± 0.00	0.00 ± 0.00
IL6	-1.07 ± 0.13	2.91 ± 0.36	2.10 ± 0.26
LTA	0.00 ± 0.00	0.00 ± 0.00	0.00 ± 0.00
MIF	-1.08 ± 0.06	1.02 ± 0.04	-1.06 ± 0.05
NFKB1	-1.04 ± 0.08	1.23 ± 0.18	1.24 ± 0.07
NOS2A	-1.03 ± 0.16	1.60 ± 0.36	1.97 ± 0.54
SERPINE1	-1.05 ± 0.08	1.51 ± 0.13	1.77 ± 0.24

Table 1.2.6: DNA damage and repair genes.

Symbol	1 h	4 h	8 h
ATM	1.25 ± 0.25	1.11 ± 0.24	1.39 ± 0.08
CHEK2	1.06 ± 0.03	-1.11 ± 0.02	1.24 ± 0.09
DDB1	1.26 ± 0.27	-1.08 ± 0.20	1.44 ± 0.37
ERCC1	1.15 ± 0.18	1.13 ± 0.17	1.07 ± 0.30
ERCC3	1.23 ± 0.21	1.12 ± 0.11	1.34 ± 0.34
RAD23A	1.07 ± 0.12	-1.07 ± 0.09	1.13 ± 0.08
RAD50	1.13 ± 0.22	-1.01 ± 0.20	1.13 ± 0.28
UGT1A4	1.14 ± 0.38	1.03 ± 0.03	0.00 ± 0.00
UNG	1.02 ± 0.09	1.01 ± 0.10	-1.01 ± 0.05
XRCC1	1.17 ± 0.11	-1.21 ± 0.15	-1.05 ± 0.32
XRCC2	1.24 ± 0.16	1.14 ± 0.15	1.43 ± 0.24

Table 1.2.7: Apoptosis signalling genes.

Symbol	1 h	4 h	8 h
ANXA5	1.06 ± 0.08	1.24 ± 0.13	1.55 ± 0.00
BAX	1.35 ± 0.15	-1.01 ± 0.11	1.32 ± 0.32
BCL2L1	1.23 ± 0.19	-1.13 ± 0.26	1.09 ± 0.43
CASP1	1.13 ± 0.16	-1.32 ± 0.35	1.31 ± 0.23
CASP10	1.14 ± 0.34	1.55 ± 0.28	1.71 ± 0.23
CASP8	1.15 ± 0.06	1.24 ± 0.10	1.62 ± 0.17
FASLG	0.00 ± 0.00	0.00 ± 0.00	0.00 ± 0.00
NFKBIA	1.08 ± 0.11	1.19 ± 0.10	-1.06 ± 0.04
TNF	-1.14 ± 0.48	1.60 ± 0.43	1.09 ± 0.23
TNFRSF1A	1.17 ± 0.20	-1.13 ± 0.20	-1.36 ± 0.40
TNFSF10	-1.08 ± 0.24	0.00 ± 0.00	0.00 ± 0.00

Values represent mean ± SEM of 3 independent experiments.

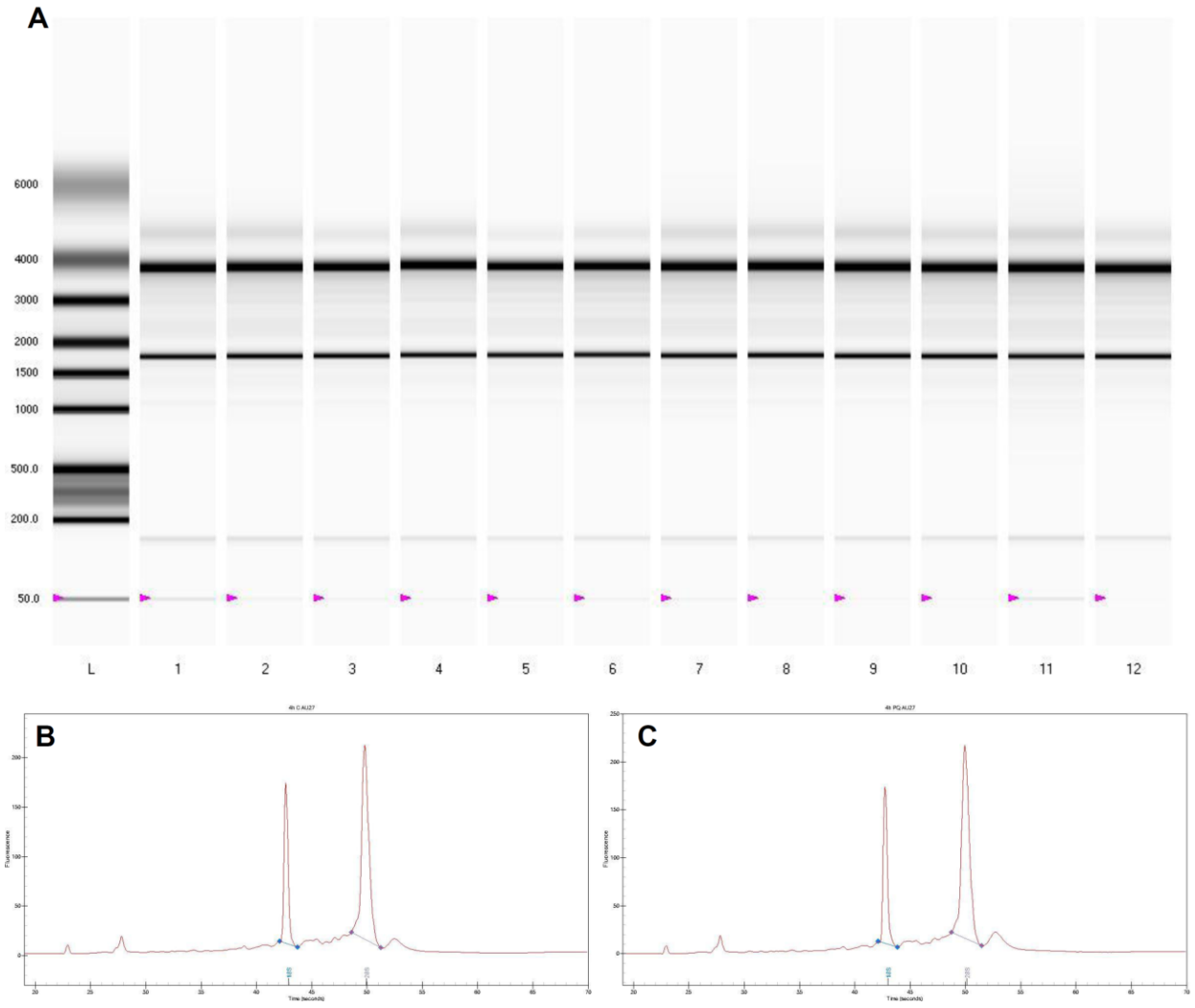

Figure 1.8: Validation of RNA integrity. Aliquots of extracted RNA from control or PQ-challenged A549 cells were assessed for RNA concentration and integrity using the Experion Automated Electrophoresis Station. Representative gels artificially depict 18 and 28 S rRNA banding (A; L: ladder; 1 - 12: extracted RNA from control or PQ-challenged cells) using data obtained from electropherograms. Representative electropherograms of samples 3 and 4 (4 h control and 0.25 mM PQ-challenged samples, respectively) display 18 and 28 S rRNA peaks (B-C).

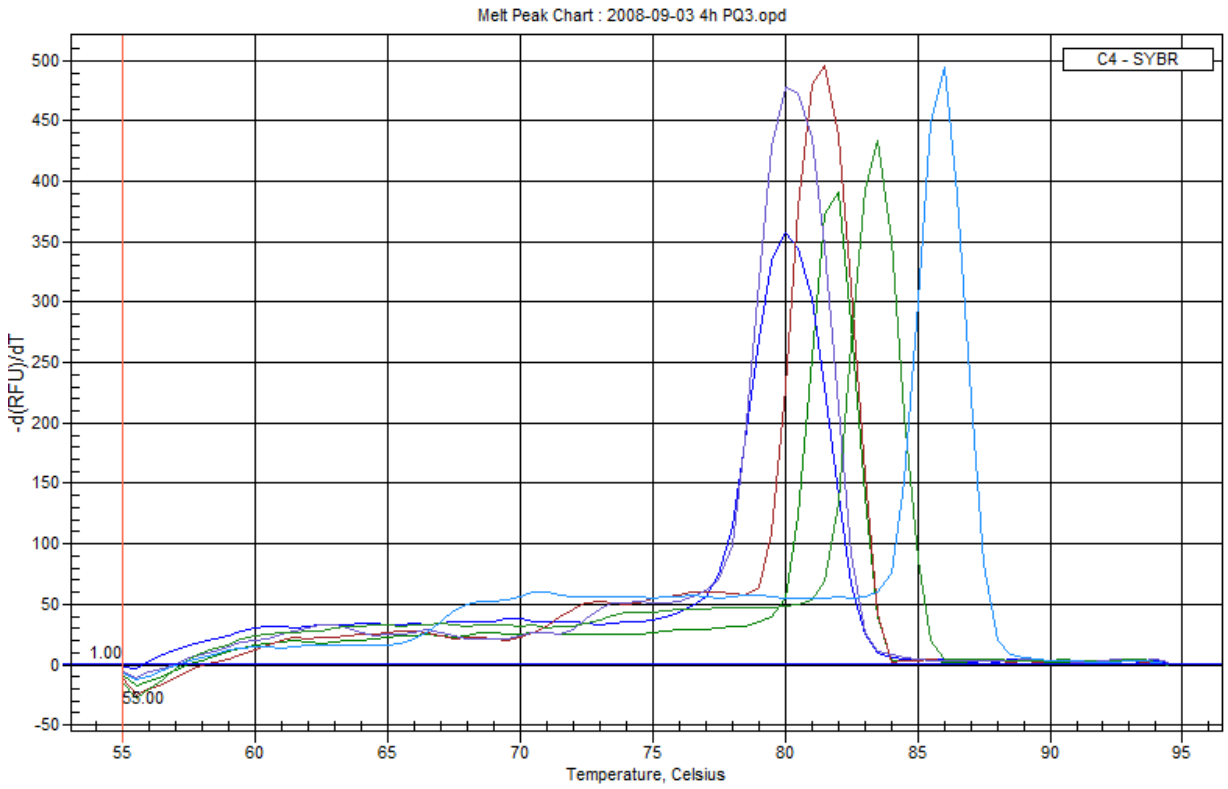

Figure 1.9: Assessment of PCR gene product quality. Representative first-derivative dissociation curves of amplified PCR product from select genes of a PCR array are depicted.

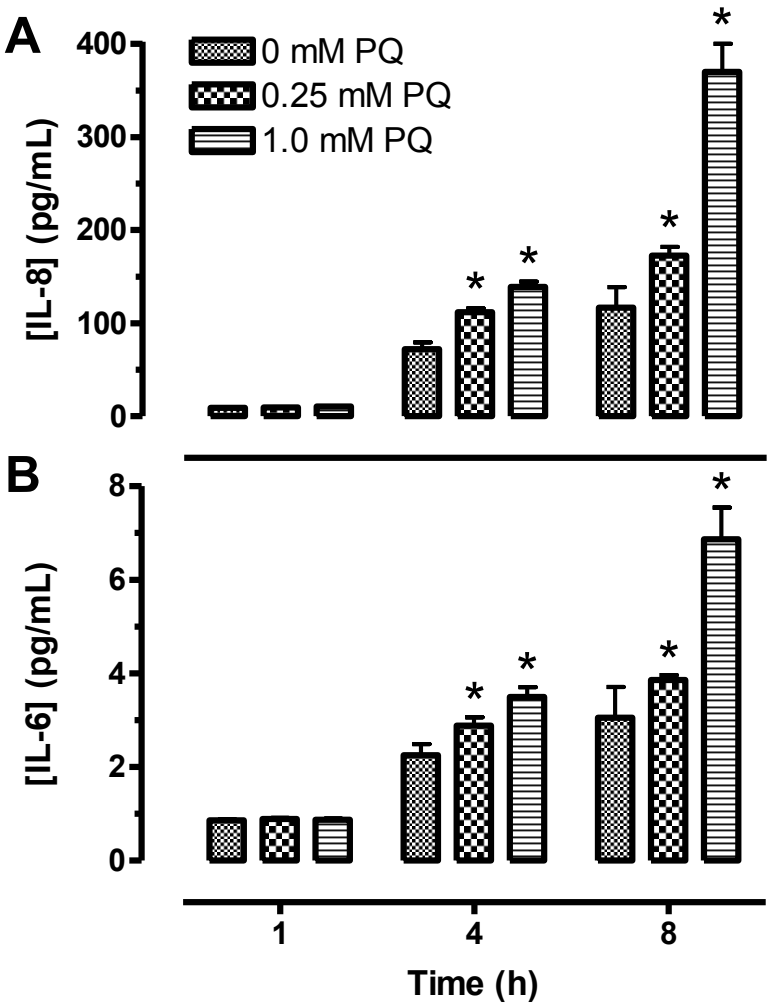

Figure 1.10: Levels of inflammatory cytokines in culture media following PQ challenge. Culture media from cells challenged with 0, 0.25, or 1.0 mM PQ for 1, 4, or 8 h were analyzed using Bio-Plex technology for levels of secreted IL-8 (A) and IL-6 (B), according to the manufacturer's instructions. Levels of IL-1β, IL-10, IL-15, and TNF-α were not detectable, while eotaxin was only consistently detectable following 1.0 mM PQ challenge for 8 h (1.393 ± 1.023 pg/mL). Bars represent mean ± S.E.M. of 3 independent trials. * denotes significant difference relative to control ($p < 0.05$).

CHAPTER II

Introduction

2.1 - Antioxidants in PQ lung toxicity

Recognizing that PQ is preferentially accumulated in the lung and exerts its cytotoxic effects via the generation of ROS, many studies have focused on increasing the antioxidant status in the lung to protect against PQ injury using various antioxidants, including antioxidant enzymes (i.e. superoxide dismutase), vitamins (i.e. ascorbic acid, α-Tocopherol), melatonin, and low-molecular weight thiol-containing antioxidants (i.e. glutathione, NAC, metallothionein). The success of these antioxidants has thus far been variable, as reviewed by Suntres (Suntres 2002).

Superoxide dismutase (SOD) administration fails to ameliorate the effects of PQ, mainly due to its inability to enter cell membranes because of its high molecular mass and its charge (Suntres 2002). A recent study found that cationization of SOD significantly increased its intracellular delivery and suppressed PQ-induced toxicity and lipid peroxidation (Ishimoto *et al.* 2006). It was also found that SOD fusion proteins containing a nuclear localization signal or membrane translocation sequence successfully transduced into the nucleus or cytosol of cells *in vitro*, increasing the viability of cells challenged with PQ (Kim *et al.* 2008). SOD mimetics were also found to have a beneficial effect against PQ toxicity in the kidney (Samai *et al.* 2008, Samai *et al.* 2007).

Curcumin (diferuloyl methane), the component of turmeric, is widely used as a potent anti-inflammatory, antioxidant, anticancer, and membrane-stabilizing agent (Venkatesan 2000, Soudamini *et al.* 1992). One study found that oral administration of curcumin to PQ-challenged rats reduced lipid peroxidation in tissues (i.e. lung, liver, kidney, and brain) of mice compared to mice challenged with PQ alone (Soudamini *et al.* 1992). In another study, curcumin was found to protect against PQ-induced toxicity in the lung by having beneficial effects on myeloperoxidase activity (an index of neutrophil content), bronchoalveolar lavage fluid protein content, thiobarbituric acid reactive substances formation, and viability (Venkatesan 2000). These protective effects were attributed to curcumin's ability to decrease neutrophil influx into the lung, stabilize cell membranes, decrease the oxidant burden, and enhance the natural cellular antioxidant defenses (i.e. GSH) (Venkatesan 2000).

3-Methyl-1-phenyl-2-pyrazolin-5-one (MCI-186), a novel free radical scavenger recently introduced clinically, has exhibited beneficial effects in acute PQ toxicity. MCI-186 improved the survival of rats treated orally with 175 mg/kg PQ from 8 to 42 % after 6 days, and from 4 to 38 % after 14 days when administered immediately following PQ. However, the beneficial effects of MCI-186 on survival were significantly diminished when administered 30 min after PQ challenge (Saibara *et al.* 2003). These therapeutic effects on acute PQ toxicity were attributed to the potent inhibitory activity of MCI-186 both on non-enzymatic lipid peroxidation and lipoxygenase activity (Saibara *et al.* 2003).

Amifostine, a thiophosphate prodrug approved by the Food and Drug Administration for the prevention of toxicities associated with cisplatin and therapeutic radiation, can be converted to its

active metabolite (WR-1065) and function as an oxygen and DNA radical scavenger (Wills *et al.* 2007). This has been shown to protect against lipoperoxidation, but a study showed that subcutaneous injections of amifostine did not improve survival or lung injury caused by PQ toxicity in mice (Wills *et al.* 2007).

Captopril, a thiol-containing angiotensin-converting enzyme inhibitor, has also provided beneficial effects against PQ-induced toxicity in the lung, attributable to its antioxidant properties (Candan and Alagozlu 2001). This molecule can scavenge free radicals independently of angiotensin-converting enzyme inhibition (Candan and Alagozlu 2001). One study showed that the simultaneous administration of captopril (50 mg/kg i.p.) and PQ (40 mg/kg i.p.) in rats, followed by an additional captopril injection 1 h later, significantly reduced lipid peroxidation, normalized the activities of SOD, GPx, and GSH content in the lung tissue, and prevented the increase in lung fibrosis (Candan and Alagozlu 2001). In another study on isolated perfused rat lungs, captopril (10μM) significantly reduced LDH leakage and lipid peroxidation, while increasing GSH and total protein content when exposed to 600 μM PQ for 1 h (Ghazi-Khansari *et al.* 2005). However, it was found that oral administration of a lower dose (10 mg/kg) of captopril had no effect on glutathione levels and lipid peroxidation in PQ (20 mg/kg; i.p.)-treated rats after 21 days, but improved pulmonary fibrosis (Ghazi-Khansari *et al.* 2007). Interestingly, the authors suggest that the antifibrotic effects of captopril may be related to the inhibition of angiotensin-converting enzyme, and not from the thiol group on captopril, since the non-thiol angiotensin-converting enzyme inhibitor enalapril exhibited similar effects to captopril (Ghazi-Khansari *et al.* 2007).

Dexamethasone, a potent synthetic glucocorticoid which acts as an anti-inflammatory and immunosuppressant (its effects are related to *de novo* synthesis of P-glycoprotein), was also found to have a protective effect in the rat lung following PQ challenge by decreasing lipid peroxidation and carbonyl groups content, normalizing myeloperoxidase activities, and preventing the increase in lung weight (Dinis-Oliveira *et al.* 2006). Dexamethasone was also responsible for decreasing PQ accumulation in the lung (Dinis-Oliveira *et al.* 2006b) and was shown to have a protective effect in the lung when combined with surfactant treatment (Chen *et al.* 2001). However, increased damage to the kidney and spleen were noted with dexamethasone treatment (Dinis-Oliveira *et al.* 2006).

Sodium salicylate (NaSAL), a nonsteroidal anti-inflammatory drug, is able to modulate inflammatory signalling and prevent oxidative stress (Dinis-Oliveira *et al.* 2007). In rats, NaSAL caused a significant reduction in PQ-induced oxidative stress, platelet activation, and NF-κB activation in the lung, while the survival of rats treated with NaSAL following PQ challenge was 100 % after 30 days, compared to 100 % mortality after 6 days in rats challenged with PQ alone (Dinis-Oliveira *et al.* 2007). One possible mechanism for this protection may involve the ability of NaSAL to chemically react with PQ (Dinis-Oliveira *et al.* 2008), a novel feature for therapeutic drugs targeted against PQ toxicity, which correlates with another study in which NaSAL decreased the herbicidal activity of PQ when simultaneously applied to plants (Silverman *et al.* 2005).

Rats fed diets containing soy protein isolate and soy peptide containing 0.025 % PQ had decreased serum thiobarbituric acid reactive substances levels and reduced lung weight

compared animals receiving PQ but no soy protein isolate or soy peptide in their diets (Takenaka *et al.* 2003). This effect was suggested to be a result of the antioxidative properties of soy protein. In another study, green tea extract mixed with food decreased PQ-induced pulmonary fibrosis in rats by suppression of oxidative stress and endothelin-1 expression (Kim *et al.* 2006).

Finally, pre- and post-treatment with ethyl pyruvate in PQ challenged rats significantly decreased the malondialdehyde levels in the lung and liver tissues, and decreased plasma nitric oxide concentrations at 6 h, but failed to show a significant change in GSH levels (Lee *et al.* 2008).

2.2 - N-acetylcysteine

2.2.1 - Antioxidant role

N-acetylcysteine (NAC), the acetylated variant of the amino acid L-cysteine, is a low-molecular weight thiol-containing antioxidant with free radical-scavenging properties and is a pre-cursor to cellular glutathione (GSH) synthesis (Sadowska *et al.* 2007, Suntres 2002, Atkuri *et al.* 2007). The scavenging capabilities of NAC are attributed to the nucleophilicity and redox interactions of its thiol group, and it is able to undergo transhydrogenation or thiol-disulfide exchange reactions with other thiol redox couples (Arakawa and Ito 2007). Additionally, NAC is a source of cysteine, often the limiting pre-cursor of *de novo* GSH synthesis (Arakawa and Ito 2007, Kelly 1998, van de Poll *et al.* 2006, Sadowska *et al.* 2007). GSH is an important antioxidant as it is the most abundant non-protein thiol present in living cells, and its levels are commonly used as

an indicator of intracellular antioxidant status. Unlike cysteine, which is taken up by the alanine-serine-cysteine system, a ubiquitous system of Na^+-dependent neutral amino acid transport, NAC is a membrane-permeable molecule that does not require active transport to enter the cell (Arakawa and Ito 2007). Once available, γ-glutamylcysteine synthetase converts L-cysteine and glutamate to γ-glutamylcysteine, after which GSH synthetase converts this product and glycine to GSH, both reactions being driven by adenosine triphosphate (Arakawa and Ito 2007). This pathway can be controlled by feedback inhibition of γ -glutamylcysteine synthetase by GSH (K_i ~ 1.5 mM) (Richman and Meister 1975), meaning that under physiologically normal conditions this enzyme is likely not operating at its maximal rate. Thus, these two modes of action make NAC an attractive therapeutic candidate for the treatment of ROS-mediated toxicity.

2.2.2 - Role in cellular signalling

Due to its antioxidant properties, NAC has been shown to influence redox-sensitive cell-signalling and transcription pathways, such as NF-κB (which regulates pro-inflammatory genes), and the p38, ERK1/2, SAPK/JNK, c-Jun, and c-Fos pathways, among others, in a wide variety of different systems (Sadowska *et al.* 2007, Pajonk *et al.* 2002, Zafarullah *et al.* 2003). NAC has been shown to promote cell growth and survival by activating the MAPK pathway in response to ROS-induced injuries (which normally lead to growth arrest and apoptosis) and is able to limit inflammatory processes, such as the release of pro-inflammatory cytokines (Zafarullah *et al.* 2003). These actions may play a role in its cytoprotective effect.

2.2.3 - Clinical uses

NAC is used clinically mainly in two capacities: as a mucolytic agent and for the treatment of acetaminophen toxicity. NAC was originally introduced as a mucolytic agent for the treatment of congestive and obstructive pulmonary diseases, particularly those associated with hyper-secretion of mucus (i.e. cystic fibrosis and chronic bronchitis), and has been used clinically in this capacity since the mid-1950s (Arakawa and Ito 2007, Henke and Ratjen 2007). The commercial formulation Mucomyst® is one of two drugs currently used in North America and Europe for aerosol administration in the treatment of cystic fibrosis (Henke and Ratjen 2007). Its sulfhydryl groups are able to reduce the disulfide bonds of the high-molecular weight glycoproteins of mucus, resulting in reduced viscosity and elasticity of mucus (Aitio 2006, Atkuri *et al.* 2007, Henke and Ratjen 2007). The mucolytic activity of NAC increases with pH, operating optimally in a range from 7.0 – 9.0 (Henke and Ratjen 2007).

In addition to its use as a mucolytic agent, NAC has been used clinically since the mid-1970s for the treatment of acetaminophen (paracetamol; N-acetyl-p-aminophenol) poisoning, one of the most commonly encountered substances to be taken deliberately in overdosage (Atkuri *et al.* 2007, Prescott 2005). During the course of acetaminophen poisoning, the metabolite N-acetyl-p-benzoquinoneimine is generated in the liver by the hepatic cytochrome P450 enzymes (Atkuri *et al.* 2007) and damages essential mitochondrial and other cellular enzymes by covalently binding to and arylating their protein sulphydryl groups (Prescott 2005). High concentrations of GSH are required to detoxify this metabolite in order to avoid permanent liver damage (Atkuri *et al.* 2007). Therefore due to the excessive GSH depletion from acetaminophen overdose, the liver

may benefit from *de novo* synthesis of hepatic GSH via the administration of NAC. Studies indicate that NAC is almost completely effective in preventing severe liver damage, renal failure, and death, provided that it is administered intravenously or orally within 8 to 10 hours of acetaminophen overdose; its efficacy was reduced when treatment was delayed beyond 15 hours (Prescott 2005). Although the arylation of sulphydryl groups by acetaminophen can be reversed by excess GSH, there is limited time as the changes eventually become permanent and lead to irreversible hepatic damage and necrosis (Prescott 2005).

In addition to cystic fibrosis and acetaminophen toxicity, NAC has been used clinically to treat HIV/AIDS, chronic obstructive pulmonary disease, and diabetes (Atkuri *et al.* 2007), and many placebo-controlled trials have reported beneficial effects regarding oral NAC treatment for various other diseases, including colon cancer, Alzheimer‟s disease, bronchitis, ARDS, pulmonary oxygen toxicity, cardiac dysfunction, and protein energy malnutrition (Arakawa and Ito 2007, Atkuri *et al.* 2007).

2.2.4 - Administration and distribution

NAC is generally administered orally, intravenously, or through aerosol inhalation (i.e. for airway mucolytic activity). The intravenous administration of NAC for acetaminophen toxicity was first used in the 1970s in the UK, and consists of a loading dose of 150 mg/kg followed by subsequent lower doses totalling 300 mg/kg in 20 ¼ hours (Prescott 2005). Oral NAC was introduced near the same time in the USA and is delivered with an initial dose of 140 mg/kg,

followed by subsequent lower doses totalling 1330 mg/kg over 3 days (Prescott 2005). Both routes of administration appear to be equally effective, though there is inevitably a delay between the administration of oral NAC and the absorption of an effective dose (Prescott 2005). When given as a chronic nutritional supplement, 300 to 600 mg NAC is administered daily (van de Poll *et al.* 2006).

NAC forms disulfides in plasma, prolonging the existence of the drug for up to 6 h (Arakawa and Ito 2007). Following a single intravenous injection of 200 mg/kg NAC in humans, the peak plasma level declined rapidly and biphasically ($\alpha T_{1/2}$ = 6 min, $\beta T_{1/2}$ = 40 min) (Cotgreave *et al.* 1987). However, the free thiol is largely undetectable following oral administration of 200 mg/kg NAC, being 5% bioavailable (Cotgreave *et al.* 1987). It is suggested that the drug itself does not accumulate in the body, but instead its oxidized forms and metabolites do. NAC is readily taken up in the stomach and gut and sent to the liver where it is largely converted to cysteine for the synthesis of glutathione, which is secreted into circulation (Atkuri *et al.* 2007). The plasma half-life is estimated to be approximately 2.5 h after oral administration, while no NAC is detectable 10-12 h after administration (Arakawa and Ito 2007). NAC is also known to cross the blood-brain barrier (Arakawa and Ito 2007), and has been reported to reverse memory impairment and reduce oxidative stress in the brain in aged SAMP8 mice (Farr *et al.* 2003).

Serious and life-threatening anaphylactoid reactions to NAC, though uncommon, have been reported and include nausea, vomiting, hypotension, flushing, urticaria, and pruritis (Atkuri *et al.* 2007, Prescott 2005). However, most reactions to intravenous administration of NAC are minor and subside rapidly following a temporary discontinuation of NAC treatment or reduction in the

rate of NAC infusion (Atkuri *et al.* 2007, Prescott 2005). Adverse reactions via oral administration are rarely mentioned, suggesting this route may be safer (Prescott 2005). Interestingly, many reactions to intravenous NAC occur during the first hour, coinciding with the greatest infusion rate during treatment, which has prompted many investigators to suggest that the incidence and severity of such reactions may be reduced by slowing the initial rate of infusion (Prescott 2005).

2.2.5 - Role in PQ toxicity

Several studies have investigated the effects of NAC on PQ toxicity in various systems. *In vitro* studies have demonstrated NAC to have a beneficial effect primarily via the amelioration of redox status. NAC exhibited a protective effect against PQ-induced cytotoxicity of isolated hepatocytes (Dawson *et al.* 1984) and alveolar type II cells (Hoffer *et al.* 1996, Cecen *et al.* 2002) via enhancement of cellular GSH content. Additionally, NAC suppressed the levels of PQ-induced ROS in normal pooled plasma and in 3T3 fibroblasts *in vitro* (Hong *et al.* 2003), and decreased apoptosis (measured 72 h following treatment) of PQ-challenged A549 cells when co-incubated or pre-treated with NAC (Cappelletti *et al.* 1998).

In vivo studies have also shown NAC to exhibit beneficial effects against PQ toxicity, particularly in the inflammatory response. PQ-challenged (70 mg/kg; i.p.) rats post-treated with NAC (100 mg/kg × 4; i.p.) exhibited an increased survival rate (Yeh *et al.* 2006). NAC was responsible for decreasing lipid peroxidation and superoxide anion production, as well as

augmenting total glutathione concentrations in the lung, liver and kidney, which played a role in limiting the destruction of the lung tissue and decreasing the infiltration of inflammatory cells in interstitial stroma (Yeh *et al.* 2006). Similarly, rats challenged with 20 mg/kg PQ (i.p.) and given 1 % NAC solution as drinking water displayed less oedema and cellular infiltration in the lung than animals not given NAC (Wegener *et al.* 1988). Finally, NAC administration (50 mg/kg; i.p.) post-PQ challenge (30 mg/kg; i.p.) reduced the release of chemoattractants in the rat lung and delayed neutrophil infiltration, suggesting NAC may delay inflammation (Hoffer *et al.* 1993, Hoffer *et al.* 1997).

Clinically, NAC has been used in combination with other treatment regimens (i.e. forced diuresis, Fuller‟s earth, gastric lavage, hemoperfusion, etc.) to ameliorate the adverse effects of PQ toxicity. One such regimen resulted in the full recovery of a patient that developed ARDS and pulmonary fibrosis following ingestion of 6650 mg PQ and 3500 mg diquat (Eisenman *et al.* 1998), while another led to recovery of a patient following ingestion of 60 g PQ (Drault *et al.* 1999). In two other cases of accidental PQ ingestion, patients had improved symptoms and undetectable levels of PQ 48 h after such treatment (Lopez Lago *et al.* 2002), and death was prevented in another patient following ingestion of a potentially lethal PQ dose (Lheureux *et al.* 1995). Finally, treatment involving NAC was successful in ameliorating PQ toxicity following 10 g PQ ingestion in an adolescent female (Dinis-Oliveira *et al.* 2006c). However, it is unclear what role, if any, NAC played in each of these cases.

2.3 - Liposomes

Liposomes are lyotropic liquid crystals consisting of an aqueous inner compartment entrapped by a bilayer of naturally-occurring phospholipids, and can be unilamellar or multilamellar (Goyal *et al.* 2005). They possess a low intrinsic toxicity, and are biocompatible, biodegradable, and non-immunogenic (Shek *et al.* 1994, Goyal *et al.* 2005). Both lipophilic and hydrophilic drug types can be incorporated into liposomes; lipophilic drugs into the phospholipid bilayer, and hydrophilic drugs into the inner aqueous compartment. Liposomes allow indiscriminate passage of drugs through biological barriers such as cellular membranes, as they are able to either fuse with the membrane and deliver their contents (Goyal *et al.* 2005) or may be taken up directly by the cell through endocytosis depending on their size (Hashimoto and Suzuki 1992). This makes liposomal encapsulation especially useful for drugs or compounds that normally cannot cross such barriers.

2.3.1 - Composition of liposomes

The specific composition of liposomes can differ, with various phospholipids or surfactants employed in various ratios. Pulmonary surfactant is a mixture of lipids and proteins that coat the inside of the mammalian lung, and is necessary to maintain proper expansion of small air sacs to avoid lung collapse (Goyal *et al.* 2005, Stone and Smith 2004). Dipalmitoyl-phosphatidylcholine (DPPC), dimyristoyl-phosphatidyl-glycerol, dimyristoyl-phosphatidylcholine, and disaturated-phosphatidylcholine, are all naturally-occurring lipids and

components of human lung surfactant (i.e. DPPC accounts for 60-70 % by weight of human lung surfactant) which can be synthetically produced and incorporated into liposomes (Bernsdorff *et al.* 1999). An important consideration for liposomal design is their encapsulation efficiency, which is determined by the composition of the liposome (i.e. lipid content and particle size), since it must be balanced with substrate permeability to achieve a useful formulation for drug administration. Enhanced drug release can be achieved by incorporating cholesterol in the liposomal membrane (Shek *et al.* 1994).

2.3.2 - Antioxidant liposomes

Antioxidant liposomes contain lipid- or water- soluble antioxidants, enzymatic antioxidants, or some combination thereof. As reviewed by Stone et al., researchers have investigated several liposomal antioxidants, such as the lipid-soluble tocopherols, carotenoids, and flavenoids, the water-soluble ascorbate, GSH, lipoic acid, and NAC, and the entrapped antioxidant enzymes SOD and catalase, and have demonstrated an improved effect for these antioxidants in various models of oxidative stress (Stone and Smith 2004). A major advantage of antioxidant liposomes is their ability to simultaneously contain and deliver both water- and lipid-soluble antioxidants for an improved effect, and they are also able to more effectively deliver antioxidant enzymes which are normally unable to cross biological barriers (i.e. cell membranes) (Stone and Smith 2004). Thus, the incorporation of antioxidants into liposomes has garnered great therapeutic interest.

2.3.3 - Administration

Antioxidant liposomes can be administered topically, intratracheally, intravenously, subcutaneously, intramuscularly, or by inhalation of its aerosolized form (Shek *et al.* 1994, Stone and Smith 2004). Topical administration is of considerable interest in the cosmetics industry for treating skin disorders such as psoriasis, inhalation and intratracheal administration can be useful in situations where pulmonary tissues are subjected to oxidative stress, such as influenza infection or in cases of PQ injury, and intravenous administration is used in situations where oxidative stress is a component of an acute trauma or disease, since it has the potential to rapidly increase the plasma and tissue concentration of antioxidants (Shek *et al.* 1994, Stone and Smith 2004). Aerosol inhalation is the most convenient and practical approach for direct liposomal drug delivery to the lung (Shek *et al.* 1994) and DPPC may be the most biocompatible phospholipid for drug delivery to the lung since it constitutes the major component of naturally-occuring lung surfactant. It is also more suitable than other lipids due to its lipid-phase transition temperature being the most physiologically relevant (41 °C), allowing slower release of the entrapped drug (Shek *et al.* 1994).

A problem with conventional liposomes, particularly when delivered intravenously, is their recognition by the immune system and rapid removal from circulation by phagocytic cells, particularly in the liver and spleen (Stone and Smith 2004, Vyas *et al.* 2006). However, recent advances have been made in the design of "stealth liposomes," which circumvent the phagocytic cells of the immune system and thus have a considerably longer half-life in circulation (Stone and Smith 2004, Vyas *et al.* 2006). Stealth liposomes are created by coating liposomes with a

layer of polyethylene glycol-phosphatidylethanolamine (PEG liposomes), which is inert in the body and creates a shield around the pegylated liposome due to its large hydrodynamic volume, protecting it from renal clearance and recognition by cells of the immune system (Stone and Smith 2004, Molineux 2002).

Others have also investigated various ways to target liposomes to specific tissues or cell types, including noncovalent association of cell-specific antibodies, coating with heat-aggregated immunoglobulin M, addition of glycoproteins or glycolipids, or covalent attachment of poly and monoclonal antibodies to the liposome (referred to as "immunoliposomes") (Goyal *et al.* 2005). Immunoliposomes are potent carriers that accelerate cellular uptake due to the recognition of the antibody by the target cell (Hatakeyama *et al.* 2007). These features make liposomes very attractive vehicles for the administration of various drugs.

2.3.4 - Clinical applications

Liposomal drug delivery has a variety of clinical applications, such as the delivery of anticancer, antimicrobial, and antiviral drugs (Goyal *et al.* 2005). The anticancer drug doxorubicin, a potent antineoplastic agent active against a wide range of human cancers, constitutes the first liposomal product (Doxil^{TM}) to be licensed in the United States (Goyal *et al.* 2005). This liposomal formulation reduced the drug's associated non-specific toxicity and maintained or enhanced its anticancer effect (Goyal *et al.* 2005). Several types of antimicrobial drugs, including those used to treat mycobacterial and fungal infections, have been incorporated into liposomes. These

formulations are able to localize in the liver and spleen, where many pathogenic microorganisms reside, and can increase intracellular targeting to these cells (Goyal *et al.* 2005). As an antiviral vehicle, liposomes have been used to treat herpes, hepatitis C, and HIV(Sinico *et al.* 2005, Ferguson *et al.* 2006, Pecheur *et al.* 2007), while antioxidant liposomes have been investigated for the treatment of acute lung injuries and respiratory distress in infants and adults (Stone and Smith 2004).

2.3.5 - Antioxidant liposomes in PQ toxicity

The effectiveness of certain antioxidant liposomes against PQ-induced lung injuries in animals has been investigated. Intratracheal administration of liposomal GSH conferred better protection than conventional GSH against PQ-induced acute lung injury, which was attributed to its increased retention in the lung (Suntres and Shek 1996). Intratracheal administration of α-tocopherol liposomes was also shown in various studies to alleviate many of the pulmonary toxic effects of PQ (Suntres *et al.* 1992, Suntres and Shek 1995a, Suntres and Shek 1995b), suggesting the protective effect of liposomal α-tocopherol in PQ toxicity may be due to the increased concentration of α-tocopherol achieved in the lung (Suntres 2002). Finally, bifunctional antioxidant liposomes containing both α-tocopherol and GSH provided increased protection against PQ-induced lung injuries compared to antioxidant liposomes containing only α-tocopherol (Suntres and Shek 1996). Thus, liposomal encapsulation improved the therapeutic potential of these antioxidants against PQ-induced lung injuries presumably due to their ability to

facilitate intracellular delivery and prolong the cellular retention of entrapped agents (Shek *et al.* 1994).

2.3.6 - Liposomal NAC

The liposomal formulation of N-acetylcysteine (L-NAC) has only recently been focused on for therapeutic potential in the lung. In 2000, Fan et al showed that liposomal antioxidants including NAC, both alone and in bifunctional liposomes with α-tocopherol, were successful in providing long-lasting protection against ARDS in rats by reducing the increase in transpulmonary albumin flux, neutrophil influx, and myeloperoxidase in the lung of shock/LPS rats (Fan *et al.* 2000). L-NAC was also shown to have a prophylactic effect against both LPS-induced lung injuries (Mitsopoulos *et al.* 2008) and LPS-induced hepatotoxicity in rats (Alipour *et al.* 2007). The use of L-NAC was also investigated in half sulfur mustard-induced acute lung injury in rats (McClintock *et al.* 2006, Hoesel *et al.* 2008) and guinea pigs (Mukherjee *et al.* 2009). McClintock et al. found that the effects of airway instillation of 2-chloroethyl ethyl sulfide (CEES), which has been shown to induce acute lung injury (assessed by the leakage of plasma albumin into the lung) in rats, were attenuated with immediate and 1 h-delayed instillation of liposomes containing reducing agents (i.e. NAC, GSH, or resveratrol) or bifunctional liposomes (containing NAC and GSH) (McClintock *et al.* 2006). Additionally, Hoesel et al. found that airway instillation of L-NAC was protective when administered 4 h following CEES application in rats, as well as 3 weeks after CEES with bifunctional α-tocopherol and NAC liposomes, though not with L-NAC alone after 3 weeks (Hoesel *et al.* 2008). Also, antioxidant liposomes

containing NAC, and α- and γ-tocopherol together were effective in providing protection 5 min and 1 h following CEES lung exposure in guinea pigs (Mukherjee *et al.* 2009). Thus, L-NAC possesses considerable therapeutic potential for the treatment of various lung diseases.

Objectives

Objective I: Characterize the uptake of NAC and L-NAC in A549 cells. The cytotoxicity of NAC will be assessed in A549 cells via the MTT assay to determine the concentration range in which NAC has no detrimental effect on cell viability, and the uptake of NAC delivered to A549 cells in both its free and liposomal formulation will be assessed via UPLC analysis of a concentration- and time-course of NAC and L-NAC exposure.

Objective II: Examine the effectiveness of NAC and L-NAC against PQ-induced cytotoxicity and delineate the mechanism(s) by which these antioxidant formulations confer their cytoprotection. PQ-challenged A549 cells pre-treated with NAC or L-NAC will be assessed for cytotoxicity via the MTT and LDH leakage assays, and the mechanism(s) of NAC and L-NAC cytoprotection will be investigated by assessing cellular PQ uptake, intracellular GSH content, ROS levels, cellular antioxidant potential, mitochondrial membrane potential, cellular gene expression, and inflammatory cytokine release.

Objective III: Assess whether the L-NAC confers a greater cytoprotective effect against PQ-induced cytotoxicity in A549 cells than NAC. This assessment will be based on the results of the aforementioned readouts (Objective II).

Methods

2.1 - Cell culture

Cell culture was performed as detailed in Chapter 1.

2.2 - N-acetylcysteine (NAC) preparation

NAC (N-acetyl-L-cysteine, SigmaUltra > 99 % TLC; Sigma-Aldrich) was dissolved in PBS and adjusted to pH 7.4 using an Accumet Basic pH Meter (Fisher Scientific) to produce a 0.1 M stock solution. Following filter sterilization (0.2 μm pore-size filters), specific volumes of NAC stock solution were added to culture media for the pre-treatment / treatment of cells. NAC stocks were made fresh daily.

2.3 - Liposomal-N-acetylcysteine preparation

Liposomal-N-acetylcysteine (L-NAC) was prepared from a mixture of DPPC (dipalmitoylphosphatidylcholine) and NAC in a 7:3 molar ratio by using a dehydration-rehydration method. The lipid was dissolved in chloroform in a 50 mL round-bottomed flask and dried at 45 °C with a rotary evaporator (Buchi Rotavapor R 205). The lipid film was dried with nitrogen to eliminate traces of chloroform and hydrated with a 2 mL sucrose-water solution (1:1; DPPC:sucrose, w/w) and subsequently sonicated (Model 500 Dismembrator, Fisher

Scientific) for 5 minutes (cycles of 40 s on and 20 s off). After formation of multilamellar vesicles, NAC was added to the solution and freeze-dried overnight. Upon rehydration with PBS (pH 6.5), the liposomal solution was placed in a water bath for 15 and 30 minutes and mixed, followed by centrifugation at 30,000 × g (TLA 110 rotor, Optima MAX Ultracentrifuge, Beckman Coulter) for 30 minutes at 4 °C to separate free-NAC. Liposomes were re-suspended in PBS (pH 7.4) and added to culture media for treatment of cells. Liposomal vesicle size was determined with a Submicron Particle Sizer (Nicomp Model 270) following rehydration and was found to have a mean diameter of 181.5 ± 19.6 nm. The encapsulation efficiency of NAC by DPPC-liposomes was measured as 18.5 %.

2.4 - PQ preparation

PQ was prepared as detailed in Chapter 1.

2.5 - Viability (MTT)

To determine the effect of NAC alone on viability, cells were treated with control or NAC-containing media (serum-free). To determine the effect of NAC or L-NAC pre-treatment on viability of PQ-challenged cells, cells were first pre-treated with control or NAC / L-NAC-containing media (5.0 mM for 4 h), followed by challenge with control or PQ-containing media (serum-free). The methodology was otherwise carried out as detailed in Chapter 1.

2.6 - Viability (LDH leakage)

Lactate dehydrogenase (LDH) leakage, an indicator of cell membrane integrity and therefore relative cell viability, was assessed using the Lactate Dehydrogenase-Based *In Vitro* Toxicology Assay Kit (Sigma-Aldrich). LDH is an enzyme that leaks out of the cell when the cellular membrane is compromised. Thus, the amount of cytoplasmic LDH released into the incubation media of treated cells can be quantified by measuring its enzymatic activity using a colorimetric-based system. This assay is based on the reduction of NAD^+ by LDH. The resulting NADH is utilized in the stoichiometric conversion of a tetrazolium dye, which can be quantified spectrophotometrically.

LDH leakage was measured in accordance with the manufacturer‟s instructions. A549 cells seeded were into sterile flat-bottom 96-well plates (Corning) at 10,000 cells/well and incubated overnight. Cells were pre-treated with control media or 5.0 mM NAC- or L-NAC-containing media for 4 h prior to 4 or 24 h PQ challenge (0, 0.25 or 1.0 mM). Following treatment, plates were centrifuged at 250 × g for 4 min to pellet debris, and 70 µL aliquots of the contents of each well were transferred to a clean 96-well plate. 46.7 µL of each of the provided LDH assay substrate, cofactor, and dye solutions were then added (collectively equalling twice the volume of sample media), and the plate was incubated at room temperature in the absence of light for 30 minutes. The reaction was terminated by the addition of 1N hydrochloric acid (20 µL) to each well, and absorbance was measured spectrophotometrically at a wavelength of 490 nm (690 nm wavelength correction) using a PowerWave XS Microplate Spectrophotometer (BioTek).

Absorbance was indirectly proportional to LDH leakage, and viabilities of treated cells were assessed relative to control cells.

2.7 - Ultra-performance liquid chromatography

To determine the uptake of NAC and its effect on intracellular GSH content, cells were treated with control or NAC / L-NAC-containing media (various concentrations and times; serum-free). To determine the effect of NAC or L-NAC pre-treatment on intracellular GSH content and levels of NAC and PQ uptake on PQ-challenged cells, cells were first pre-treated with control or NAC / L-NAC- containing media (5.0 mM for 4 h), followed by challenge with control or PQ-containing media (various concentrations and times; serum-free). The methodology was otherwise carried out as detailed in Chapter 1.

2.8 - Total protein assay

The total protein assay was performed as detailed in Chapter 1.

2.9 - Reactive oxygen species levels

To determine the effect of NAC or L-NAC pre-treatment on intracellular ROS levels in PQ-challenged cells, cells were first pre-treated with control or NAC / L-NAC- containing media (5.0 mM for 4 h), followed by challenge with control or PQ-containing media (0.25 or 1.0 mM for 4 h; serum-free). The methodology was otherwise carried out as detailed in Chapter 1.

2.10 - Total antioxidant potential

Total antioxidant potential was determined using the Bioxytech AOP-490 Colorimetric Quantitative Assay for Total Antioxidant Potential (Oxis International) in accordance with the manufacturer"s instructions. This assay is based upon the reduction of Cu^{++} to Cu^{+} by the combined actions of all the antioxidants present in the sample. Bathocuproine (2,9-dimethyl-4,7-diphenyl-1,10-phenanthroline), a chromogenic reagent, selectively forms a 2:1 complex with Cu^{+} and has a maximal absorbance at 490 nm. Briefly, cells were grown to 80 % confluence in sterile 150 cm^2 culture flasks (Corning) and pre-treated for 4 h with control media or 5.0 mM NAC- or L-NAC-containing media (serum-free) followed by challenge with 1.0 mM PQ for 4 h. Adherent cells were detached via trypsinization, washed once with PBS, and suspended in 100 µL PBS. Following sonication (20 s, 100 % amplitude; Sonic Dismembrator Model 500, Fisher Scientific), samples were centrifuged at 16,000 × g for 5 minutes at 4 ºC and aliquots of the supernatant were diluted 1:40 (i.e. 8 µL in 320 µL) with R1 reagent (containing bathocuproine) in a flat-bottom 96-well plate. Following a reference measurement (490 nm), 40 µL of R2

reagent (containing Cu^{++}) was added and incubated for 3 minutes. The reaction was terminated by the addition of a stop solution (40 µL), and the reference absorbance was subtracted from the final absorbance at 490 nm. Values were expressed as mM Uric Acid Equivalents by comparing the absorbance to a standard curve generated using uric acid.

2.11 - Superoxide dismutase activity

The activity of superoxide dismutase (SOD) enzymes in cell extracts was assessed using the Superoxide Dismutase Kit (R&D Systems, Minneapolis, MN, USA). In this assay, superoxide anions, generated by the conversion of xanthine to uric acid and H_2O_2 by xanthine oxidase, converted NBT to NBT-diformazan (absorbs light at 560 nm). SOD reduces superoxide ion concentrations and thus lowers the rate of NBT-diformazan formation. The percent inhibition of the formation of NBT-diformazan by SOD was converted to the relative SOD activity of the sample. Cells were seeded into sterile 150 cm^2 culture flasks (Corning) and grown to 80 % confluence. To determine the effect of NAC or L-NAC pre-treatment on the activity of SOD in PQ-challenged cells, cells were first pre-treated for 4 h with control or NAC / L-NAC-containing media (5.0 mM; serum-free), followed by 4 h challenge with control or PQ-containing media (0.25 mM; serum-free). Cells were lysed and relative SOD activity was assessed in accordance with the manufacturer‟s instructions using a PharmaSpec UV-1700 Visible Spectrophotometer (Shimadzu, Columbia, MD, USA).

2.12 - Mitochondrial membrane potential

To determine the effect of NAC or L-NAC pre-treatment on mitochondrial membrane potential in PQ-challenged cells, cells were first pre-treated with control or NAC / L-NAC- containing media (5.0 mM for 4 h), followed by challenge with control or PQ-containing media (0.25 or 1.0 mM for 4 h; serum-free). The methodology was otherwise carried out as detailed in Chapter 1.

2.13 – Quantitative polymerase chain reaction (qPCR)

To determine the effect of NAC or L-NAC pre-treatment on gene expression in PQ-challenged cells using the Human Stress & Toxicity PathwayFinder RT^2 Profiler PCR Array (SA Biosciences), cells were first pre-treated with control or NAC / L-NAC- containing media (5.0 mM for 4 h), followed by challenge with control or PQ-containing media (0.25 mM for 4 h; serum-free). The methodology was otherwise carried out as detailed in Chapter 1.

To determine the effect of NAC or L-NAC pre-treatment on gene expression in PQ-challenged cells using the RT^2 qPCR Primer Assays (Table 2.1; SA Biosciences), cells were first pre-treated with control or NAC / L-NAC- containing media (5.0 mM for 4 h), followed by challenge with control or PQ-containing media (0.25 mM for 4 h; serum-free). The methodology (RNA Isolation, Experion, First Strand cDNA Synthesis, and Real-Time PCR) was carried out similar to that detailed in Chapter 1, with the exception that 1 μL of the appropriate primer was manually

added to each well of the iCycler iQ 96 well PCR Plates (Bio-Rad), and were covered with Microseal „B" Film (Bio-Rad).

2.14 - Bio-Plex

To determine the effect of NAC or L-NAC pre-treatment on the secretion of inflammatory cytokines in PQ-challenged cells, cells were first pre-treated with control or NAC / L-NAC-containing media (5.0 mM for 4 h), followed by challenge with control or PQ-containing media (0.25 or 1.0 mM for 4 h; serum-free). The methodology was otherwise carried out as detailed in Chapter 1.

2.15 - Interleukin-8 secretion

Levels of interleukin-8 (IL-8) in cell culture supernatants were assessed using the Quantikine Human CXCL8/IL-8 Immunoassay (R&D Systems), a quantitative sandwich enzyme immunoassay technique. Briefly, cells were seeded into sterile flat-bottom 6-well plates (Corning) at 0.6×10^6 cells/well and grown to 80 % confluence overnight. To determine the effect of NAC or L-NAC pre-treatment on the secretion of IL-8 in PQ-challenged cells, cells were first pre-treated for 4 h with control or NAC / L-NAC- containing media (5.0 mM; serum-free), followed by 4 or 24 h challenge with control or PQ-containing media (0.25 mM; serum-free). Immediately following treatment, aliquots of cell culture supernatants were added to the

provided microplate pre-coated with a monoclonal antibody specific for IL-8. Thus, any IL-8 present in the sample was bound by the immobilized antibody and, after washing unbound substances, an enzyme-linked polyclonal antibody specific for IL-8 was added. Following washes to remove unbound antibody-enzyme reagent, a substrate solution was added and colour developed in proportion to the amount of IL-8 bound in the initial step. Absorbance values (measured at 450 nm, with wavelength correction at 570 nm) were interpolated to IL-8 concentrations via a standard curve of known values using a recombinant human IL-8 standard.

2.16 - Statistics

Statistical analysis was performed as detailed in Chapter 1.

Table 2.1: RT^2 qPCR Primer Assays gene table.

Unigene	GeneBank	Symbol	Description	Gene Name
Hs.502302	NM_001752	CAT	Catalase	MGC138422
Hs.72912	NM_000499	CYP1A1	Cytochrome P450, family 1, subfamily A, polypeptide 1	AHH/AHRR
Hs.25647	NM_005252	FOS	V-fos FBJ murine osteosarcoma viral oncogene homolog	
Hs.1722	NM_000575	IL1A	Interleukin 1, alpha	IL-1A/IL1
Hs.126256	NM_000576	IL1B	Interleukin 1, beta	IL-1/IL1-BETA
Hs.654458	NM_000600	IL6	Interleukin 6 (interferon, beta 2)	BSF2/HGF
Hs.624	NM_000548	IL8	Interleukin 8	
Hs.193717	NM_000572	IL10	Interleukin 10	
Hs.861	NM_002746	MAPK3	Mitogen-activated protein kinase 3	
Hs. 138211	NM_002750	MAPK8	Mitogen-activated protein kinase 8	
Hs.588289	NM_001315	MAPK14	Mitogen-activated protein kinase 14	
Hs.155396	NM_006164	NFE2L2	Nuclear factor (erythroid-derived 2)-like 2	
Hs.654408	NM_003998	NFKB1	Nuclear factor of kappa light polypeptide gene enhancer in B-cells 1 (p105)	DKFZp686C01211/EBP-1
Hs.81328	NM_020529	NFKBIA	Nuclear factor of kappa light polypeptide gene enhancer in B-cells inhibitor, alpha	IKBA/MAD-3
Hs.523185	NM_012423	RPL13A	Ribosomal protein L13a	RPL13A
Hs.443914	NM_000454	SOD1	Superoxide dismutase 1, soluble (amyotrophic lateral sclerosis 1 (adult))	ALS/ALS1

Results

Effect of NAC alone on viability of A549 cells. Viability of cells treated with NAC alone was unchanged following 24 h with concentrations ranging from 0 - 10.0 mM. However, a 30 % decrease in viability relative to control cells was observed following treatment with 50.0 mM NAC (Figure 2.1).

Uptake of NAC in A549 cells and its effect on cellular GSH content. The uptake of NAC by A549 cells was assessed using UPLC following treatment with 5.0 mM NAC- or L-NAC-containing media for 0, 1, 2, 4, 8, and 24 h (Figure 2.2 A). Treatment with free-NAC resulted in increased NAC uptake following 1 and 2 h treatment, with levels remaining unchanged between 2 and 24 h. Cells treated with L-NAC exhibited increased uptake over time, with maximal levels achieved following 4 h treatment. However, levels of NAC uptake in L-NAC-treated cells decreased between 4 and 24 h treatment. Interestingly, under all investigated conditions, the uptake of NAC by A549 cells was significantly greater following treatment with the liposomal formulation compared to free-NAC.

In addition, intracellular GSH content of samples was measured in concert with NAC uptake via UPLC. GSH levels remained relatively constant through 8 h of treatment with free- and liposomal-NAC, but decreased significantly in both cases following 24 h treatment relative to 4 h treated cells (Figure 2.2 B). Based on Figures 2.1 – 2.2, the treatment conditions which resulted in optimal uptake of NAC without compromising cell viability or intracellular redox status (i.e.

GSH levels) were found to be 5.0 mM for 4 h. These conditions were used for all subsequent NAC and L-NAC pre-treatments.

Effect of NAC and L-NAC pre-treatment on cell viability post-PQ challenge. Viability of cells challenged with PQ (0.1 and 0.5 mM) for 24 h, as assessed by measuring the activity of mitochondrial and cytosolic dehydrogenases via the MTT assay, was higher in those cells pre-treated with L-NAC (Figure 2.3). In contrast, NAC pre-treatment did not confer any observable effect on cell viability of PQ-challenged cells under these conditions. In addition, no significant changes in the amount of LDH leakage was observed following 4 h PQ exposure (Figure 2.4 A), though both NAC or L-NAC pre-treatment protected against LDH leakage following 24 h exposure with both 0.25 and 1.0 mM PQ, returning leakage to basal levels in each case (Figure 2.4 B). LDH leakage is frequently used as an indicator of cell membrane integrity and viability.

Effect of NAC and L-NAC pre-treatment on cellular redox status and PQ uptake following PQ challenge. Exposure of cells to increasing concentrations of PQ for 24 h significantly decreased intracellular GSH content, which correlated with increases in cellular PQ uptake, as measured by UPLC analysis (Figure 2.5). Pre-treatment with L-NAC was effective in increasing intracellular GSH content of cells exposed to 0.1 or 0.5 mM PQ compared to cells without pre-treatment, while NAC pre-treatment was only effective in increasing GSH content of 0.5 mM PQ-challenged cells. Pre-treatment with NAC or L-NAC had no effect on the linear ($R^2 = 0.969$) uptake of PQ in A549 cells challenged with increasing concentrations of PQ (Figure 2.5 B). In

accordance with the data on intracellular GSH content under the studied conditions, ROS levels increased following PQ exposure, but pre-treatment with NAC or L-NAC significantly reduced levels of ROS in 0.25 and 1.0 mM PQ-challenged cells (4 h) to either basal or sub-basal levels as assessed via flow cytometric analysis of CM-H_2DCFDA stained cells (Figure 2.6). In fact, pre-treatment of control cells also reduced levels of intracellular ROS below basal levels. In addition cells challenged with 0.25 mM PQ for 4 h exhibited decreased cellular antioxidant potential, but this was returned to basal levels when pre-treated with either NAC or L-NAC (Figure 2.7). Finally, preliminary data regarding the enzymatic activity of cellular superoxide dismutases in cells challenged with 0.25 mM PQ for 4 h indicated that activities were increased following PQ exposure compared to untreated control cells, but decreased when pre-treated with L-NAC (Figure 2.8). No apparent difference in superoxide dismutase activity was observed in PQ-challenged cells pre-treated with NAC.

Effect of NAC or L-NAC pre-treatment on mitochondrial membrane potential following PQ challenge. The mitochondrial membrane potential of cells challenged with 0.25 mM PQ for 4 h was significantly decreased relative to untreated control cells, and was further decreased following 1.0 mM PQ challenge. Pre-treatment with L-NAC was effective in preventing the decreases of mitochondrial membrane potential in both 0.25 and 1.0 mM PQ-challenged cells, returning it to basal levels in the former, as well as increasing it nearly 2-fold in untreated control cells (Figure 2.9). Conversely, pre-treatment with NAC only significantly prevented the decrease in mitochondrial membrane potential of 0.25 mM PQ-challenged cells, having no apparent effect on untreated control or 1.0 mM PQ-challenged cells.

Effect of NAC or L-NAC pre-treatment on cellular gene expression following PQ challenge. Changes in gene expression were assessed using a PCR array designed to study genes involved in cellular stress and toxicity. The magnitude of gene expression in cells pre-treated with NAC or L-NAC prior to 0.25 mM PQ challenge for 4 h was generally decreased relative to challenged cells with no pre-treatment (Figure 2.10). Fold changes (relative to control cells) of each gene of the array following PQ challenge with no pre-treatment, NAC pre-treatment, or L-NAC pre-treatment are listed in Table 2.2.

The expression of many oxidative or metabolic stress-related genes, including CAT, GPX1, MT2A, PRDX1, SOD1, and SOD2, remained unchanged relative to control cells following PQ challenge regardless of pre-treatment (Table 2.2.1). However, the expression patterns of other genes were altered, such as the 4.6-fold increase in CYP1A1 in PQ-challenged cells with L-NAC pre-treatment compared to a 1.4-fold decrease with no pre-treatment. Also noteworthy is the expression of POR, which was down-regulated 1.7-fold following PQ challenge with no pre-treatment, but was up-regulated 2.2-fold with NAC pre-treatment. With respect to the expression of heat shock genes, DNAJA1 and DNAJB4 were increased 1.6- and 1.7-fold, respectively following PQ challenge with no pre-treatment, but NAC pre-treatment limited this increase and L-NAC pre-treatment maintained expression at control levels (Table 2.2.2). The expression of heat shock genes was otherwise not substantially altered under the studied conditions. In regards to genes involved with proliferation and carcinogenesis, the expression of EGR1 was increased 2.8-fold in PQ challenged cells with no pre-treatment, and though NAC pre-treatment did not significantly alter this, L-NAC pre-treatment prevented expression from increasing beyond control levels (Table 2.2.3). GDF15 expression was increased following PQ challenge with no

pre-treatment, and though NAC pre-treatment did not significantly alter GDF15 expression levels, the increase was limited in cells pre-treated with L-NAC (i.e. 1.5-fold increase with L-NAC pre-treatment compared to 1.9-fold increase with no pre-treatment; Table 2.2.4). The expression patterns of several inflammatory genes were also altered in PQ-challenged cells pre-treated with NAC and/or L-NAC relative to cells with no pre-treatment. For instance, the increases in expression of certain genes (i.e. IL18 and SERPINE1) in PQ-challenged cells with no pre-treatment were limited when pre-treated with L-NAC (Table 2.2.5). IL-6 was found to be highly up-regulated in all studied conditions, with greatest up-regulation following L-NAC pre-treatment of PQ-challenged cells. Alternatively, LTA was significantly decreased (2.3-fold) in PQ-challenged cells pre-treated with L-NAC compared with the fold changes from the other studied conditions, while other genes were not found to be expressed (i.e. CCL21, CCL3, CCL4, CSF2, and CXCL10). Expression of the majority of DNA damage and repair genes were not substantially altered between conditions with the exception of ATM, which was increased 2.3-fold in PQ-challenged cells with no pre-treatment, but NAC and L-NAC pre-treatment prevented its expression from changing from control levels (Table 2.2.6). Finally, the expression of many apoptosis signalling genes were not altered under the studied conditions with the exception of CASP10, which was increased in PQ-challenged cells with no pre-treatment. This increase was limited when pre-treated with NAC, and further limited with L-NAC pre-treatment (Table 2.2.7).

Individual primer assays were also performed under the same conditions to confirm findings obtained from the gene arrays. For these assays, an additional condition was performed in which PQ-challenged cells were pre-treated with empty liposomes (EL). Similar gene expression patterns were observed for the majority of the genes (i.e. CAT, CYP1A1, IL1A, NFKB1,

NFKBIA, SOD1, and TNF) analyzed by both gene array and individual primer assays (Table 2.3).

The expression patterns of additional genes not analyzed via the gene array were investigated with individual primer assays (Table 2.4). The expression of FOS was unchanged from control levels following PQ challenge with no pre-treatment, but NAC pre-treatment caused a significant increase in expression (2.2-fold). IL8 expression was significantly increased in non-pre-treated cells challenged with PQ, but this increase was limited with NAC or L-NAC pre-treatment. Expression of IL10 exhibited a similar pattern where NAC and L-NAC pre-treatment ameliorated the 3-fold decrease in expression of PQ-challenged cells with no pre-treatment. Finally, NFE2L2 exhibited increased expression in PQ-challenged cells with no pre-treatment, but this increase was limited with L-NAC pre-treatment.

Measures were taken throughout the quantitative gene expression procedure for both the gene array and individual primer assays to ensure that reliable results were obtained. Figure 1.8 depicts representative gels and electropherograms of extracted RNA samples, achieved using the Experion automated electrophoresis station, indicating high RNA integrity with little or no apparent degradation of 18 and 28 S rRNA. Additionally, a single peak (or zero if no product was amplified) was present in first-derivative dissociation curves for every PCR reaction on all arrays and individual primer assays, indicating that only a single PCR product (i.e. the gene of interest) was amplified in each case (Figure 1.9 depicts representative dissociation curves of individual primer assays).

Effect of NAC or L-NAC pre-treatment on the secretion of inflammatory cytokines post-PQ challenge. Levels of IL-8 secreted by cells exposed to 0.25 mM and 1.0 mM PQ were significantly increased relative to untreated control cells (Figure 2.12 A). Both NAC and L-NAC pre-treatments decreased IL-8 levels in untreated control cells and 0.25 mM PQ-challenged cells, while L-NAC, but not NAC, was also able to significantly reduce levels of IL-8 following 1.0 mM PQ challenge. Pre-treatment of PQ-challenged cells was less effective in altering IL-6 secretion (Figure 2.12 B). Though both NAC and L-NAC pre-treatment lowered IL-6 levels in untreated control cells, only NAC pre-treatment was able to significantly decrease IL-6 levels of 0.25 mM PQ-challenged cells. Levels of IL-1β, IL-10, IL15, TNF-α, and eotaxin were not reliably detectable under these conditions. In addition, a second method of IL-8 detection was employed to confirm the results achieved using Bio-Plex analysis. A quantitative sandwich enzyme immunoassay of cells challenged for 24 h with 0.25 mM PQ indicated that both NAC and L-NAC pre-treatments decreased the more than 4-fold increase in IL-8 secretion caused by PQ exposure by 1.6- and 2.1-fold, respectively (Figure 2.13).

Discussion

The protective effect of the thiol-containing antioxidant N-acetylcysteine (NAC), both in its free and liposomal (L-NAC) form, was investigated in PQ-induced cytotoxicity. In addition to directly scavenging ROS via its thiol group, the membrane-permeable NAC is also a source of cysteine, the limiting pre-cursor to intracellular glutathione synthesis (Arakawa and Ito 2007, Sadowska *et al.* 2007, Atkuri *et al.* 2007). These two modes of action make NAC a suitable candidate for the amelioration of PQ-induced toxicity.

The optimal pre-treatment conditions for NAC and L-NAC in A549 cells were investigated for subsequent experiments involving PQ challenge. NAC has been reported to exhibit cytotoxicity at variable concentrations depending on cell type: 10 mM NAC was non-toxic in human bronchial epithelial cells (Sadowska *et al.* 2007), 40 mM was non-toxic in 3T3 fibroblasts (Hong *et al.* 2003), and 50 mM was non-toxic in aortic endothelial cells (Sadowska *et al.* 2007); however, 30 mM was cytotoxic in vascular smooth muscle cells, monocytes and neutrophils (Sadowska *et al.* 2007), and as low as 5.0 mM NAC was cytotoxic in porcine aortic endothelial cells (Sadowska *et al.* 2007). Studies involving NAC in A549 cells have generally employed concentrations ranging from 1 to 10 mM (Cappelletti *et al.* 1998, Kim *et al.* 2007, Rogalska *et al.* 2008, Woo *et al.* 2008, Wu *et al.* 2005, Heberlein *et al.* 2000, Alexandre *et al.* 2006). Our results indicate that concentrations of 10.0 mM or less had no negative impact on viability, while a greater concentration (i.e. 50.0 mM) resulted in significantly decreased viability after 24 h (Figure 2.1). Since the uptake of NAC in A549 cells has yet to be well characterized, the cellular uptake of 5.0 mM NAC and L-NAC, a concentration within the non-cytotoxic range, was

assessed using UPLC over a 24 h time-course. The cellular uptake of NAC, when delivered in its free form, was found to plateau after 2 h incubation, while uptake with L-NAC incubation was optimal after 4 h (Figure 2.2 A). It should be noted that liposomes enhanced the delivery of NAC in the A549 cells since the cellular uptake of this antioxidant was greater (i.e. up to 4-fold) under all conditions when delivered as L-NAC compared to free-NAC (Figure 2.2 A). These results, in concert with intracellular GSH data under the same conditions (Figure 2.2 B), indicated that the optimal conditions for the uptake of NAC via both the free and liposomal formulations, without compromising cell viability or cellular redox status (i.e. GSH levels), was 5.0 mM for 4 h. These conditions were used for all subsequent pre-treatments in this study.

The effect of NAC or L-NAC pre-treatment on the viability of PQ-challenged cells was assessed via the MTT and LDH leakage assays. L-NAC pre-treatment limited the decrease in viability of 24 h PQ-challenged cells by up to 23 % at various PQ concentrations (i.e. 0.1 and 0.5 mM) as measured by the MTT assay, while NAC pre-treatment did not exhibit any significant protective effect (Figure 2.3). Assessment of LDH-leakage indicated that, while there were no significant changes in 4 h PQ-challenged cells (Figure 2.4 A), NAC or L-NAC pre-treatment of 24 h PQ-challenged cells (i.e. 0.25 or 1.0 mM) prevented the increase in LDH leakage observed in cells with no pre-treatment (Figure 2.4 B), correlating with similar findings in PQ-challenged hepatocytes co-incubated with NAC (Dawson *et al.* 1984). Since NAC or L-NAC pre-treatment had no effect on intracellular PQ levels in A549 cells (Figure 2.5 B), agreeing with data obtained by Hoffer et al. in alveolar type II cells (Hoffer *et al.* 1996), it is evident that pre-treatment with NAC or L-NAC conferred protection against PQ-induced cytotoxicity independent of PQ uptake.

The effects of NAC's antioxidant properties in PQ-induced cytotoxicity were investigated by assessing the cellular redox status of PQ-challenged cells pre-treated with NAC or L-NAC. Pre-treatment with NAC significantly limited the decrease of cellular GSH content in cells challenged with 0.5 mM PQ for 24 h, while L-NAC pre-treatment exhibited the same effect in cells challenged with both 0.1 and 0.5 mM PQ (Figure 2.5 A). It is unclear whether this is a result of NAC's direct scavenging properties or the *de novo* synthesis of GSH using NAC as a precursor. The effect of NAC or L-NAC pre-treatment of PQ-challenged cells was further investigated by assessing intracellular ROS levels. In addition to decreasing basal levels of ROS in control cells, pre-treatment with either formulation limited ROS to basal or sub-basal levels following both 0.25 and 1.0 mM PQ challenges (Figure 2.6). Similarly, the total antioxidant potential (i.e. the total reducing capacity of all cellular antioxidants) of PQ-challenged cells (0.25 mM for 4 h) was decreased relative to control cells, but pre-treatment with NAC or L-NAC maintained basal levels following PQ challenge (Figure 2.7). Finally, preliminary data indicated that the increased activity of SOD observed following 0.25 mM PQ challenge for 4 h was modulated with L-NAC, but not NAC, pre-treatment (Figure 2.8). These data indicate that NAC, either in its free or liposomal form, confers some level of protection against PQ-induced cytotoxicity by maintaining a normal cellular redox status. These effects were more prominent in cells pre-treated with L-NAC, which can be attributed to the greater intracellular NAC levels achieved via liposomal delivery.

The mitochondria are thought to be essential targets of PQ and important in its toxicity. In fact, there is evidence that PQ disrupts the mitochondrial electron transfer chain resulting in a reduction of metabolic function, and it is suggested that lesions due to PQ first occur in the

mitochondria (Fukushima *et al.* 2002). Pre-treatment with NAC or L-NAC exhibited a beneficial effect on the mitochondrial membrane potential of PQ-challenged cells (Figure 2.9). NAC or L-NAC pre-treatment increased the membrane potential above control levels in 0.25 mM PQ-challenged cells for 4 h, while L-NAC, but not NAC, pre-treatment limited the decrease of membrane potential in cells exposed to 1.0 mM PQ. Interestingly, control cells pre-treated with L-NAC exhibited nearly a 2-fold increase in fluorescence intensity relative to control cells with no pre-treatment. Previous studies by Suntres et al. (1993) have shown that radioactively-labelled liposomal antioxidant vesicles were associated with mitochondria, and antioxidants that are selectively accumulated into mitochondria can inhibit mitochondrial oxidative damage that contributes to a range of degenerative diseases related to oxidative stress (Suntres *et al.* 1993).

In order to further investigate the protective effects of NAC or L-NAC pre-treatment in PQ-challenged cells, cellular gene expression was investigated in 4 h PQ-challenged cells with or without pre-treatment using PCR arrays specific for genes relating to cellular stress and toxicity. Gene expression was investigated under these conditions since many genes were found to be differentially expressed after 4 h in 0.25 mM PQ-challenged cells (Table 1.2). In this study, the magnitude of gene expression in cells pre-treated with NAC or L-NAC prior to 0.25 mM PQ challenge for 4 h was generally decreased relative to challenged cells with no pre-treatment (Figure 2.10). Although the exact mechanism(s) by which NAC affected the pathways involved in signal transduction and gene expression cannot be delineated from the results of this study, it is possible that these pathways are regulated by oxidants and redox-sensitive steps since increasing levels of intracellular NAC (Figures 2.1 and 2.2) affect the steady state level of oxidants (Figure 2.6) and can modify the redox status of the cell (Figures 2.5 and 2.7), an effect

known to exert a regulatory effect on transcriptional activation and gene expression (Zafarullah *et al.* 2003, Garcia-Ruiz and Fernandez-Checa 2007, Oktyabrsky and Smirnova 2007). In the next few paragraphs, the modulation of gene expression of PQ-challenged cells by NAC and L-NAC is discussed.

Several genes known to be induced in cases of cellular stress were differentially expressed. Expression of GDF15, which is present in a wide variety of epithelial cells, is known to be dramatically increased in response to acute injury (Bauskin *et al.* 2006). Accordingly, our data indicates this gene was up-regulated 1.9-fold in PQ-challenged cells, and its expression was ameliorated with L-NAC, but not NAC, pre-treatment (Table 2.2.4). Additionally, NFE2L2, a gene coding for a transcription factor that induces cytoprotective genes in response to various stressors (Yang *et al.* 2007), was up-regulated over 3-fold in PQ-challenged cells with no pre-treatment, but this was ameliorated in challenged cells pre-treated with L-NAC (Table 2.4). ATM, which is up-regulated in response to DNA damage (Zenz *et al.* 2008), was also up-regulated over 2-fold in PQ-challenged cells with no pre-treatment, but its expression was maintained at basal levels when challenged cells were pre-treated with NAC or L-NAC (Table 2.2.6). Lastly, the expression of CASP10, which codes for the initiator caspase-10 involved in the death-inducing signalling complex during apoptosis (Bidere *et al.* 2006), was up-regulated 1.9-fold in PQ-challenged cells with no pre-treatment, but was ameliorated in challenged cells pre-treated with L-NAC (Table 2.2.7).

The expression and/or secretion of a variety of inflammatory mediators in PQ-challenged cells were modulated with NAC or L-NAC pre-treatment. The expression of IL8, the gene coding for

the pro-inflammatory neutrophil chemoattractant IL-8, was up-regulated in 4 h PQ-challenged cells with no pre-treatment, but its expression was substantially modulated with NAC or L-NAC pre-treatment (Table 2.4). This correlated with decreased IL-8 protein secretion in the cell culture supernatant of PQ-challenged cells pre-treated with NAC or L-NAC (Figures 2.13 A and 2.14). This effect was observed via Bio-Plex after 4 h PQ challenge (Figure 2.13 A), where NAC or L-NAC pre-treatment reduced IL-8 secretion in 0.25 mM PQ-challenged cells, but only L-NAC pre-treatment was able to significantly reduce IL-8 protein secretion following 1.0 mM PQ exposure. This effect was confirmed after 24 h PQ challenge (0.25 mM) via a quantitative sandwich enzyme immunoassay technique (Figure 2.14). These effects exhibited by NAC are in accordance with other studies: the increased IL-8 gene (Bianchi *et al.* 1993) and protein (Horiguchi *et al.* 1993) expression of PQ-challenged peripheral blood mononuclear cells was blocked by NAC (Horiguchi *et al.* 1993), and NAC administration was found to inhibit the release of chemotactic factors for neutrophils and consequently reduce their infiltration into the lungs of PQ-challenged rats (Hoffer *et al.* 1993). The protective effects of NAC on IL-8 gene and protein expressions in our study were more evident in cells pre-treated with the liposomal formulation than free-NAC, which is attributed to the increased intracellular NAC levels achieved via liposomal delivery.

Other inflammatory genes were also differentially expressed under the conditions studied. IL10, which codes for the anti-inflammatory cytokine interleukin-10 (IL-10), is down-regulated 3-fold following PQ-challenge (Table 2.4), suggesting that the cell may be actively repressing anti-infammatory mediators in favor of pro-inflammatory mediators (i.e. IL-8). However, expression of IL10 is maintained at basal levels with L-NAC pre-treatment, suggesting that the

inflammatory response is tempered due to L-NAC‟s cytoprotection. Since this effect is present in challenged cells pre-treated with L-NAC, but not NAC or EL (i.e. the liposomes themselves have no direct effect), it is thus attributable to the increased intracellular NAC content achieved via liposomal delivery.

The expressions of other pro-inflammatory cytokines in PQ-challenged cells were affected by NAC or L-NAC pre-treatment. IL18 expression, which was slightly up-regulated in PQ-challenged cells with no pre-treatment, was ameliorated in challenged cells with L-NAC pre-treatment (Table 2.2.5). LTA, a characteristic cytokine of Th1 cells which codes for TNF-β/lymphotoxin (Lin *et al.* 2008), was found to become down-regulated in the L-NAC pre-treated group while remaining at basal levels in PQ-challenged cells with no pre-treatment or NAC pre-treatment.

Finally, certain genes relating to the cell cycle were differentially expressed under the conditions examined. EGR1, which encodes a transcriptional regulator that activates genes (including p53) required for differentiation and mitogenesis (Sperandio *et al.* 2009), was substantially up-regulated in PQ-challenged cells with no pre-treatment, but its expression was ameliorated with L-NAC pre-treatment, where basal expression was maintained (Table 2.2.3). The expression of E2F1, which codes for a transcription factor that regulates several important genes involved in cell cycle progression (i.e. G_1/S and G_2/M progression) (Tategu *et al.* 2008), was further down-regulated in the L-NAC, but not NAC, pre-treatment group compared to challenged cells with no pre-treatment (Table 2.2.3).

Gene array data was validated using quantitative RT-PCR of various genes (Table 2.3), the majority of which (i.e. CAT, CYP1A1, IL1A, NFKB1, NFKBIA, SOD1, and TNF) exhibited similar expression patterns to those achieved via gene array analysis. In addition, only quality RNA samples showing no signs of degradation were used for both gene array and quantitative RT-PCR analyses (Figure 2.11), and a first-derivative dissociation curve was created following each PCR reaction to ensure the presence of a single PCR product (Figure 2.12).

Based on these data, it was evident that NAC pre-treatment, both in its free and liposomal form, conferred cytoprotection against PQ-induced toxicity in A549 cells. This was mainly attributed to its ability to ameliorate cellular redox status (i.e. intracellular GSH content, ROS levels, and total antioxidant potential), and was independent of PQ uptake. In addition, antioxidant pre-treatment conferred a beneficial effect on mitochondrial membrane potential, and decreased the expression of a variety of genes known to be up-regulated under acute stress conditions (i.e. GDF15, NFE2L2, and ATM). NAC and/or L-NAC pre-treatment also lessened the inflammatory response of A549 cells to PQ toxicity, in particular decreasing both IL-8 gene and protein expressions and modulating IL-10 gene expression. These protective effects were more evident in cells pre-treated with L-NAC, which is attributed, at least in part, to the increased NAC levels achieved via liposomal delivery.

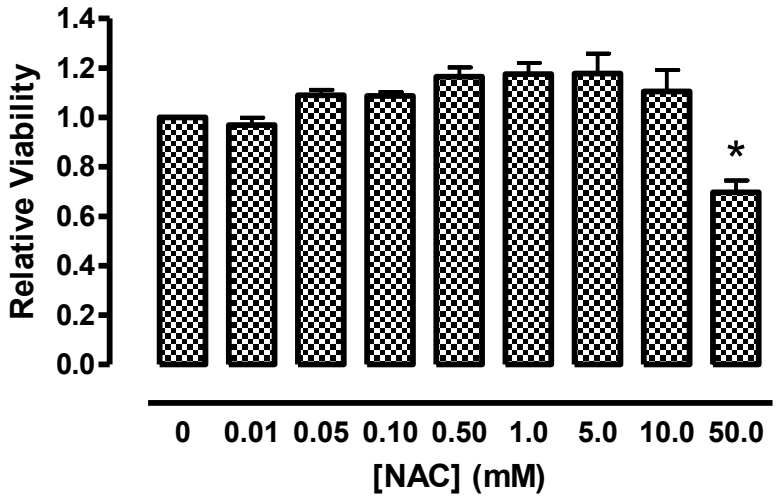

Figure 2.1: Effect of NAC concentration on the viability of A549 cells. Viabilities of cells treated for 24 h with increasing concentrations of NAC (0 - 50.0 mM) were assessed using the MTT colorimetric assay. Cells were seeded into 96-well plates at 10,000 cells/well and grown to 80 % confluence prior to treatment. Absorbance was measured spectrophotometrically at 570 nm (650 nm correction wavelength), and viability of treated cells was assessed relative to control cells. Bars represent mean ± S.E.M. of 3 independent experiments performed in octuplet. * denotes significant difference relative to control ($p < 0.05$).

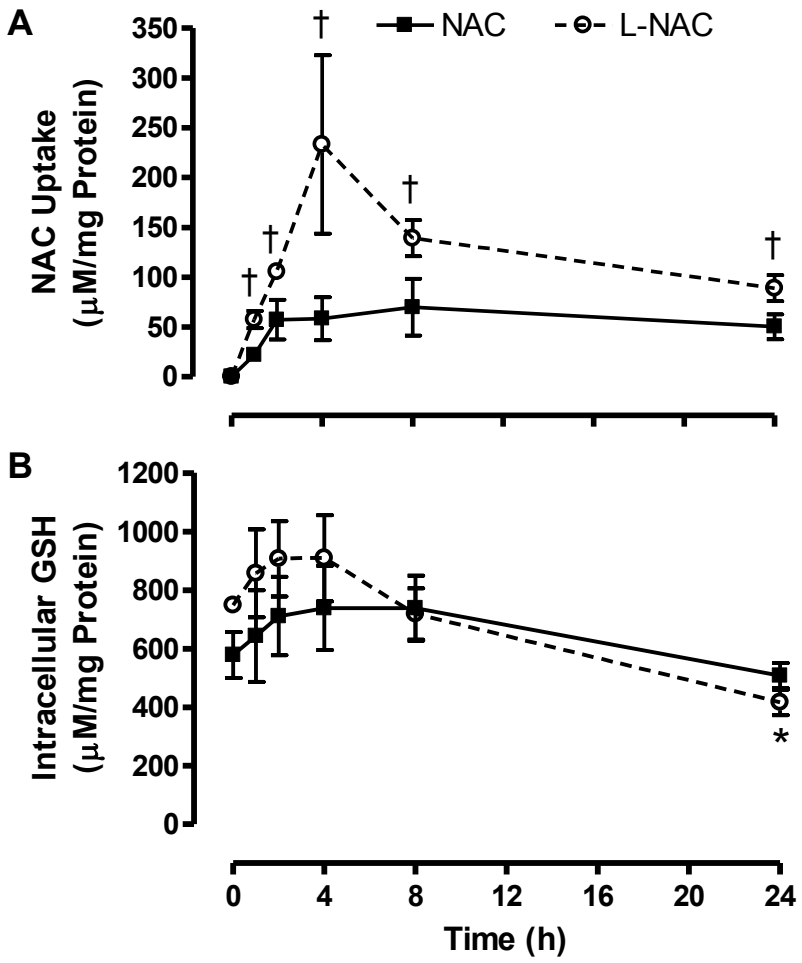

Figure 2.2: Uptake of NAC in A549 cells and its effect on cellular GSH content. Cells were treated with either 5.0 mM NAC- or L-NAC-containing media for various time-points up to 24 h. NAC uptake (A) and intracellular GSH content (B) were measured concomitantly via UPLC (solid line: NAC treatment; dotted line: L-NAC treatment). Lysates were normalized to total protein. Data points represent mean ± S.E.M. of 3 independent experiments performed in duplicate. † denotes significant difference relative to NAC-treated group; * denotes significant difference relative to 0 h untreated control ($p < 0.05$).

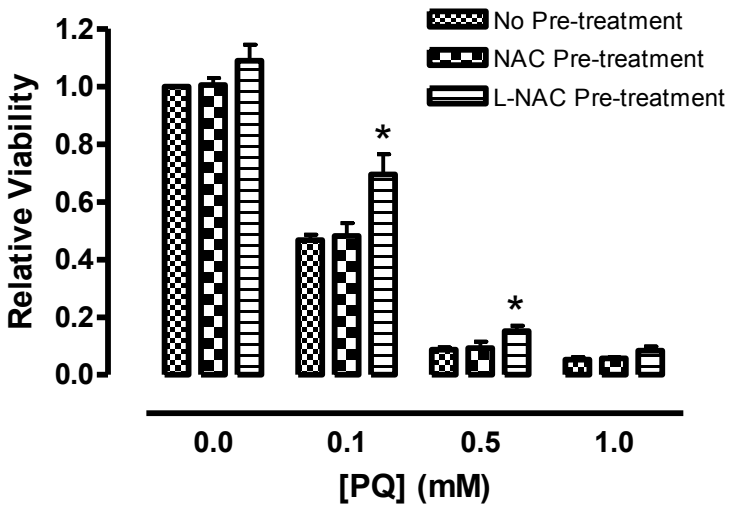

Figure 2.3: Effect of NAC or L-NAC pre-treatment on viability of PQ-challenged cells. The viability of cells pre-treated with control media (No Pre-treatment), or 5.0 mM NAC- (NAC Pre-treatment) or L-NAC-containing media (L-NAC Pre-treatment) for 4 h prior to 24 h PQ challenge (0, 0.1, 0.5, or 1.0 mM) was assessed using the MTT colorimetric assay. Viability of challenged cells was assessed relative to untreated control cells. Bars represent mean ± S.E.M. of 3 independent experiments performed in octuplet. * denotes significant difference relative to cells with no pre-treatment ($p < 0.05$).

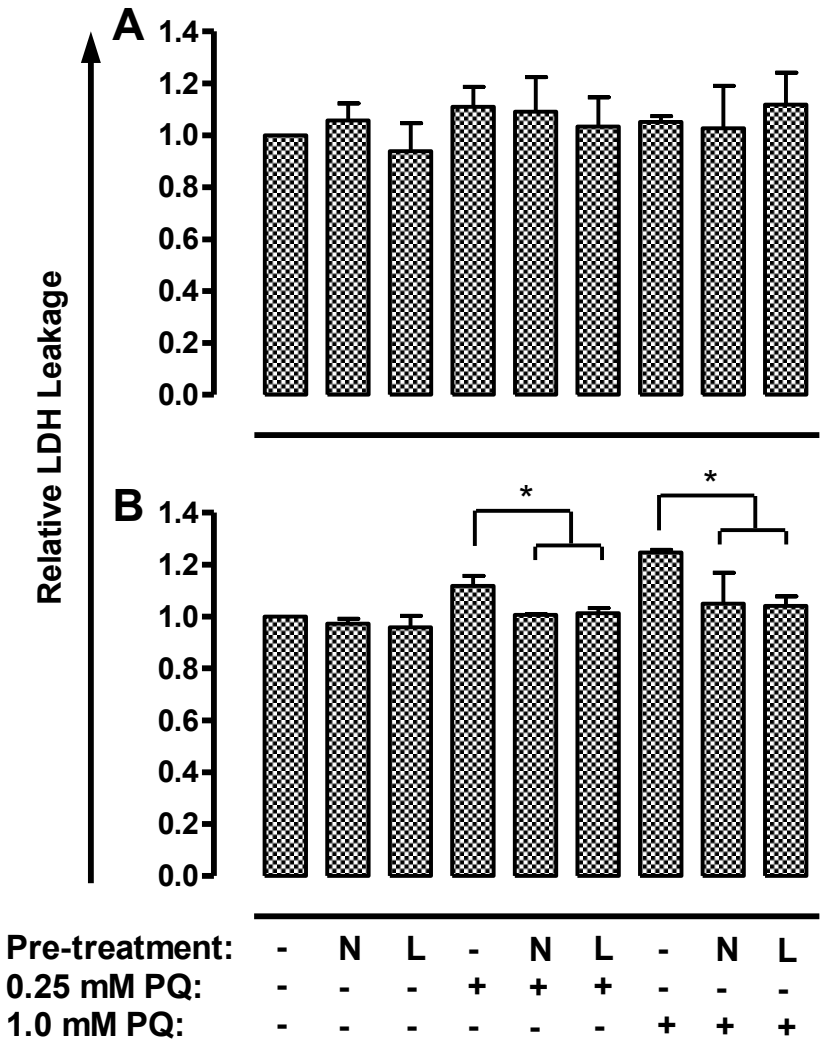
A
B
Relative LDH Leakage
1.4
1.2
1.0
0.8
0.6
0.4
0.2
0.0
*
*
Pre-treatment: - N L - N L - N L
0.25 mM PQ: - - - + + + - - -
1.0 mM PQ: - - - - - - + + +

Figure 2.4: Effect of NAC or L-NAC pre-treatment on LDH leakage in PQ-challenged cells. The cellular membrane integrity of cells pre-treated for 4 h with control media or 5.0 mM NAC-(N) or L-NAC-containing media (L) prior to 4 (A) or 24 h (B) PQ exposure (0, 0.25, or 1.0 mM) was assessed by measuring the relative amounts of LDH leakage into cell culture supernatants from control and challenged cells. Absorbance was measured spectrophotometrically at 490 nm (690 nm correction wavelength), and LDH leakage was assessed relative to untreated control cells. Bars represent mean ± S.E.M. of 3 independent experiments performed in octuplet. * denotes significant difference relative to PQ-challenged cells with no pre-treatment ($p < 0.05$).

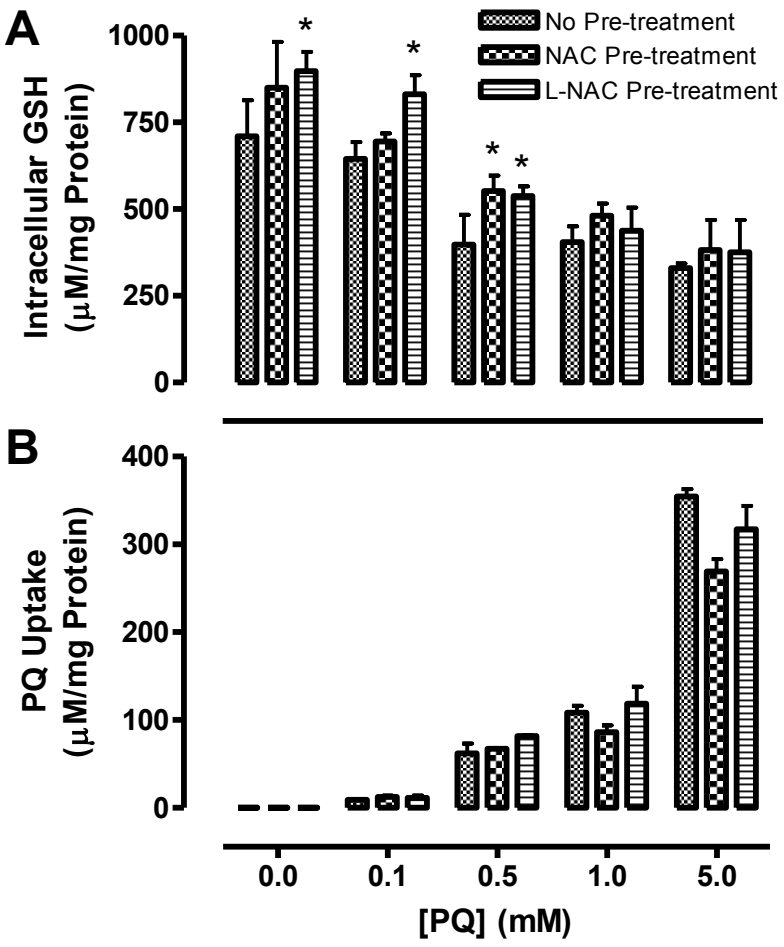

Figure 2.5: Effect of NAC or L-NAC pre-treatment on GSH content and PQ uptake of PQ-challenged cells. Cells pre-treated for 4 h with control media (No Pre-treatment) or 5.0 mM NAC- (NAC Pre-treatment) or L-NAC-containing media (L-NAC Pre-treatment) were challenged with increasing PQ concentrations (0, 0.1, 0.5, 1.0, and 5.0 mM) for 24 h. Cells were harvested and lysed for the determination of intracellular GSH content (A) and PQ uptake (B) via UPLC analysis. Lysates were normalized to total protein. Bars represent mean ± S.E.M. of 3 independent experiments performed in duplicate. * denotes significant difference relative to cells with no pre-treatment ($p < 0.05$).

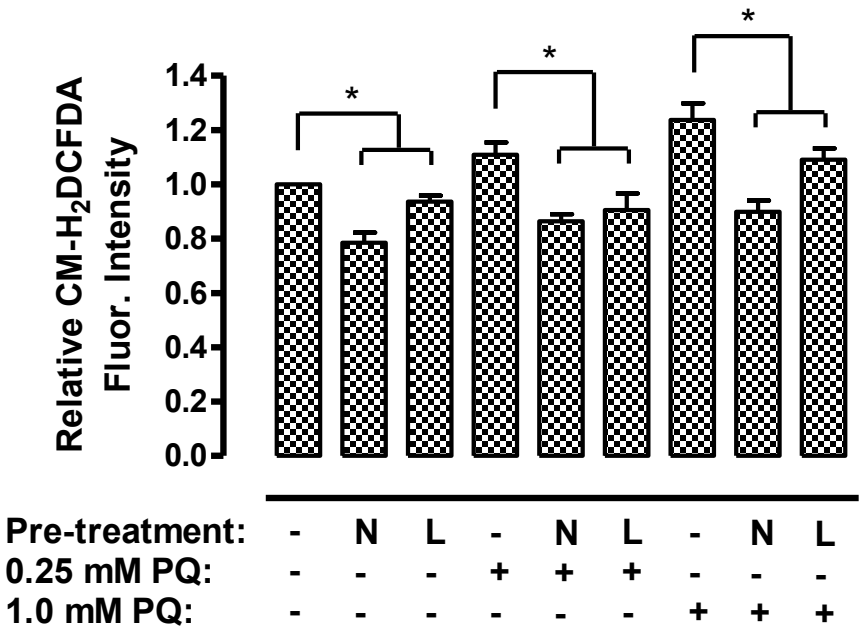

Figure 2.6: Effect of NAC or L-NAC pre-treatment on levels of intracellular ROS following PQ challenge. Cells pre-treated for 4 h with control media or 5.0 mM NAC- (N) or L-NAC-containing media (L) were challenged with 0, 0.25 or 1.0 mM PQ for 4 h. Cells were stained for 30 min post-treatment with the cell permeable CM-H_2DCFDA fluorescent dye specific for oxidative species. Adherent cells were scraped and analyzed flow cytometrically using the FL1-H channel. Bars represent mean ± S.E.M. of 3 independent experiments. * denotes significant difference relative to cells with no pre-treatment ($p < 0.05$).

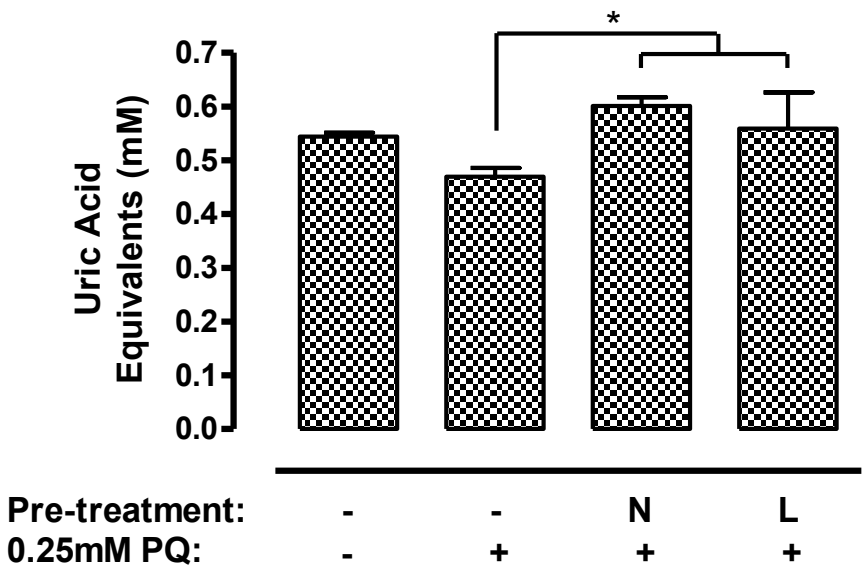

Figure 2.7: Effects of NAC or L-NAC pre-treatment on total antioxidant potential in PQ-challenged cells. Cells were pre-treated for 4 h with 5 mM NAC- (N) or L-NAC-containing media (L), followed by 0 or 0.25 mM PQ challenge for 4 h. Absorbance of cell lysates was measured at 490 nm following the addition of a chromogenic reagent, which formed a complex with Cu^{+} upon its reduction by cellular antioxidants. Total cellular antioxidant potential was measured in uric acid equivalents. Bars represent mean ± S.E.M. of 3 independent experiments. * denotes significant difference relative to PQ-challenged cells with no pre-treatment ($p < 0.05$).

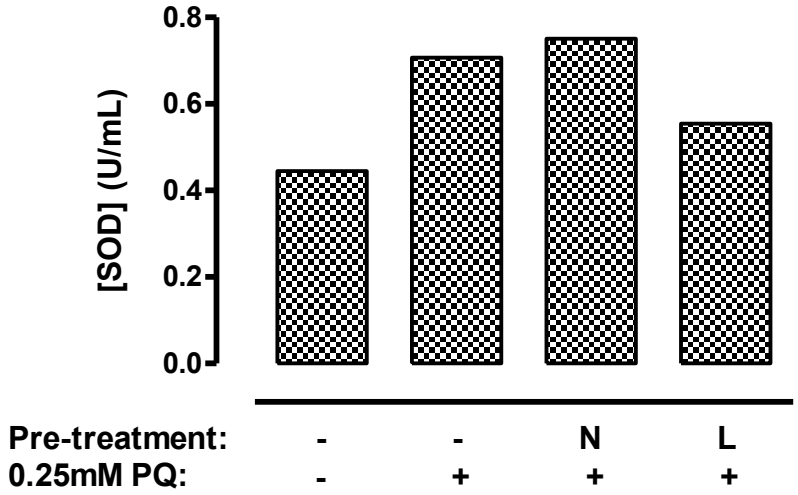

Figure 2.8: Effects of NAC and L-NAC pre-treatment on SOD activity in PQ-challenged cells. Cells were pre-treated for 4 h with control media or 5.0 mM NAC- (N) or L-NAC-containing media (L), followed by 0 or 0.25 mM PQ challenge for 4 h. Activity of cellular SOD enzymes was assessed by monitoring the rate of inhibition of absorbance at 560 nm for 5 min (measured in U/mL, where one unit is that amount of SOD which inhibits the rate of increase in absorbance due to NBT-diformazan formation by 50 %). Bars represent values of 1 independent experiment.

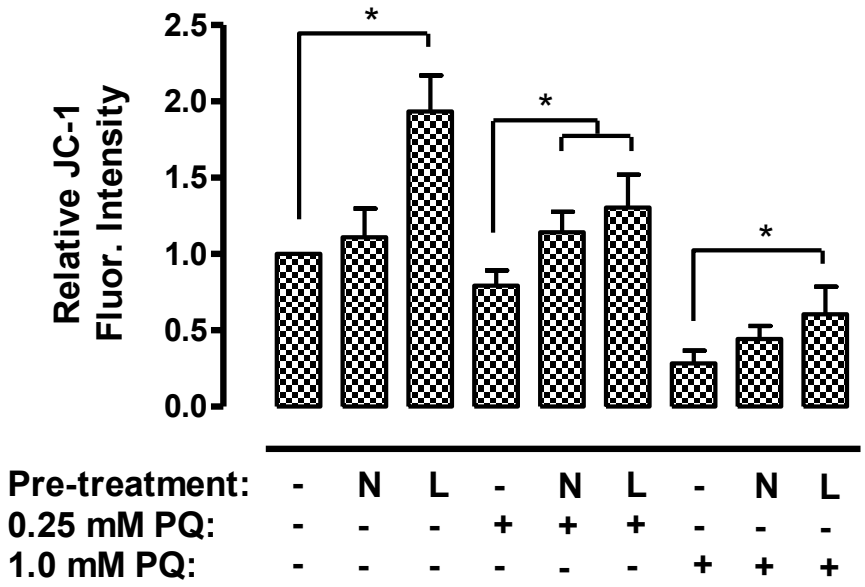

Figure 2.9: Effect of NAC or L-NAC pre-treatment on mitochondrial membrane potential following PQ challenge. Cells pre-treated for 4 h with control media or 5.0 mM NAC- (N) or L-NAC-containing media (L) were challenged with 0, 0.25, or 1.0 mM PQ for 4 h. Cells were stained for 30 min post-treatment with the cell permeable JC-1 fluorescent dye. Aggregation of the dye due to high mitochondrial membrane potential produced red fluorescence, measured flow cytometrically on the FL2-H channel, while depolarized mitochondrial membranes resulted in decreased red fluorescence. Bars represent mean ± S.E.M. of 3 independent experiments. * denotes significant difference relative to cells with no pre-treatment ($p < 0.05$).

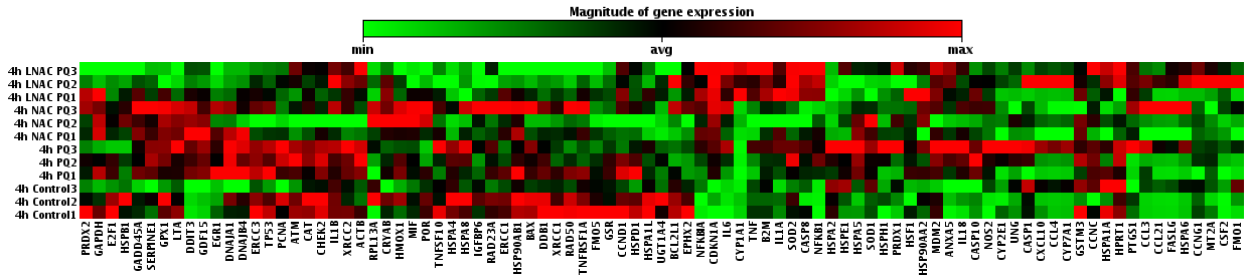

Figure 2.10: Effect of pre-treatment on the magnitude of gene expression in PQ-challenged cells. RNA was extracted from cells challenged with 0 or 0.25 mM PQ for 4 h following pre-treatment with 5.0 mM NAC- or L-NAC-containing media, and analyzed via quantitative reverse-transcription PCR using a gene array. The magnitude of expression of each gene is expressed on a scale ranging from minimal (intense green) to maximal (intense red) expression (n = 3 independent trials).

Table 2.2: Relative expression, via gene array analysis, of genes involved with cellular stress and toxicity in cells pre-treated with control media or NAC- or L-NAC-containing media prior to 0.25 mM PQ challenge for 4 h. Fold change is expressed relative to control using the housekeeping genes B2M, HPRT1, RPL13A, and GAPDH.

Table 2.2.1: Oxidative or metabolic stress-related genes.

Gene	No Pre-treatment	NAC Pre-treatment	L-NAC Pre-treatment
CAT	-1.02 ± 0.11	-1.26 ± 0.25	-1.15 ± 0.13
CRYAB	1.22 ± 0.17	1.50 ± 0.20	1.35 ± 0.05
CYP1A1	-1.38 ± 0.14	1.11 ± 0.11	4.65 ± 0.93
CYP2E1	0.00 ± 0.00	0.00 ± 0.00	0.00 ± 0.00
CYP7A1	0.00 ± 0.00	0.00 ± 0.00	0.00 ± 0.00
EPHX2	-1.86 ± 0.60	-1.01 ± 0.35	-1.53 ± 0.34
FMO1	0.00 ± 0.00	0.00 ± 0.00	0.00 ± 0.00
FMO5	-1.27 ± 0.09	-1.52 ± 0.13	-1.60 ± 0.06
GPX1	-1.04 ± 0.07	-1.00 ± 0.07	-1.01 ± 0.00
GSR	-1.07 ± 0.12	-1.54 ± 0.23	-1.44 ± 0.14
GSTM3	-1.18 ± 0.07	-1.16 ± 0.12	-1.24 ± 0.13
HMOX1	1.16 ± 0.14	1.36 ± 0.20	-1.15 ± 0.10
MT2A	1.02 ± 0.04	-1.09 ± 0.13	-1.15 ± 0.28
POR	-1.74 ± 0.58	2.19 ± 0.53	-2.19 ± 1.02
PRDX1	1.07 ± 0.05	1.02 ± 0.06	1.05 ± 0.07
PRDX2	-1.10 ± 0.14	1.06 ± 0.28	-1.26 ± 0.07
PTGS1	-1.37 ± 0.06	1.03 ± 0.08	1.53 ± 0.23
SOD1	1.04 ± 0.01	1.00 ± 0.07	-1.10 ± 0.04
SOD2	1.18 ± 0.06	-1.07 ± 0.10	1.29 ± 0.05

Table 2.2.2: Heat shock genes.

Gene	No Pre-treatment	NAC Pre-treatment	L-NAC Pre-treatment
DNAJA1	1.63 ± 0.23	1.37 ± 0.09	-1.07 ± 0.10
DNAJB4	1.69 ± 0.23	1.47 ± 0.14	-1.02 ± 0.09
HSF1	1.10 ± 0.05	1.08 ± 0.04	1.13 ± 0.07
HSPA1A	-1.15 ± 0.08	-1.32 ± 0.18	1.02 ± 0.14
HSPA1L	-1.26 ± 0.19	-1.57 ± 0.37	-1.40 ± 0.17
HSPA2	-1.01 ± 0.05	-1.40 ± 0.05	-1.41 ± 0.06
HSPA4	-1.05 ± 0.10	-1.43 ± 0.24	-1.69 ± 0.15
HSPA5	1.35 ± 0.03	1.24 ± 0.10	-1.00 ± 0.03
HSPA6	0.00 ± 0.00	0.00 ± 0.00	0.00 ± 0.00
HSPA8	1.04 ± 0.16	-1.05 ± 0.22	-1.32 ± 0.14
HSPB1	-1.23 ± 0.08	1.10 ± 0.12	-1.26 ± 0.18
HSP90AA2	1.02 ± 0.08	1.14 ± 0.03	1.10 ± 0.09
HSP90AB1	-1.06 ± 0.11	1.34 ± 0.19	-1.58 ± 0.21
HSPD1	1.06 ± 0.04	-1.12 ± 0.19	-1.03 ± 0.09
HSPE1	1.07 ± 0.02	-1.09 ± 0.06	-1.07 ± 0.02
HSPH1	1.03 ± 0.03	1.13 ± 0.04	1.01 ± 0.06

Table 2.2.3: Proliferation / carcinogenesis related genes.

Gene	No Pre-treatment	NAC Pre-treatment	L-NAC Pre-treatment
ACTB	1.57 ± 0.23	-1.27 ± 0.00	1.25 ± 0.17
CCNC	1.02 ± 0.06	-1.18 ± 0.10	1.21 ± 0.20
CCND1	-1.03 ± 0.03	-1.22 ± 0.28	1.05 ± 0.10
CCNG1	-1.00 ± 0.05	1.04 ± 0.06	1.17 ± 0.05
E2F1	-1.45 ± 0.18	-1.07 ± 0.32	-2.61 ± 0.58
EGR1	2.78 ± 0.65	2.23 ± 0.36	-1.24 ± 0.08
PCNA	1.16 ± 0.14	-1.07 ± 0.13	-1.03 ± 0.08

Table 2.2.4: Growth arrest and senescence related genes.

Gene	No Pre-treatment	NAC Pre-treatment	L-NAC Pre-treatment
CDKN1A	1.44 ± 0.10	1.73 ± 0.11	1.88 ± 0.08
DDIT3	1.88 ± 0.09	2.17 ± 0.11	1.72 ± 0.14
GADD45A	1.31 ± 0.17	1.38 ± 0.16	1.01 ± 0.11
GDF15	1.91 ± 0.13	1.96 ± 0.11	1.53 ± 0.02
IGFBP6	-1.04 ± 0.05	1.07 ± 0.20	-1.52 ± 0.29
MDM2	1.30 ± 0.23	1.04 ± 0.23	1.51 ± 0.27
TP53	1.15 ± 0.12	-1.06 ± 0.21	-1.02 ± 0.09

Table 2.2.5: Inflammatory genes.

Gene	No Pre-treatment	NAC Pre-treatment	L-NAC Pre-treatment
CCL21	0.00 ± 0.00	0.00 ± 0.00	0.00 ± 0.00
CCL3	0.00 ± 0.00	0.00 ± 0.00	0.00 ± 0.00
CCL4	0.00 ± 0.00	0.00 ± 0.00	0.00 ± 0.00
CSF2	0.00 ± 0.00	0.00 ± 0.00	0.00 ± 0.00
CXCL10	0.00 ± 0.00	0.00 ± 0.00	0.00 ± 0.00
IL18	1.67 ± 0.19	1.54 ± 0.11	1.29 ± 0.11
IL1A	1.66 ± 0.29	1.83 ± 0.16	1.92 ± 0.26
IL1B	1.00 ± 0.13	-1.87 ± 0.52	-1.34 ± 0.33
IL6	3.20 ± 0.62	3.63 ± 0.59	4.88 ± 0.20
LTA	1.34 ± 0.43	1.45 ± 0.33	-2.27 ± 0.16
MIF	1.02 ± 0.01	1.08 ± 0.06	-1.09 ± 0.03
NFKB1	1.22 ± 0.03	1.12 ± 0.06	1.36 ± 0.02
NOS2A	2.90 ± 0.39	1.94 ± 0.28	2.30 ± 0.65
SERPINE1	1.40 ± 0.16	1.39 ± 0.27	1.02 ± 0.08

Table 2.2.6: DNA damage and repair genes.

Gene	No Pre-treatment	NAC Pre-treatment	L-NAC Pre-treatment
ATM	2.26 ± 0.83	-1.26 ± 0.39	1.20 ± 0.28
CHEK2	1.03 ± 0.10	-1.29 ± 0.21	-1.21 ± 0.14
DDB1	-1.10 ± 0.09	-1.19 ± 0.29	-1.54 ± 0.06
ERCC1	-1.14 ± 0.13	1.17 ± 0.33	-1.41 ± 0.32
ERCC3	1.09 ± 0.12	1.07 ± 0.27	-1.19 ± 0.06
RAD23A	1.06 ± 0.15	1.07 ± 0.29	-1.17 ± 0.24
RAD50	-1.27 ± 0.10	-1.01 ± 0.38	-1.87 ± 0.17
UGT1A4	-1.26 ± 0.21	-1.92 ± 0.49	-1.76 ± 0.02
UNG	1.12 ± 0.07	-1.00 ± 0.10	-1.01 ± 0.03
XRCC1	-1.24 ± 0.11	-1.24 ± 0.26	-1.64 ± 0.05
XRCC2	1.21 ± 0.12	-1.23 ± 0.22	1.11 ± 0.11

Table 2.2.7: Apoptosis signalling genes.

Gene	No Pre-treatment	NAC Pre-treatment	L-NAC Pre-treatment
ANXA5	1.44 ± 0.14	1.25 ± 0.03	1.43 ± 0.07
BAX	-1.02 ± 0.12	-1.08 ± 0.20	-1.29 ± 0.08
BCL2L1	-1.44 ± 0.14	-1.26 ± 0.37	-1.33 ± 0.34
CASP1	-1.20 ± 0.22	-1.46 ± 0.13	-1.76 ± 0.27
CASP10	1.93 ± 0.22	1.60 ± 0.22	1.35 ± 0.08
CASP8	1.15 ± 0.07	-1.08 ± 0.06	1.37 ± 0.12
FASLG	0.00 ± 0.00	0.00 ± 0.00	0.00 ± 0.00
NFKBIA	1.20 ± 0.04	1.35 ± 0.07	1.47 ± 0.06
TNF	-1.03 ± 0.16	-1.32 ± 0.11	1.22 ± 0.03
TNFRSF1A	-1.29 ± 0.10	-1.07 ± 0.29	-1.62 ± 0.16
TNFSF10	-1.36 ± 0.23	-1.28 ± 0.04	-2.25 ± 0.56

Values represent mean ± SEM of 3 independent experiments.

Table 2.3: Relative expression of selected genes in cells pre-treated with control media or NAC-, L-NAC-, or empty liposome (EL)-containing media prior to 0.25 mM PQ challenge for 4 h. Data was obtained using individual primer assays. Fold change is expressed relative to untreated control using the housekeeping gene RPL13A.

Gene	No Pre-treatment	NAC Pre-treatment	L-NAC Pre-treatment	EL Pre-treatment
CAT	-1.11 ± 0.11	-1.13 ± 0.29	-1.26 ± 0.23	-1.24 ± 0.09
CYP1A1	1.88 ± 0.83	2.18 ± 0.61	3.79 ± 1.33	3.35 ± 1.66
IL1A	1.09 ± 0.07	1.49 ± 0.14	1.66 ± 0.12	1.40 ± 0.23
IL1B	1.03 ± 0.13	1.95 ± 0.09	2.63 ± 0.59	1.42 ± 0.15
IL6	1.45 ± 0.30	1.23 ± 0.28	1.23 ± 0.03	1.08 ± 0.22
NFKB1	-1.05 ± 0.20	1.33 ± 0.04	1.17 ± 0.06	1.08 ± 0.20
NFKBIA	1.34 ± 0.18	1.46 ± 0.11	1.73 ± 0.24	1.57 ± 0.17
SOD1	1.01 ± 0.21	1.08 ± 0.23	-1.30 ± 0.41	-1.22 ± 0.14
TNF	-1.15 ± 0.22	-1.37 ± 0.45	1.35 ± 0.20	-1.85 ± 1.02

Values represent mean ± SEM of 3 independent experiments.

Table 2.4: Relative expression of selected genes in cells pre-treated with control media or NAC-, L-NAC-, or empty liposome (EL)-containing media prior to 0.25 mM PQ challenge for 4 h. Data was obtained using individual primer assays. Fold change is expressed relative to untreated control using the housekeeping gene RPL13A.

Gene	No Pre-treatment	NAC Pre-treatment	L-NAC Pre-treatment	EL Pre-treatment
FOS	1.05 ± 0.19	2.22 ± 0.51	1.14 ± 0.25	1.09 ± 0.22
IL8	2.68 ± 0.32	1.84 ± 0.09	1.53 ± 0.23	1.80 ± 0.30
IL10	-3.03 ± 0.88	-1.73 ± 0.38	1.13 ± 0.22	-2.45 ± 0.62
ILK	-1.25 ± 0.05	-1.53 ± 0.05	-1.92 ± 0.38	-1.50 ± 0.17
ITGB1	1.24 ± 0.06	1.38 ± 0.11	1.33 ± 0.08	1.26 ± 0.12
JUN	1.41 ± 0.13	1.63 ± 0.08	1.53 ± 0.23	1.49 ± 0.24
MAPK3	1.48 ± 0.13	1.90 ± 0.32	1.42 ± 0.02	2.06 ± 0.21
MAPK8	1.20 ± 0.13	1.45 ± 0.08	1.06 ± 0.15	-1.05 ± 0.16
MAPK14	-1.26 ± 0.04	1.32 ± 0.35	-1.00 ± 0.10	-1.02 ± 0.45
NFE2L2	3.17 ± 0.31	2.55 ± 0.61	2.25 ± 0.29	1.67 ± 0.48
TGFB1	1.15 ± 0.15	1.34 ± 0.08	1.27 ± 0.09	1.35 ± 0.21

Values represent mean ± SEM of 3 independent experiments.

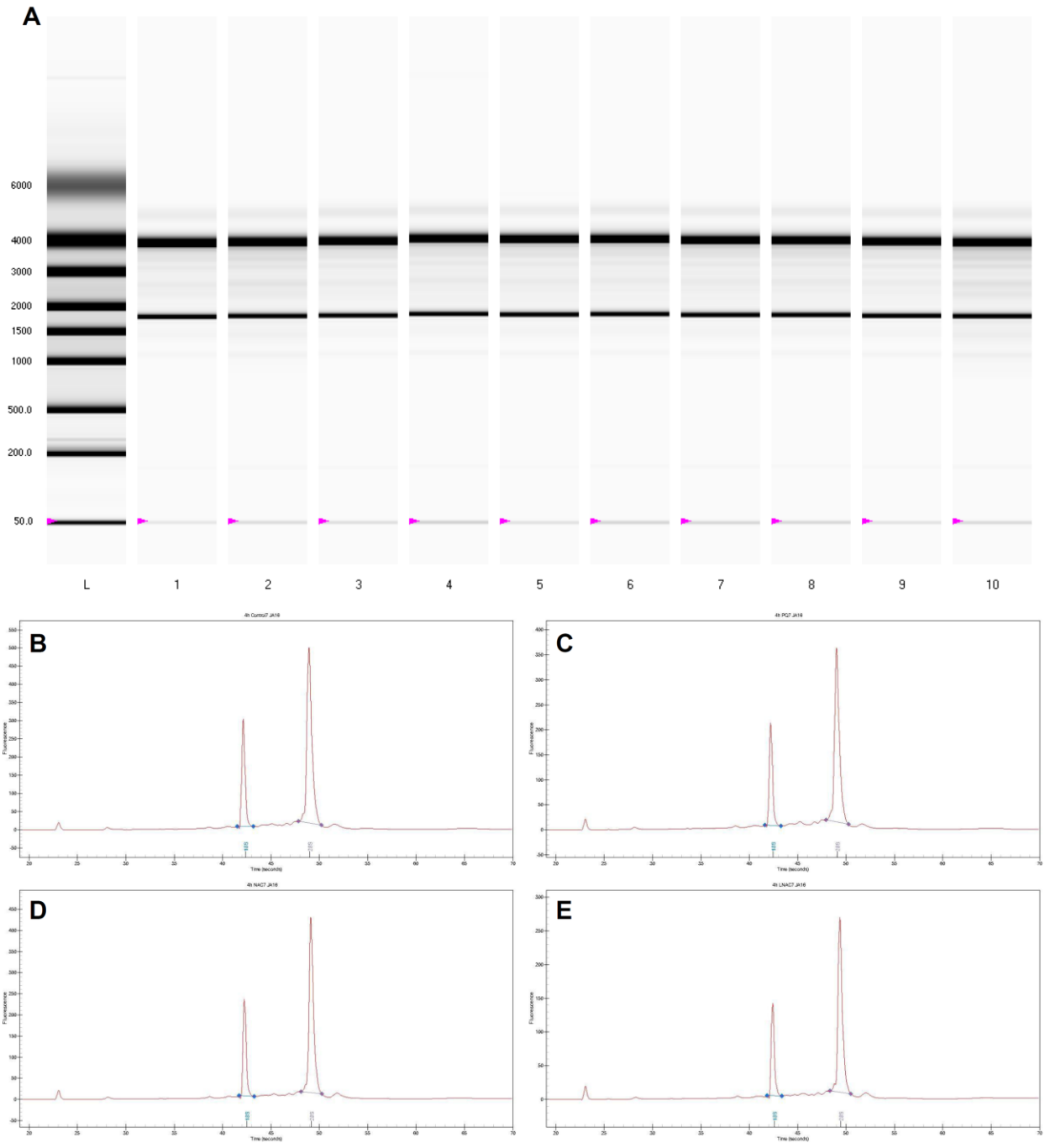
A
6000
4000
3000
2000
1500
1000
500.0
200.0
50.0
L
1
2
3
4
5
6
7
8
9
10
B
C
D
E

Figure 2.11: Validation of RNA integrity. Aliquots of extracted RNA from control or PQ-challenged A549 cells with or without pre-treatment were assessed for RNA concentration and integrity using the Experion Automated Electrophoresis Station. Representative gels artificially depict 18 and 28 S rRNA banding (A; L: ladder; 1 - 12: extracted RNA samples) using data obtained from electropherograms. Representative electropherograms of samples 1 - 4 display 18 and 28 S rRNA peaks (B-E, respectively).

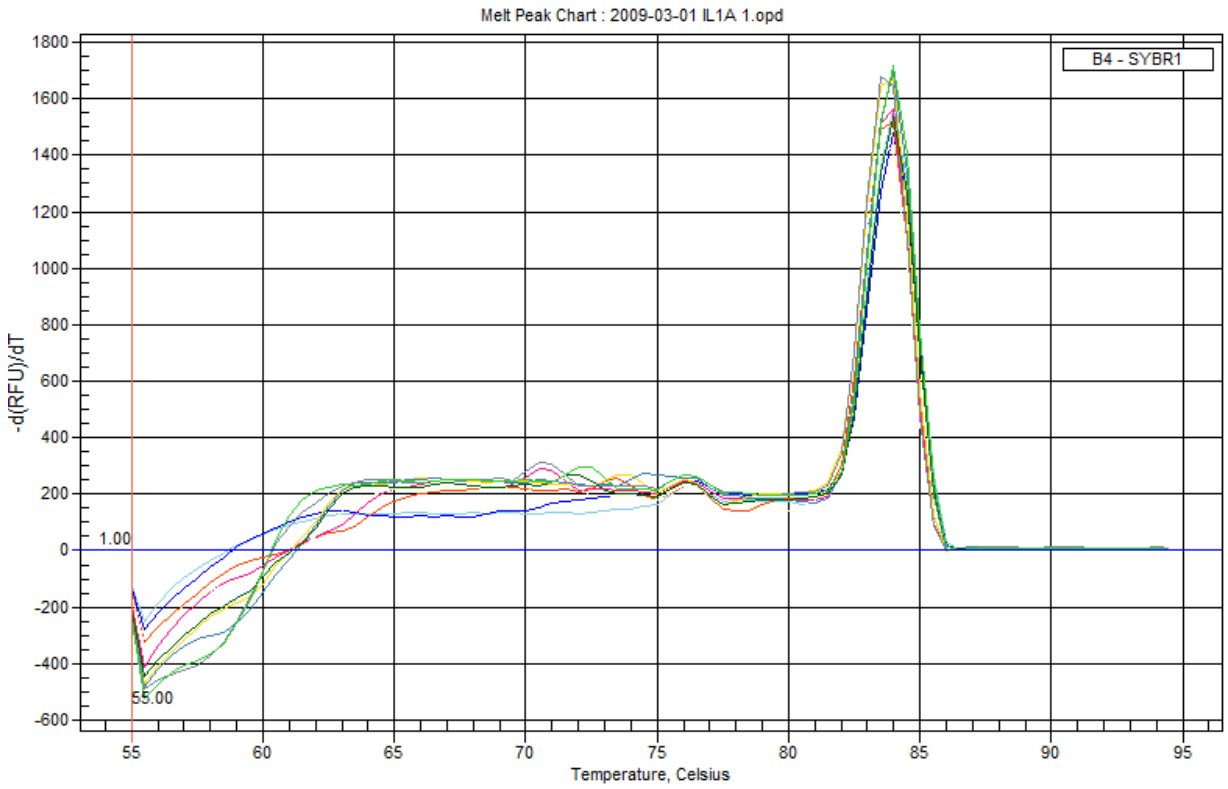

Figure 2.12: Assessment of PCR gene product quality. Representative first-derivative dissociation curves of amplified PCR product of IL1A were obtained via individual primer assays. Depicted samples are from 4 h control and PQ-challenged cells pre-treated with control media or NAC- or L-NAC-containing media.

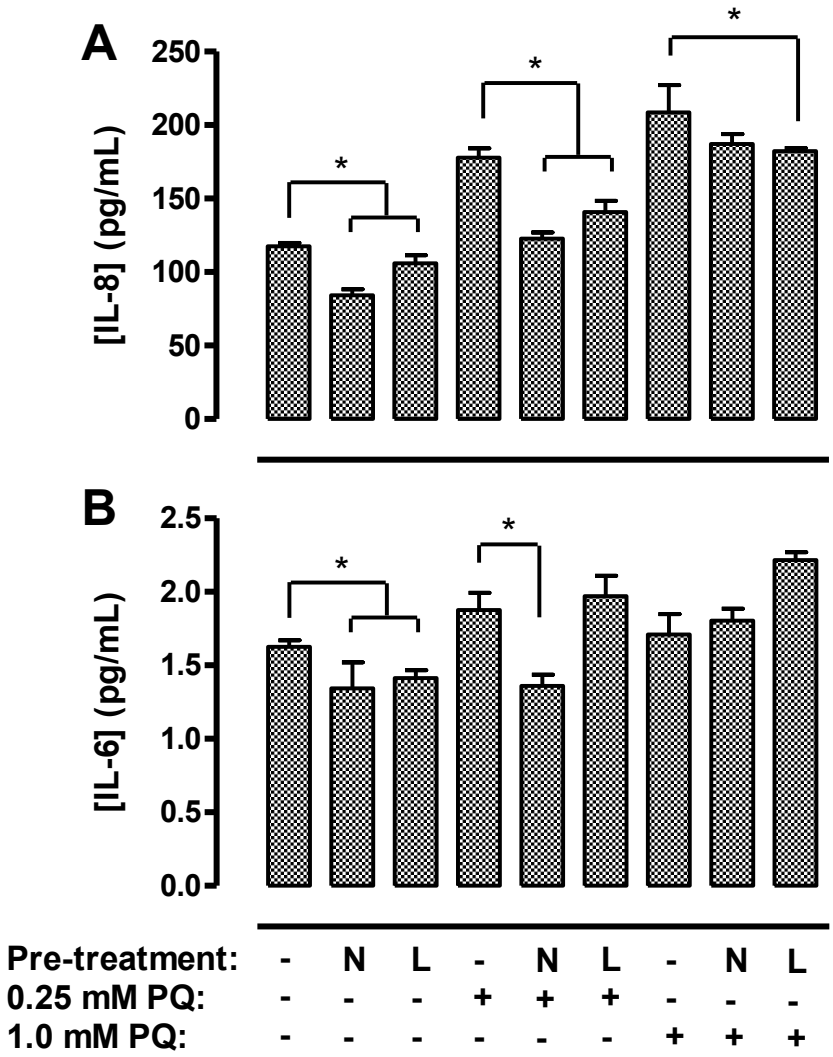

Figure 2.13: Effect of NAC or L-NAC pre-treatment on inflammatory cytokine levels post-PQ exposure. Cells pre-treated for 4 h with control media or 5.0 mM NAC- (N) or L-NAC-containing media (L) were challenged with 0, 0.25, or 1.0 mM PQ for 4 h. Cell culture supernatants were collected immediately following challenge and concomitantly analyzed for IL-8 (A), IL-6 (B), and other cytokines (IL-1β, IL-10, IL-15, TNF-α, and eotaxin; data not shown) using Bio-Plex technology. Bars represent mean ± S.E.M. of 3 independent experiments. * denotes significant difference relative to cells with no pre-treatment ($p < 0.05$).

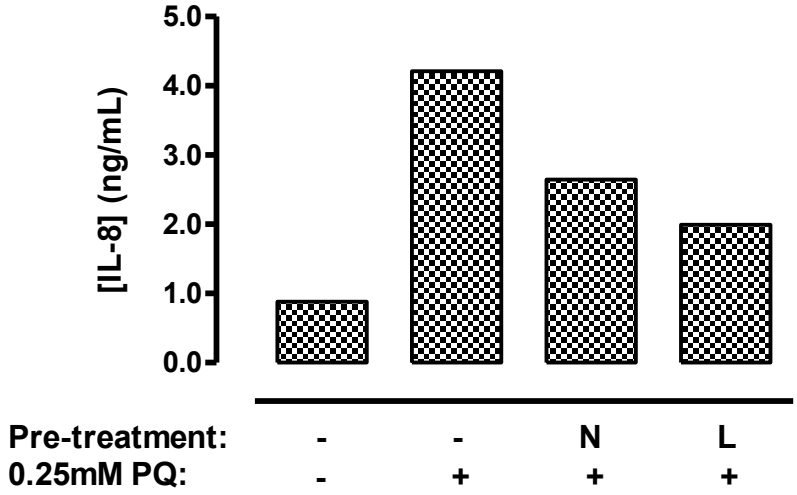

Figure 2.14: Effect of NAC or L-NAC pre-treatment on IL-8 levels following PQ challenge. Cells pre-treated for 4 h with control media or 5.0 mM NAC- (N) or L-NAC-containing media (L) were challenged with 0 or 0.25 mM PQ for 24 h. Cell culture supernatants were collected immediately post-challenge and analyzed for IL-8 using a quantitative sandwich enzyme immunoassay technique. Absorbance was measured at 450 nm (570 nm wavelength correction) and converted to IL-8 concentrations based on a standard curve of known values. Bars represent values of 1 independent experiment.

Conclusion

Paraquat is a chemical that induces its toxicity in biological systems via the generation of ROS. The results of this *in vitro* study demonstrated that PQ exhibits concentration- and time-dependent toxicity in A549 cells, primarily via dysregulation of cellular redox balance, resulting in necrotic, but not apoptotic, cell death. PQ also increased the expression of pro-inflammatory mediators at both the gene and protein level, suggesting alveolar type II epithelial cells contribute to the inflammatory response associated with PQ lung toxicity. The antioxidant NAC, delivered to A549 cells both in its free and liposomal form, conferred protection against PQ-induced cytotoxicity primarily through the maintenance of cellular redox status and independent of PQ uptake, and played a role in regulating the immune response of alveolar cells to this challenge, as indicated by gene and protein expression of inflammatory mediators. These protective effects were more evident in cells pre-treated with L-NAC, which is attributed to the greater cellular NAC levels achieved via liposomal administration. These data suggest that studies examining the protective effects of L-NAC *in vivo* are warranted in order to further explore the use of liposomal antioxidants for the treatment of conditions associated with oxidative stress.

References

Aitio ML., 2006. N-acetylcysteine -- passe-partout or much ado about nothing? Br J Clin Pharmacol 61, 5-15.

Alexandre J, Batteux F, Nicco C, Chereau C, Laurent A, Guillevin L, Weill B, Goldwasser F., 2006. Accumulation of hydrogen peroxide is an early and crucial step for paclitaxel-induced cancer cell death both in vitro and in vivo. Int J Cancer 119, 41-48.

Alipour M, Omri A, Smith MG, Suntres ZE., 2007. Prophylactic effect of liposomal N-acetylcysteine against LPS-induced liver injuries. J Endotoxin Res 13, 297-304.

Amondham W, Parkpian P, Polprasert C, DeLaune RD, Jugsujinda A., 2006. Paraquat adsorption, degradation, and remobilization in tropical soils of Thailand. J Environ Sci Health B 41, 485-507.

Arakawa M, Ito Y., 2007. N-acetylcysteine and neurodegenerative diseases: Basic and clinical pharmacology. Cerebellum 1-7.

Atkuri KR, Mantovani JJ, Herzenberg LA, Herzenberg LA., 2007. N-Acetylcysteine--a safe antidote for cysteine/glutathione deficiency. Curr Opin Pharmacol 7, 355-359.

Bateman DN., 2008. New formulation of paraquat: a step forward but in the wrong direction. PLoS Med 5, e58.

Bauskin AR, Brown DA, Kuffner T, Johnen H, Luo XW, Hunter M, Breit SN., 2006. Role of macrophage inhibitory cytokine-1 in tumorigenesis and diagnosis of cancer. Cancer Res 66, 4983-4986.

Bernsdorff C, Reszka R, Winter R., 1999. Interaction of the anticancer agent Taxol (paclitaxel) with phospholipid bilayers. J Biomed Mater Res 46, 141-149.

Bianchi M, Fantuzzi G, Bertini R, Perin L, Salmona M, Ghezzi P., 1993. The pneumotoxicant paraquat induces IL-8 mRNA in human mononuclear cells and pulmonary epithelial cells. Cytokine 5, 525-530.

Bidere N, Su HC, Lenardo MJ., 2006. Genetic disorders of programmed cell death in the immune system. Annu Rev Immunol 24, 321-352.

Bilska A, Wlodek L., 2005. Lipoic acid - the drug of the future? Pharmacol Rep 57, 570-577.

Bove J, Prou D, Perier C, Przedborski S., 2005. Toxin-induced models of Parkinson's disease. NeuroRx 2, 484-494.

Bromilow RH., 2004. Paraquat and sustainable agriculture. Pest Manag Sci 60, 340-349.

Burns RG, Audus LJ., 1970. Distribution and breakdown of paraquat in soil. Weed Res 10, 49-58.

Bus JS, Aust SD, Gibson JE., 1976. Paraquat toxicity: proposed mechanism of action involving lipid peroxidation. Environ Health Perspect 16, 139-146.

Bus JS, Gibson JE., 1984. Paraquat: model for oxidant-initiated toxicity. Environ Health Perspect 55, 37-46.

Candan F, Alagozlu H., 2001. Captopril inhibits the pulmonary toxicity of paraquat in rats. Hum Exp Toxicol 20, 637-641.

Cant JS, Lewis DR., 1968. Ocular damage due to paraquat and diquat. Br Med J 2, 224.

Cappelletti G, Incani C, Maci R., 1994. Paraquat induces irreversible actin cytoskeleton disruption in cultured human lung cells. Cell Biol Toxicol 10, 255-263.

Cappelletti G, Maggioni MG, Maci R., 1998. Apoptosis in human lung epithelial cells: triggering by paraquat and modulation by antioxidants. Cell Biol Int 22, 671-678.

Cecen SS, Cengiz G, Soylemezoglu T., 2002. The protective effects of N-acetylcysteine in paraquat-induced toxicity. J Fac Pharm Anakara 31, 259-271.

Chen CM, Fang CL, Chang CH., 2001. Surfactant and corticosteroid effects on lung function in a rat model of acute lung injury. Crit Care Med 29, 2169-2175.

Cheng WH, Quimby FW, Lei XG., 2003. Impacts of glutathione peroxidase-1 knockout on the protection by injected selenium against the pro-oxidant-induced liver aponecrosis and signaling in selenium-deficient mice. Free Radic Biol Med 34, 918-927.

Chester G, Ward RJ., 1984. Occupational exposure and drift hazard during aerial application of paraquat to cotton. Arch Environ Contam Toxicol 13, 551-563.

Choi Y, Cho K, Yoon S, Lee H, Choi Y., 2008. A case of paraquat intoxication caused by intravenous injection. Am J Emerg Med 26, 836.e3-836.e4.

Chopra M, Reuben JS, Sharma AC., 2009. Acute lung injury:apoptosis and signaling mechanisms. Exp Biol Med (Maywood) 234, 361-371.

Ciencewicki J, Trivedi S, Kleeberger SR., 2008. Oxidants and the pathogenesis of lung diseases. J Allergy Clin Immunol 122, 456-68; quiz 469-70.

Clark DG, McElligott TF, Hurst EW., 1966. The toxicity of paraquat. Br J Ind Med 23, 126-132.

Costantini P, Petronilli V, Colonna R, Bernardi P., 1995. On the effects of paraquat on isolated mitochondria. Evidence that paraquat causes opening of the cyclosporin A-sensitive permeability transition pore synergistically with nitric oxide. Toxicology 99, 77-88.

Cotgreave IA, Eklund A, Larsson K, Moldeus PW., 1987. No penetration of orally administered N-acetylcysteine into bronchoalveolar lavage fluid. Eur J Respir Dis 70, 73-77.

Dawson JR, Norbeck K, Anundi I, Moldeus P., 1984. The effectiveness of N-acetylcysteine in isolated hepatocytes, against the toxicity of paracetamol, acrolein, and paraquat. Arch Toxicol 55, 11-15.

Day BJ, Crapo JD., 1996. A metalloporphyrin superoxide dismutase mimetic protects against paraquat-induced lung injury in vivo. Toxicol Appl Pharmacol 140, 94-100.

Dinis-Oliveira RJ, de Pinho PG, Ferreira AC, Silva AM, Afonso C, Bastos MD, Remiao F, Duarte JA, Carvalho F., 2008. Reactivity of paraquat with sodium salicylate: Formation of stable complexes. Toxicology 249, 130-139.

Dinis-Oliveira RJ, Duarte JA, Remiao F, Sanchez-Navarro A, Bastos ML, Carvalho F., 2006. Single high dose dexamethasone treatment decreases the pathological score and increases the survival rate of paraquat-intoxicated rats. Toxicology 227, 73-85.

Dinis-Oliveira RJ, Duarte JA, Sanchez-Navarro A, Remiao F, Bastos ML, Carvalho F., 2008. Paraquat poisonings: mechanisms of lung toxicity, clinical features, and treatment. Crit Rev Toxicol 38, 13-71.

Dinis-Oliveira RJ, Remiao F, Carmo H, Duarte JA, Navarro AS, Bastos ML, Carvalho F., 2006a. Paraquat exposure as an etiological factor of Parkinson's disease. Neurotoxicology 27, 1110-1122.

Dinis-Oliveira RJ, Remiao F, Duarte JA, Ferreira R, Sanchez Navarro A, Bastos ML, Carvalho F., 2006b. P-glycoprotein induction: an antidotal pathway for paraquat-induced lung toxicity. Free Radic Biol Med 41, 1213-1224.

Dinis-Oliveira RJ, Sarmento A, Reis P, Amaro A, Remiao F, Bastos ML, Carvalho F., 2006c. Acute paraquat poisoning: report of a survival case following intake of a potential lethal dose. Pediatr Emerg Care 22, 537-540.

Dinis-Oliveira RJ, Sousa C, Remiao F, Duarte JA, Navarro AS, Bastos ML, Carvalho F., 2007. Full survival of paraquat-exposed rats after treatment with sodium salicylate. Free Radic Biol Med 42, 1017-1028.

Drault JN, Baelen E, Mehdaoui H, Delord JM, Flament F., 1999. Massive paraquat poisoning. Favorable course after treatment with n-acetylcysteine and early hemodialysis. Ann Fr Anesth Reanim 18, 534-537.

Eddleston M, Wilks MF, Buckley NA., 2003. Prospects for treatment of paraquat-induced lung fibrosis with immunosuppressive drugs and the need for better prediction of outcome: a systematic review. QJM 96, 809-824.

Eisenman A, Armali Z, Raikhlin-Eisenkraft B, Bentur L, Bentur Y, Guralnik L, Enat R., 1998. Nitric oxide inhalation for paraquat-induced lung injury. J Toxicol Clin Toxicol 36, 575-584.

Fan J, Shek PN, Suntres ZE, Li YH, Oreopoulos GD, Rotstein OD., 2000. Liposomal antioxidants provide prolonged protection against acute respiratory distress syndrome. Surgery 128, 332-338.

Farr SA, Poon HF, Dogrukol-Ak D, Drake J, Banks WA, Eyerman E, Butterfield DA, Morley JE., 2003. The antioxidants alpha-lipoic acid and N-acetylcysteine reverse memory impairment and brain oxidative stress in aged SAMP8 mice. J Neurochem 84, 1173-1183.

Farrington JA, Ebert M, Land EJ, Fletcher K., 1973. Bipyridylium quaternary salts and related compounds. V. Pulse radiolysis studies of the reaction of paraquat radical with oxygen. Implications for the mode of action of bipyridyl herbicides. Biochim Biophys Acta 314, 372-381.

Ferguson MR, Rojo DR, Somasunderam A, Thiviyanathan V, Ridley BD, Yang X, Gorenstein DG., 2006. Delivery of double-stranded DNA thioaptamers into HIV-1 infected cells for antiviral activity. Biochem Biophys Res Commun 344, 792-797.

Fernandes AF, Zhou J, Zhang X, Bian Q, Sparrow JR, Taylor A, Pereira P, Shang F., 2008. Oxidative inactivation of the proteasome in RPE: A potential link between oxidative stress and upregulation of IL-8. J Biol Chem

Freeman BA, Turrens JF, Mirza Z, Crapo JD, Young SL., 1985. Modulation of oxidant lung injury by using liposome-entrapped superoxide dismutase and catalase. Fed Proc 44, 2591-2595.

Fukuda Y, Ferrans VJ, Schoenberger CI, Rennard SI, Crystal RG., 1985. Patterns of pulmonary structural remodeling after experimental paraquat toxicity. The morphogenesis of intraalveolar fibrosis. Am J Pathol 118, 452-475.

Fukushima T, Tanaka K, Lim H, Moriyama M., 2002. Mechanism of Cytotoxicity of Paraquat. Environ Health Prev Med 7, 89-94.

Garcia-Ruiz C, Fernandez-Checa JC., 2007. Redox regulation of hepatocyte apoptosis. J Gastroenterol Hepatol 22 Suppl 1, S38-42.

Ghazi-Khansari M, Mohammadi-Karakani A, Sotoudeh M, Mokhtary P, Pour-Esmaeil E, Maghsoud S., 2007. Antifibrotic effect of captopril and enalapril on paraquat-induced lung fibrosis in rats. J Appl Toxicol 27, 342-349.

Ghazi-Khansari M, Nasiri G, Honarjoo M., 2005. Decreasing the oxidant stress from paraquat in isolated perfused rat lung using captopril and niacin. Arch Toxicol 79, 341-345.

Goyal P, Goyal K, Vijaya Kumar SG, Singh A, Katare OP, Mishra DN., 2005. Liposomal drug delivery systems--clinical applications. Acta Pharm 55, 1-25.

Gram TE., 1997. Chemically reactive intermediates and pulmonary xenobiotic toxicity. Pharmacol Rev 49, 297-341.

Hashimoto Y, Suzuki S., 1992. Basic approach to application of liposomes for cancer chemotherapy. Tohoku J Exp Med 168, 361-369.

Hatakeyama H, Akita H, Ishida E, Hashimoto K, Kobayashi H, Aoki T, Yasuda J, Obata K, Kikuchi H, Ishida T, Kiwada H, Harashima H., 2007. Tumor targeting of doxorubicin by anti-MT1-MMP antibody-modified PEG liposomes. Int J Pharm 342, 194-200.

Heberlein W, Wodopia R, Bartsch P, Mairbaurl H., 2000. Possible role of ROS as mediators of hypoxia-induced ion transport inhibition of alveolar epithelial cells. Am J Physiol Lung Cell Mol Physiol 278, L640-8.

Henke MO, Ratjen F., 2007. Mucolytics in cystic fibrosis. Paediatr Respir Rev 8, 24-29.

Hoesel LM, Flierl MA, Niederbichler AD, Rittirsch D, McClintock SD, Reuben JS, Pianko MJ, Stone W, Yang H, Smith M, Sarma JV, Ward PA., 2008. Ability of antioxidant liposomes to prevent acute and progressive pulmonary injury. Antioxid Redox Signal 10, 973-981.

Hoet PH, Nemery B., 2000. Polyamines in the lung: polyamine uptake and polyamine-linked pathological or toxicological conditions. Am J Physiol Lung Cell Mol Physiol 278, L417-33.

Hoffer E, Avidor I, Benjaminov O, Shenker L, Tabak A, Tamir A, Merzbach D, Taitelman U., 1993. N-acetylcysteine delays the infiltration of inflammatory cells into the lungs of paraquat-intoxicated rats. Toxicol Appl Pharmacol 120, 8-12.

Hoffer E, Baum Y, Tabak A, Taitelman U., 1996. N-acetylcysteine increases the glutathione content and protects rat alveolar type II cells against paraquat-induced cytotoxicity. Toxicol Lett 84, 7-12.

Hoffer E, Shenker L, Baum Y, Tabak A., 1997. Paraquat-induced formation of leukotriene B4 in rat lungs: modulation by N-acetylcysteine. Free Radic Biol Med 22, 567-572.

Hong SY, Yang JO, Lee EY, Lee ZW., 2003. Effects of N-acetyl-L-cysteine and glutathione on antioxidant status of human serum and 3T3 fibroblasts. J Korean Med Sci 18, 649-654.

Horiguchi H, Mukaida N, Okamoto S, Teranishi H, Kasuya M, Matsushima K., 1993. Cadmium induces interleukin-8 production in human peripheral blood mononuclear cells with the concomitant generation of superoxide radicals. Lymphokine Cytokine Res 12, 421-428.

Ishida Y, Takayasu T, Kimura A, Hayashi T, Kakimoto N, Miyashita T, Kondo T., 2006. Gene expression of cytokines and growth factors in the lungs after paraquat administration in mice. Leg Med (Tokyo) 8, 102-109.

Ishimoto N, Nemoto T, Nagayoshi K, Yamashita F, Hashida M., 2006. Improved anti-oxidant activity of superoxide dismutase by direct chemical modification. J Control Release 111, 204-211.

Kelly GS., 1998. Clinical applications of N-acetylcysteine. Altern Med Rev 3, 114-127.

Kim CH, Han SI, Lee SY, Youk HS, Moon JY, Duong HQ, Park MJ, Joo YM, Park HG, Kim YJ, Yoo MA, Lim SC, Kang HS., 2007. Protein kinase C-ERK1/2 signal pathway switches glucose depletion-induced necrosis to apoptosis by regulating superoxide dismutases and suppressing reactive oxygen species production in A549 lung cancer cells. J Cell Physiol 211, 371-385.

Kim DW, Kim SY, Lee SH, Lee YP, Lee MJ, Jeong MS, Jang SH, Park J, Lee KS, Kang TC, Won MH, Cho SW, Kwon OS, Eum WS, Choi SY., 2008. Protein transduction of an antioxidant enzyme: subcellular localization of superoxide dismutase fusion protein in cells. BMB Rep 41, 170-175.

Kim HR, Park BK, Oh YM, Lee YS, Lee DS, Kim HK, Kim JY, Shim TS, Lee SD., 2006. Green tea extract inhibits paraquat-induced pulmonary fibrosis by suppression of oxidative stress and endothelin-l expression. Lung 184, 287-295.

King KL, Cidlowski JA., 1998. Cell cycle regulation and apoptosis. Annu Rev Physiol 60, 601-617.

Lee J, Kwon W, Jo Y, Suh G, Youn Y., 2008. Protective effects of ethyl pyruvate treatment on paraquat-intoxicated rats. Hum Exp Toxicol 27, 49-54.

Lehmann T, Kohler C, Weidauer E, Taege C, Foth H., 2001. Expression of MRP1 and related transporters in human lung cells in culture. Toxicology 167, 59-72.

Lheureux P, Leduc D, Vanbinst R, Askenasi R., 1995. Survival in a case of massive paraquat ingestion. Chest 107, 285-289.

Lin P, Lu YR, Zhang J, Wei YQ, Wang XJ, Li SF, Wang Q, Xiong ZJ, Ning QZ, Lei S, Mao YQ, Cheng JQ., 2008. Antitumor effect of lung cancer vaccine with umbilical blood dendritic cells in reconstituted SCID mice. Cancer Biother Radiopharm 23, 321-331.

Lopez Lago AM, Rivero Velasco C, Galban Rodriguez C, Marino Rozados A, Pineiro Sande N, Ferrer Vizoso E., 2002. Paraquat poisoning and hemoperfusion with activated charcoal. An Med Interna 19, 310-312.

Mak JC., 2008. Pathogenesis of COPD. Part II. Oxidative-antioxidative imbalance. Int J Tuberc Lung Dis 12, 368-374.

McClintock SD, Hoesel LM, Das SK, Till GO, Neff T, Kunkel RG, Smith MG, Ward PA., 2006. Attenuation of half sulfur mustard gas-induced acute lung injury in rats. J Appl Toxicol 26, 126-131.

Mitsopoulos P, Omri A, Alipour M, Vermeulen N, Smith MG, Suntres ZE., 2008. Effectiveness of liposomal-N-acetylcysteine against LPS-induced lung injuries in rodents. Int J Pharm 363, 106-111.

Molineux G., 2002. Pegylation: engineering improved pharmaceuticals for enhanced therapy. Cancer Treat Rev 28 Suppl A, 13-16.

Moran JM, Gonzalez-Polo RA, Ortiz-Ortiz MA, Niso-Santano M, Soler G, Fuentes JM., 2008. Identification of genes associated with paraquat-induced toxicity in SH-SY5Y cells by PCR array focused on apoptotic pathways. J Toxicol Environ Health A 71, 1457-1467.

Mukherjee S, Stone WL, Yang H, Smith MG, Das SK., 2009. Protection of half sulfur mustard gas-induced lung injury in guinea pigs by antioxidant liposomes. J Biochem Mol Toxicol 23, 143-153.

Oktyabrsky ON, Smirnova GV., 2007. Redox regulation of cellular functions. Biochemistry (Mosc) 72, 132-145.

O'Malley YQ, Reszka KJ, Britigan BE., 2004. Direct oxidation of 2',7'-dichlorodihydrofluorescein by pyocyanin and other redox-active compounds independent of reactive oxygen species production. Free Radic Biol Med 36, 90-100.

Oyadomari S, Mori M., 2004. Roles of CHOP/GADD153 in endoplasmic reticulum stress. Cell Death Differ 11, 381-389.

Pajonk F, Riess K, Sommer A, McBride WH., 2002. N-acetyl-L-cysteine inhibits 26S proteasome function: implications for effects on NF-kappaB activation. Free Radic Biol Med 32, 536-543.

Pecheur EI, Lavillette D, Alcaras F, Molle J, Boriskin YS, Roberts M, Cosset FL, Polyak SJ., 2007. Biochemical mechanism of hepatitis C virus inhibition by the broad-spectrum antiviral arbidol. Biochemistry 46, 6050-6059.

Prescott L., 2005. Oral or intravenous N-acetylcysteine for acetaminophen poisoning? Ann Emerg Med 45, 409-413.

Preston C, Soar CJ, Hidayat I, Greenfield KM, Powles SB., 2005. Differential translocation of paraquat in paraquat-resistant populations of *Hordeum leporinum*. Weed Research 45, 289-295.

Quinlan T, Spivack S, Mossman BT., 1994. Regulation of antioxidant enzymes in lung after oxidant injury. Environ Health Perspect 102 Suppl 2, 79-87.

Raggi MA, Mandrioli R, Casamenti G, Musiani D, Marini M., 1998. HPLC determination of glutathione and other thiols in human mononuclear blood cells. Biomed Chromatogr 12, 262-266.

Rahman I, Biswas SK, Kode A., 2006. Oxidant and antioxidant balance in the airways and airway diseases. Eur J Pharmacol 533, 222-239.

Rao HV, Thirumangalakudi L, Grammas P., 2009. Cyclin C and cyclin dependent kinases 1, 2 and 3 in thrombin-induced neuronal cell cycle progression and apoptosis. Neurosci Lett 450, 347-350.

Richman PG, Meister A., 1975. Regulation of gamma-glutamyl-cysteine synthetase by nonallosteric feedback inhibition by glutathione. J Biol Chem 250, 1422-1426.

Roberts TR, Dyson JS, Lane MC., 2002. Deactivation of the biological activity of paraquat in the soil environment: a review of long-term environmental fate. J Agric Food Chem 50, 3623-3631.

Rogalska A, Koceva-Chyla A, Jozwiak Z., 2008. Aclarubicin-induced ROS generation and collapse of mitochondrial membrane potential in human cancer cell lines. Chem Biol Interact 176, 58-70.

Ruiz-Bailen M, Serrano-Corcoles MC, Ramos-Cuadra JA., 2001. Tracheal injury caused by ingested paraquat. Chest 119, 1956-1957.

Sadowska AM, Manuel-Y-Keenoy B, De Backer WA., 2007. Antioxidant and anti-inflammatory efficacy of NAC in the treatment of COPD: discordant in vitro and in vivo dose-effects: a review. Pulm Pharmacol Ther 20, 9-22.

Saibara T, Toda K, Wakatsuki A, Ogawa Y, Ono M, Onishi S., 2003. Protective effect of 3-methyl-1-phenyl-2-pyrazolin-5-one, a free radical scavenger, on acute toxicity of paraquat in mice. Toxicol Lett 143, 51-54.

Saito K., 1986. Effects of paraquat on macromolecule synthesis in cultured pneumocytes. Tohoku J Exp Med 148, 303-312.

Samai M, Hague T, Naughton DP, Gard PR, Chatterjee PK., 2008. Reduction of paraquat-induced renal cytotoxicity by manganese and copper complexes of EGTA and EHPG. Free Radic Biol Med 44, 711-721.

Samai M, Sharpe MA, Gard PR, Chatterjee PK., 2007. Comparison of the effects of the superoxide dismutase mimetics EUK-134 and tempol on paraquat-induced nephrotoxicity. Free Radic Biol Med 43, 528-534.

Sarkar S, Sharma C, Yog R, Periakaruppan A, Jejelowo O, Thomas R, Barrera EV, Rice-Ficht AC, Wilson BL, Ramesh GT., 2007. Analysis of stress responsive genes induced by single-walled carbon nanotubes in BJ Foreskin cells. J Nanosci Nanotechnol 7, 584-592.

Sato M, Tanaka T, Maemura K, Uchiyama T, Sato H, Maeno T, Suga T, Iso T, Ohyama Y, Arai M, Tamura J, Sakamoto H, Nagai R, Kurabayashi M., 2004. The PAI-1 gene as a direct target of endothelial PAS domain protein-1 in adenocarcinoma A549 cells. Am J Respir Cell Mol Biol 31, 209-215.

Shareef MM, Cui N, Burikhanov R, Gupta S, Satishkumar S, Shajahan S, Mohiuddin M, Rangnekar VM, Ahmed MM., 2007. Role of tumor necrosis factor-alpha and TRAIL in high-dose radiation-induced bystander signaling in lung adenocarcinoma. Cancer Res 67, 11811-11820.

Shek PN, Suntres ZE, Brooks JI., 1994. Liposomes in pulmonary applications: physicochemical considerations, pulmonary distribution and antioxidant delivery. J Drug Target 2, 431-442.

Silverman FP, Petracek PD, Fledderman CM, Ju Z, Heiman DF, Warrior P., 2005. Salicylate activity. 1. Protection of plants from paraquat injury. J Agric Food Chem 53, 9764-9768.

Sinico C, De Logu A, Lai F, Valenti D, Manconi M, Loy G, Bonsignore L, Fadda AM., 2005. Liposomal incorporation of Artemisia arborescens L. essential oil and in vitro antiviral activity. Eur J Pharm Biopharm 59, 161-168.

Slade P., 1966. The fate of paraquat applied to plants. Weed Res 6, 158-167.

Smith LL., 1985. Paraquat toxicity. Philos Trans R Soc Lond B Biol Sci 311, 647-657.

Smith LL, Lewis CP, Wyatt I, Cohen GM., 1990. The importance of epithelial uptake systems in lung toxicity. Environ Health Perspect 85, 25-30.

Smith P, Heath D., 1976. Paraquat. CRC Crit Rev Toxicol 4, 411-445.

Smith P, Heath D., 1975. The pathology of the lung in paraquat poisoning. J Clin Pathol Suppl (R Coll Pathol) 9, 81-93.

Soloukides A, Moutzouris DA, Kassimatis T, Metaxatos G, Hadjiconstantinou V., 2007. A fatal case of paraquat poisoning following minimal dermal exposure. Ren Fail 29, 375-377.

Soudamini KK, Unnikrishnan MC, Soni KB, Kuttan R., 1992. Inhibition of lipid peroxidation and cholesterol levels in mice by curcumin. Indian J Physiol Pharmacol 36, 239-243.

Sperandio S, Fortin J, Sasik R, Robitaille L, Corbeil J, de Belle I., 2009. The transcription factor Egr1 regulates the HIF-1alpha gene during hypoxia. Mol Carcinog 48, 38-44.

Spiewak R., 2001. Pesticides as a cause of occupational skin diseases in farmers. Ann Agric Environ Med 8, 1-5.

Stone WL, Smith M., 2004. Therapeutic uses of antioxidant liposomes. Mol Biotechnol 27, 217-230.

Stoyanova T, Roy N, Kopanja D, Bagchi S, Raychaudhuri P., 2009. DDB2 decides cell fate following DNA damage. Proc Natl Acad Sci U S A 106, 10690-10695.

Suntres ZE., 2002. Role of antioxidants in paraquat toxicity. Toxicology 180, 65-77.

Suntres ZE, Hepworth SR, Shek PN., 1993. Pulmonary uptake of liposome-associated alpha-tocopherol following intratracheal instillation in rats. J Pharm Pharmacol 45, 514-520.

Suntres ZE, Hepworth SR, Shek PN., 1992. Protective effect of liposome-associated alpha-tocopherol against paraquat-induced acute lung toxicity. Biochem Pharmacol 44, 1811-1818.

Suntres ZE, Shek PN., 1996. Alleviation of paraquat-induced lung injury by pretreatment with bifunctional liposomes containing alpha-tocopherol and glutathione. Biochem Pharmacol 52, 1515-1520.

Suntres ZE, Shek PN., 1995a. Intratracheally administered liposomal alpha-tocopherol protects the lung against long-term toxic effects of paraquat. Biomed Environ Sci 8, 289-300.

Suntres ZE, Shek PN., 1995b. Liposomal alpha-tocopherol alleviates the progression of paraquat-induced lung damage. J Drug Target 2, 493-500.

Takenaka A, Annaka H, Kimura Y, Aoki H, Igarashi K., 2003. Reduction of paraquat-induced oxidative stress in rats by dietary soy peptide. Biosci Biotechnol Biochem 67, 278-283.

Tategu M, Nakagawa H, Sasaki K, Yamauchi R, Sekimachi S, Suita Y, Watanabe N, Yoshid K., 2008. Transcriptional regulation of human polo-like kinases and early mitotic inhibitor. J Genet Genomics 35, 215-224.

Tomita M, Katsuyama H, Okuyama T, Hidaka K, Minatogawa Y., 2005. Changes in gene expression level for defense system enzymes against oxidative stress and glutathione level in rat administered paraquat. Int J Mol Med 15, 689-693.

Tomita M, Okuyama T, Katsuyama H, Miura Y, Nishimura Y, Hidaka K, Otsuki T, Ishikawa T., 2007. Mouse model of paraquat-poisoned lungs and its gene expression profile. Toxicology 231, 200-209.

van de Poll MC, Dejong CH, Soeters PB., 2006. Adequate range for sulfur-containing amino acids and biomarkers for their excess: lessons from enteral and parenteral nutrition. J Nutr 136, 1694S-1700S.

Venkatesan N., 2000. Pulmonary protective effects of curcumin against paraquat toxicity. Life Sci 66, PL21-8.

Volobоueva LA, Liu J, Suh JH, Ames BN, Miller SS., 2005. (R)-alpha-lipoic acid protects retinal pigment epithelial cells from oxidative damage. Invest Ophthalmol Vis Sci 46, 4302-4310.

Vyas SP, Rawat M, Rawat A, Mahor S, Gupta PN., 2006. Pegylated protein encapsulated multivesicular liposomes: a novel approach for sustained release of interferon alpha. Drug Dev Ind Pharm 32, 699-707.

Walker M, Dugard PH, Scott RC., 1983. Absorption through human and laboratory animal skins: In vitro comparisons. Acta Pharm Suec 20, 52-53.

Wegener T, Sandhagen B, Chan KW, Saldeen T., 1988. N-acetylcysteine in paraquat toxicity: toxicological and histological evaluation in rats. Ups J Med Sci 93, 81-89.

Weidauer E, Lehmann T, Ramisch A, Rohrdanz E, Foth H., 2004. Response of rat alveolar type II cells and human lung tumor cells towards oxidative stress induced by hydrogen peroxide and paraquat. Toxicol Lett 151, 69-78.

Wester RC, Maibach HI, Bucks DA, Aufrere MB., 1984. In vivo percutaneous absorption of paraquat from hand, leg, and forearm of humans. J Toxicol Environ Health 14, 759-762.

Wills BK, Aks S, Maloney GE, Rhee J, Brand R, Sekosan M., 2007. The effect of amifostine, a cytoprotective agent, on paraquat toxicity in mice. J Med Toxicol 3, 1-6.

Woo HD, Kim BM, Kim YJ, Lee YJ, Kang SJ, Cho YH, Choi JY, Chung HW., 2008. Quercetin prevents necrotic cell death induced by co-exposure to benzo(a)pyrene and UVA radiation. Toxicol In Vitro 22, 1840-1845.

Wu XJ, Kassie F, Mersch-Sundermann V., 2005. The role of reactive oxygen species (ROS) production on diallyl disulfide (DADS) induced apoptosis and cell cycle arrest in human A549 lung carcinoma cells. Mutat Res 579, 115-124.

Yang W, Chen L, Ding Y, Zhuang X, Kang UJ., 2007. Paraquat induces dopaminergic dysfunction and proteasome impairment in DJ-1-deficient mice. Hum Mol Genet 16, 2900-2910.

Yeh ST, Guo HR, Su YS, Lin HJ, Hou CC, Chen HM, Chang MC, Wang YJ., 2006. Protective effects of N-acetylcysteine treatment post acute paraquat intoxication in rats and in human lung epithelial cells. Toxicology 223, 181-190.

Zafarullah M, Li WQ, Sylvester J, Ahmad M., 2003. Molecular mechanisms of N-acetylcysteine actions. Cell Mol Life Sci 60, 6-20.

Zenz T, Benner A, Dohner H, Stilgenbauer S., 2008. Chronic lymphocytic leukemia and treatment resistance in cancer: the role of the p53 pathway. Cell Cycle 7, 3810-3814.